Dissertation

submitted to the

Combined Faculties for the Natural Sciences and for Mathematics

of the Ruperto-Carola University of Heidelberg, Germany

for the degree of

Doctor of Natural Sciences

presented by

Diplom biologist Alexandra Wojtalla

Born in: Mannheim, Germany

Oral examination:

Bonn 2011

Liver fibrosis and endocannabinoids

Referees Prof. Dr. Stefan Wölfl

Prof. Dr. Andreas Zimmer

Kurzfassung

Leberfibrose ist die Folge einer chronischen hepatischen Schädigung und resultiert aus einer vermehrten Ablagerung von narbigem Bindegewebe durch aktivierte hepatische Sternzellen (HSZs). Während der Zelltod von Hepatozyten, den Parenchymzellen der Leber, eine kausale Rolle bei der Leberfibrosierung spielt, verstärkt der Zelltod von aktivierten HSZs die Rückbildung der Leberfibrose und der daraus resultierenden Komplikationen, welche für die hohe Sterberate dieser Krankheit verantwortlich sind.

In der vorliegenden Arbeit konnte zum ersten Mal gezeigt werden, dass die Endocannabinoide Virodhamin, Noladin Ether und N-Arachidonoyl Dopamin (NADA) zu spezifischem Zelltod von HSZs führen. Hepatozyten sind durch starke Abwehrmechanismen wie Antioxidanzien und durch eine hohe Expression des Abbauenzyms von NADA resistent gegenüber NADA-induziertem Zelltod. Das Synthese-Enzym von NADA wird in Hepatozyten, jedoch nicht in HSZs, exprimiert. NADA stellt somit eine potentielle antifibrotische Substanz dar, die für therapeutische Zwecke genutzt werden kann.

Des Weiteren wurde in früheren Studien eine starke Hochregulation des Endocannabinoids 2-Arachidonoyl Glycerol (2-AG) in der geschädigten Leber beobachtet, während in dem ungeschädigten Organ nur niedrige 2-AG Level gemessen wurden. In dieser Arbeit konnte gezeigt werden, dass Nichtparenchymzellen der Leber den zellulären Ursprung von 2-AG darstellen. Die erhöhten 2-AG Level während hepatischer Schädigung kommen zum einen durch erhöhte Expression des Synthese-Enzyms und zum anderen durch die Herabsetzung der Degradations-Enzym-Level zustande.

Aus früheren Studien ist bekannt, dass 2-AG zu apoptotischem Zelltod in HSZs, jedoch nicht in Hepatozyten, führt. HSZs und Hepatozyten weisen einen signifikanten Unterschied in der Expression von COX-2 auf, was eine unterschiedliche Metabolisierung des Endocannabinoids 2-AG bedingt. Die Produktion von PGD_2-GE durch COX-2 in HSZs trägt möglicherweise zur disparaten Empfindlichkeit von Hepatozyten und HSCs gegenüber 2-AG-induzierter Apoptose bei.

Schlussendlich sollen die neuen Erkenntnisse über die Rolle Endocannabinoid-vermittelter Signalwege bei Leberschädigung ermöglichen, spezifische Komponenten dieses Systems zu beeinflussen um dadurch hepatische Fibrogenese zu reduzieren.

Abstract

Liver fibrosis is the response to chronic hepatic injury and results from an increased deposition of connective scar tissue by activated hepatic stellate cells (HSCs). Removal of activated HSCs preceded amelioration of fibrosis and can prevent further severe complications of chronic hepatic injury, which result in a high mortality rate worldwide.

In this thesis it was shown the first time, that the endocannabinoids virodhamine, noladin ether and N-arachidonoyl dopamine (NADA) specifically induce cell death in HSCs but not in hepatocytes. Due to the selective expression of effective defence systems like antioxidants and the NADA degradation enzyme fatty acid amide hydrolase (FAAH), hepatocytes showed resistance to NADA-induced cell death. The synthesising enzyme of NADA was shown to be strongly expressed in hepatocytes but not in HSCs. Thus, NADA has therapeutic potential as an antifibrotic endogenous agent.

Moreover, in a recent study it was shown that the endocannabinoid 2-arachidonoyl glycerol (2-AG) is strongly upregulated in the injured liver. In this thesis it is shown that elevated 2-AG levels during liver fibrogenesis are due to elevated expression of the 2-AG synthesising enzyme and decreased levels of the 2-AG degradation enzyme. The data further points to non-parenchymal cells rather than to hepatocytes being the most important cells in 2-AG metabolism in the liver.

Recently it was shown that 2-AG specifically induces cell death in HScs but not in hepatocytes. HSCs and hepatocytes differentially express COX-2, leading to differential metabolism of 2-AG. The generation of pro-apoptotic PGD_2-GE by COX-2 in HSCs possibly contributes to the different susceptibility of hepatocytes and HSCs towards 2-AG-induced cell death.

In conclusion, the understanding of the role of endocannabinoid-mediated pathways in liver injury and fibrosis will make it possible to specifically target components of this system to decrease fibrogenesis.

Abbreviations

2-AG	2-arachidonoyl glycerol
Noladin ether	2-arachidonoyl glycerol ether
NADA	N-arachidonoyl dopamine
AEA	Arachidonoyl ethanolamine (Anandamide)
ALD	Alcoholic liver disease
BCP	Bromo chloropropane
BSA	Bovine serum albumine
bw	Body weight
CB	Cannabinoid
DAG	Diacylglycerol
DAGL	Diacylglycerol lipase
DEPC	diethylpyrocarbonate
DMEM	Dulbecco`s Modified Eagl Medium
DMSO	Dimethylsulfoxid
DNA	Desoxyribonucleic acid
DTT	Dithiothreitol
EC	Endocannabinoid
ECM	Extracellular matrix
EDTA	Ethylene glycol tetraacetic acid
ELISA	Enzyme-linked immunosorbent assay
EtOH	Ethanol
FAAH	Fatty acid amide hydrolase
FasL	Fas ligand
FCS	Fetal calf serum
g	Gram
h	Hour
HBSS	Hank`s buffered salt solution
HBV	Hepatitis B virus
HCV	Hepatitis C virus
HGF	Hepatocyte growth factor
HSC	Hepatic stellate cells
i.p.	Intraperitoneal
KC	Kupffer cells
kDa	Kilodalton

kg	Kilogram
LDH	Lactate dehydrooxygenase
LPS	Lipopolysaccharide
m	Metre
M.musculus	Mus musculus (house mouse)
mA	Milliampere
mA	Milliampere
MGL	Monoacyl glycerol lipase
min	Minutes
mRNA	Messenger RNA
ms	Milliseconds
n	Sample size
n.s.	Not significant
NAFLD	Non-alcoholic liver disease
ng	Nanogram
OD	Optical density
PA	Polyacrylamide
PBS	Phosphate buffered saline
PCR	Polymerase chain reaction
RNA	Ribonucleic acid
SDS PAGE	Sodium dodecyl sulfate polyacrylamide gel electrophoresis
s	Seconds
SEM	Standard error of the mean
TGF	Transforming growth factor
TNF	Tumor necrosis factor
Tris	Tris (hydroxymethyl) aminomethane
TRPV1	Transient receptor potential vanilloid type 1
U	(Enzyme) *Unit*
Δ^9-THC	Δ^9-Tetrahydrocannabinol
µl	Microlitre
µM	Micromolar

INDEX

1 INTRODUCTION

During the last decade, the endocannabinoid system (ECS) has emerged as a key regulator of the pathogenesis of chronic liver diseases. This thesis focuses on the role of the ECS, including their ligands, receptors and the enzymes, which are involved in the synthesis and degradation of endocannabinoids, in hepatic fibrosis. To provide an insight into the topic, the introduction starts with a section about the pathology of this disease. Consecutively, the second section presents the hepatic stellate cell (HSC), whose activation plays a pivotal role in the pathogenesis of liver fibrosis. Moreover, for a better understanding of the ECS in general, I will give a short overview of endocannabinoids, their synthesis and degradation. Last but not least, the last sections highlight the role of endocannabinoids in hepatic fibrosis and the aim of this thesis.

1.1 Pathogenesis of liver fibrosis

Acute injury of the liver leads to a self-limited wound healing process, which restores the architecture and function of the liver. Increased amounts of extracellular matrix (ECM) proteins like collagen and elastin are expressed to replace the damaged cells. After cessation of acute liver injury, the parenchyma regenerates and the ECM is degraded by metalloproteinases (Arthur, 2000).

If the hepatic injury persists and becomes chronic, an inflammatory and pro-fibrogenic environment develops. This entails a perpetuating wound healing reaction with an excessive deposition of ECM proteins and a failure to degrade these proteins. The consequence is a substitution of parenchymal cells by scar tissue. This process is called hepatic fibrosis and leads in the worst case to cirrhosis, the end stage of fibrosis (Bataller & Brenner, 2005; Friedman, 2000).

The main causes of chronic liver disease are viral hepatitis B and C infection. According to the world health organization (WHO), more than 500 million people are chronically infected by hepatitis B or C virus (HBV; HCV, respectively), which spread primarily by direct contact with human blood through for example unscreened blood transfusions or re-use of needles. There exists an effective HBV vaccine since 1982 resulting in a significant reduction of chronic hepatitis B infection in infants (Chang et al., 1997). In contrast, three to four million persons become newly infected by HCV each year (WHO, 2002).

Another main cause is alcohol abuse leading to alcoholic liver disease (ALD) (Farrell & Larter, 2006; Leon, Shkolnikov, McKee, Kiryanov, & Andreev, 2010). In industrial countries, ALD accounts for more than half of all cirrhotic livers (Siegmund, Dooley, & Brenner, 2005a)

and according to the WHO, 20 % of heavy drinkers develop fatty liver disease and 10-15 % of these cirrhosis (Miranda-Mendez, Lugo-Baruqui, & Armendariz-Borunda, 2010).

In the last few decades, non-alcoholic fatty liver disease (NAFLD) arose emerging from increasing rates of obese patients presenting increased insulin resistance and hypertriglyceridaemia. After progression into steatohepatitis, this liver disease resembles alcoholic hepatitis occurring in non-drinkers. It was first observed 30 years ago (Ludwig, Viggiano, McGill, & Oh, 1980). Although only 20 % of overweight people develop NAFLD, it is still a severe problem through the dramatically increasing prevalence of obesity (Day, 2005).

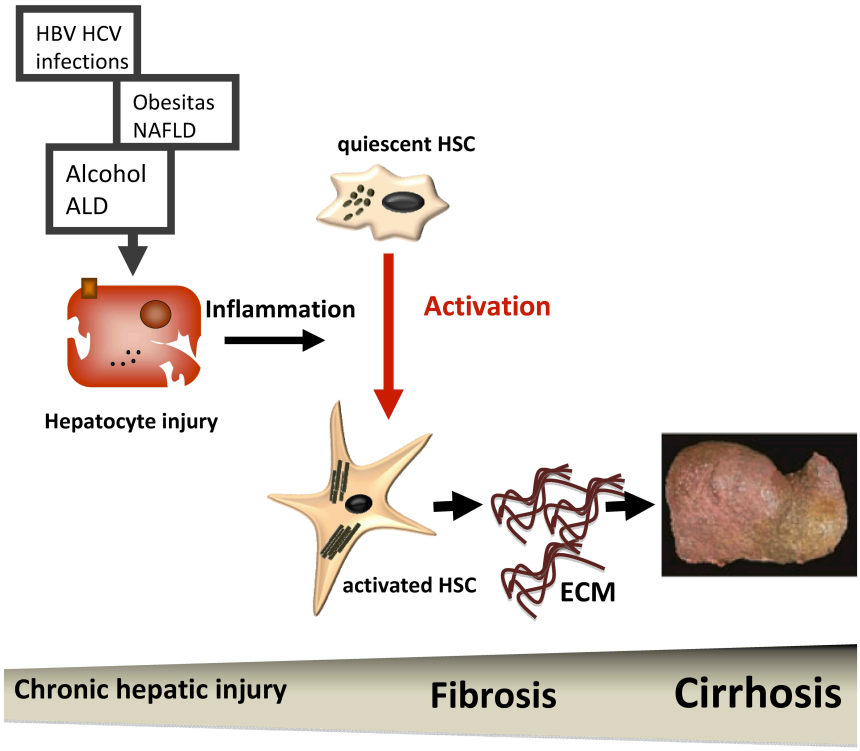

Figure 1. Liver fibrosis results from chronic damage to the liver parenchyma due to for example hepatitis B or C virus (HBV or HCV, respectively) infections, alcohol abuse leading to alcoholic liver disease (ALD) or obesitas leading to non-alcoholic fatty liver disease (NAFLD). Upon liver injury, quiescent hepatic stellate cells (HSCs) activate to myofibroblast like cells. Activated HSCs are the main extracellular matrix (ECM) producing cells. This overproduction of ECM proteins leads to hepatic fibrosis and in the worst case to cirrhosis.

Chronic liver diseases represent a major health problem, which is now in the top ten causes of mortality worldwide (Lotersztajn et al., 2005). The high mortality rate caused by chronic liver diseases is mainly due to hepatic cirrhosis and the resulting severe clinical complications. Portal hypertension is a common consequence of cirrhosis. The blood flow through the portal vein is retarded by the inflamed and fibrotic tissue. Blood pressure increases resulting in ascites, which represent the most common complication of cirrhosis with 50 % mortality of patients in five years. Spontaneous bacterial infections causing peritonitis is seen in 30 % of patients with severe cirrhosis. The survival rate of these patients

is less than one year. Moreover, cirrhosis represents a risk factor for the development of hepatocellular carcinoma (Dong & Saab, 2008).

Up to now, removal of the causative agent is the most effective way to treat fibrosis (Bataller et al., 2005; Siegmund et al., 2005a). Alcohol withdrawal, eradication of the toxic agent (Okazaki, Watanabe, Hozawa, Arai, & Maruyama, 2000; Sobesky et al., 1999) (Dufour & Oneta, 2004) or weight loss in patients with NAFLD can significantly reduce inflammation or even reverse fibrosis (Dixon, Bhathal, Hughes, & O'Brien, 2004).

However, what if the removal of the causative agent cannot be achieved like chronic viral infections? In this case, alternative treatment options are strongly required.

1.2 The hepatic stellate cell: good or bad guy?

The overproduction of ECM following scarring of the liver results from an activation of myofibroblast-like cells. The primary source of connective tissue presents the hepatic stellate cell (HSC), the main fibrogenic cell type in the liver (Bataller et al., 2005; Friedman, 2000).

HSCs are first described by Kupffer in the 19th century and play pivotal roles in the response to hepatic injury and fibrosis (Bataller et al., 2005; Friedman, 2004; Iredale, 2007; Wake, 1971).

HSCs reside in their quiescent state in the space of Disse between the hepatocytes and the sinusoidal endothelial cells, which are lining the liver sinusoids. They represent one third of the entire non-parenchymal cell population and 8-14 % of the total number of resident cells in the liver (Giampieri, Jezequel, & Orlandi, 1981).

In the healthy liver, HSCs play a central role in uptake and storage of vitamin A (Wake, 1971). Following liver injury of any etiology, HSCs activate, transdifferentiate into myofibroblast-like cells and start to produce high amounts of ECM proteins, which replace the damaged parenchymal cells (Figure 1). Kupffer cells (KCs), the resident macrophages in the liver, have been found to be essential for the activation of HSCs by secreting profibrogenic cytokines like transforming growth factor (TGF) β and by recruiting inflammatory cells to the side of injury (Duffield et al., 2005; Matsuoka & Tsukamoto, 1990; Rivera et al., 2001). After cessation of the acute damage, these inflammatory cells together with the HSCs degrade the extracellular tissue. Thus, after an acute injury of the liver, activation of HSCs is an important and beneficial step to restore liver architecture and function.

If hepatic injury becomes chronic, the removal of the ECM is no longer achieved. Instead, HSCs, KC and recruited inflammatory cells continue to secrete proinflammatory mediators. HSCs produce excessive amounts of extracellular matrix proteins, which replace also the healthy liver parenchyma and lead to scarring of the liver (Maher, 2001) (Pinzani & Marra, 2001). In such an environment, activated HSCs not contribute to maintain liver architecture

but rather destroy the whole liver cell organisation and function.

Primary HSCs cultivated on uncoated plastic tissue culture plates display many characteristics of activated HSCs *in vivo*; they start to proliferate, loose the vitamin A stores and increase the cytosceletal protein expression (Friedman, 2008b). Therefore, isolation of HSCs is an excellent *in vitro* model for the examination of the role of these cells in hepatic fibrosis.

Due to their pivotal role in the pathophysiology of the disease, HSCs display an interesting target for the treatment of hepatic fibrosis. During amelioration of liver fibrosis in rats, a selective cell death in activated HSCs takes place (Iredale et al., 1998). Several endogenous mediators including Fas ligand (FasL), tumor necrosis factor (TNF) α or nerve growth factor (NGF) are capable to induce cell death in HSCs (Lang, Schoonhoven, Tuvia, Brenner, & Rippe, 2000; Saile, Knittel, Matthes, Schott, & Ramadori, 1997; Trim et al., 2000). However, these mediators act on cellular receptors that are also highly expressed in hepatocytes and other hepatic cell populations. Thus, these endogenous mediators are unsuitable candidates for the treatment of liver fibrosis.

It was recently demonstrated that the endogenous cannabinoids N-arachidonoyl ethanolamine (anandamide, AEA) and 2-arachidonoyl glycerol (2-AG) are highly efficient in inducing cell death in HSCs, but not in hepatocytes (Siegmund et al., 2007; Siegmund et al., 2006; Siegmund, Uchinami, Osawa, Brenner, & Schwabe, 2005b). Moreover, AEA and 2-AG levels in the liver are significantly upregulated during fibrogenesis *in vivo* and can reach concentrations that induce cell death in HSCs *in vitro* (Siegmund et al., 2007).

Based on these findings, endocannabinoids may potentially act as endogenous antifibrotic mediators.

1.3 The endocannabinoid system

The first natural cannabinoid, the main psychoactive compound of *Cannabis Sativa*, Δ^9-THC (delta-9-tetrahydrocannabinol) has been isolated in 1971 (Gaoni & Mechoulam, 1971). Endogenous cannabinoids started to be characterised in the early 90s. Endocannabinoids, their receptors and the molecules that are responsible for their uptake, synthesis and degradation form a signalling system (endocannabinoid system, ECS) that plays pivotal roles in a number of physiological processes including nociception, food intake, intestinal motility or inflammation (Capasso et al., 2005; Di Marzo, Bifulco, & De Petrocellis, 2004; Di Marzo & Matias, 2005; Storr, Yuce, & Goke, 2006). Moreover, the ECS is involved in the pathophysiology of several diseases including atherosclerosis, fatty liver disease or liver fibrosis (Fisar, 2009; Osei-Hyiaman et al., 2005; Siegmund & Schwabe, 2008).

Endocannabinoids (ECs) are endogenous ligands for the cannabinoid receptors. There are at least two seven-transmembrane-domain cannabinoid receptors (CB_1 and CB_2) that are

coupled to $G_{i/o}$-proteins. The CB_1 receptor was cloned in 1990 and is mostly expressed in the central nervous system (Matsuda, Lolait, Brownstein, Young, & Bonner, 1990), but also in peripheral tissues including the gastrointestinal tract, the lung and the liver (Osei-Hyiaman et al., 2005). The CB_2 receptor was cloned in 1993 (Munro, Thomas, & Abu-Shaar, 1993) and shows high expression levels in immune cells and peripheral tissues like tonsils and spleen, but is also present in the central nervous system (Brown, Wager-Miller, & Mackie, 2002; Klein et al., 2003; Onaivi et al., 2006).

The N-acyl ethanolamide N-arachidonoylethanolamide (anandamide; AEA) and the monoacylglycerol 2-arachidonoyl glycerol (2-AG) represent the two most studied endocannabinoids. AEA was discovered in 1992 and can act as an endogenous ligand for CB_1 receptors and with low efficiency to CB_2 receptors (Devane et al., 1992). Moreover, it can bind to transient receptor vanilloid type 1 (TRPV1) (van der Stelt et al., 2005) and to the G protein-coupled receptor GPR55 (Ryberg et al., 2007). 2-AG was discovered as a second endogenous ligand, which is a full CB_1 and CB_2 receptor agonist (Mechoulam et al., 1995).

In 2001, 2-arachidonoyl glycerol ether (noladin ether) was isolated from porcine brain (Hanus et al., 2001). One year later it was found in amounts similar to AEA in rat tissue (Fezza et al., 2002). It binds very weakly to the CB_2 receptor but has a high affinity to CB_1 receptors (Steffens, Zentner, Honegger, & Feuerstein, 2005). Noladin ether has anti-proliferative effects in prostate carcinoma cells by a cannabinoid receptor-independent pathway, but other functional activities are rarely known so far (Hanus et al., 2001; Nithipatikom, Isbell, Endsley, Woodliff, & Campbell). Nevertheless, Sugiura and colleagues could not find any noladin ether in rat brain (Oka et al., 2003). Although its affinity to cannabinoid receptors is not in discussion, its physiological role is undetermined so far.

Shortly after, by developing a bioanalytical method to measure anandamide in tissue, a substance was found with the same molecular weight than anandamide but with a shorter retention time. This analyte was O-arachidonoyl-ethanolamine (virodhamine), an arachidonic acid and ethanolamine joined by an ester linkage. In the brain, virodhamine showed similar concentrations to that of AEA and in peripheral tissues the levels of virodhamine are even higher than that of AEA. At the CB_2 receptor, virodhamine acts as a full agonist. However, less is known about the effects of virodhamine: it produces hypothermia in mice and reflected vasorelexant activities in mesenteric arteries in rats (Ho & Hiley, 2004; Porter et al., 2002). Moreover, virodhamine causes a relaxation of human pulmonary arteries and as such could control the vascular tone (Kozlowska et al., 2008). Nevertheless, virodhamine has been shown to be partly converted to AEA, which should be taken into consideration when looking at virodhamine-induced effects (Saario, Savinainen, Laitinen, Jarvinen, & Niemi, 2004).

N-arachidonoyl dopamine (NADA) was recently identified as an endogenous ligand for CB_1 receptors and TRPV1. It belongs to the endovanilloid class of endocannabinoids (Bisogno et

al., 2000; Huang et al., 2002). It also shows low affinity to CB_2 receptors (Bisogno et al., 2000; Di Marzo et al., 2004). In peripheral organs such as isolated bronchi or urinary bladder of the guinea pig, NADA showed constrictory effects mediated by TRPV1 signalling (Harrison et al., 2003). In contrast, NADA initiated vasorelaxant effects also via the activation of TRPV1 and CB_1 receptors in small mesenteric vessels, superior mesenteric artery or aorta in rats (O'Sullivan, Kendall, & Randall, 2004; 2005). Moreover, NADA induces cell death in a human neuroblastoma cell line and in human peripheral blood mononuclear cells via TRPV1 activation (Davies, Hainsworth, Guerin, & Lambert; Saunders, Fassett, & Geraghty, 2009). However, further roles of NADA as a representative of this novel endovanilloid class of endocannabinoids in peripheral tissues need to be elucidated (Hu et al., 2009; Huang et al., 2002).

1.3.1 Endocannabinoid synthesis and degradation

The endocannabinoids AEA and 2-AG are arachidonic acid-derived lipid mediators. Unlike many other signalling molecules, they are not stored intracellularly, but synthesised on demand in response to specific signals such as an increase in intracellular Ca^{2+} (Straiker & Mackie, 2006). AEA is produced from membrane phospholipids through hydrolysis of N-arachidonyl-phosphatidyl-ethanolamine (NAPE) by a Ca^{2+}-sensitive NAPE-phospholipase D (NAPE-PLD) (Okamoto, Morishita, Tsuboi, Tonai, & Ueda, 2004). 2-AG is produced in two steps via generation of diacylglycerols (DAG) from phosphatidylinositol and subsequent hydrolysis of DAG with arachidonate in the second position by the enzyme DAG lipase (DAGL) (Di Marzo et al., 1999) (Figure 2).

Less is known about the biosynthesis of the most recent discovered endocannabinoids.

Indeed, the biosynthetic pathway of noladin ether is unknown so far, while virodhamine is believed to have a synthesis pathway related to AEA due to their structural similarities (Porter et al., 2002) (Ho et al., 2004). The proposed mechanism of NADA biosynthesis is the condensation of arachidonic acid and tyrosine followed by a transformation of N-arachidonoyl-tyrosine into NADA. This reaction is catalysed by tyrosine hydroxylase, an enzyme catalysing also the biosynthesis of dopamine from tyrosine (Hu et al., 2009) (Figure 2).

The hydrolysis of endocannabinoids, which results in the termination of endocannabinoid signalling, is an intracellular event. Endocannabinoids are lipophilic substances and can cross cell membranes by simple diffusion. However, the existence of a putative endocannabinoid transporter is also under discussion (Beltramo & Piomelli, 2000; Glaser et al., 2003). Anandamide is degraded by fatty acid amide hydrolase (FAAH) to ethanolamine and arachidonic acid (Cravatt et al., 1996). Pharmacological blocking of FAAH as well as genetic deletion leads to strongly enhanced AEA levels (Muccioli, 2010).

Although it has been recently shown that FAAH is also able to degrade 2-AG *in vitro*, 2-AG levels are not increased in FAAH knockout mice ($FAAH^{-/-}$ mice) (Muccioli; Patel et al., 2005). Indeed, 2-AG is mainly hydrolysed by the serine hydrolase monoacylglycerol lipase (MGL) to glycerol and arachidonic acid (Dinh, Kathuria, & Piomelli, 2004) (Figure 2).

In human neocortex, virodhamine interacts with FAAH (Steffens et al., 2005) and a specific FAAH inhibitor attenuated the vasorelaxant effect of virodhamine suggesting an involvement of this enzyme in its metabolism (Ho et al., 2004).

NADA is rapidly taken up in glioma cells by an unknown mechanism and is hydrolysed by FAAH but significantly slower than AEA (Figure 2). Another mechanism for deactivation of NADA could be the metabolism to the less potent 3-O-methyl derivative by catechol-O-methyl transferase (COMT) (Hu et al., 2009).

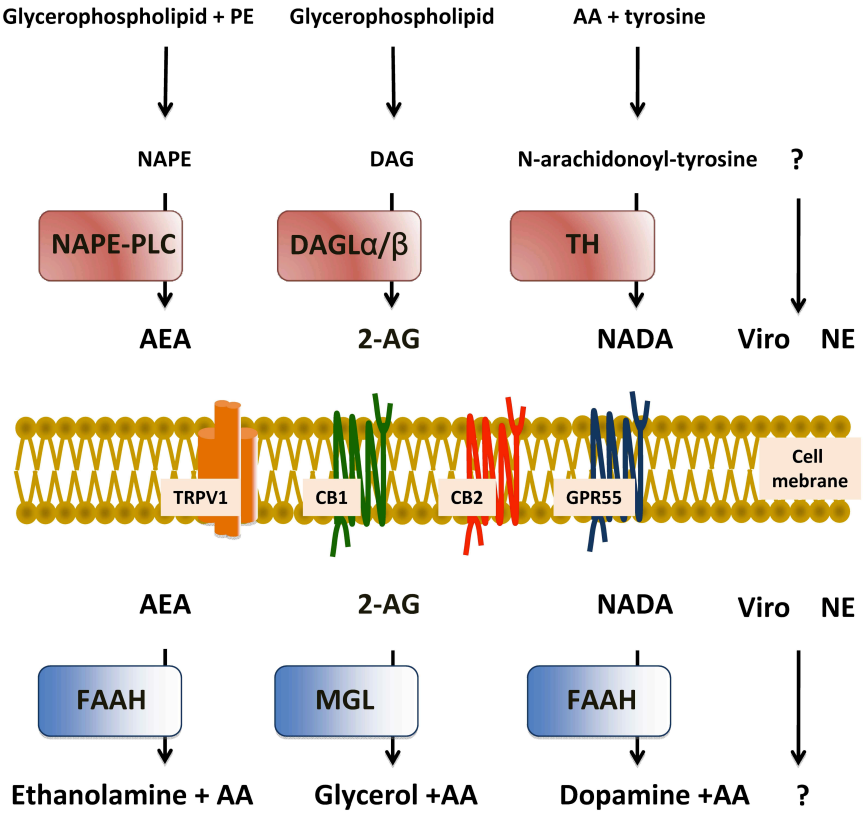

Figure 2. Biosynthesis and breakdown of the endocannabinoids anandamide (AEA), 2-arachidonoyl glycerol (2-AG) and N-arachidonoyl dopamine (NADA). AEA is synthesised by N-transacylation of a glycerophospholipid to phosphatidylethanolamine (PE) resulting in N-acyl-phosphatidlyethanolamine (NAPE). Afterwards, NAPE is transformed to AEA catalysed by an NAPE-phospholipase C (NAPE-PLC). After synthesis, AEA is rapidly deactivated via degradation by fatty acid amide hydrolase (FAAH). 2-AG is synthesised from diacylglycerol (DAG) via the actions of DAG lipase (DAGL). In addition, 2-AG is hydrolysed by monoacylglycerol lipase (MGL) to yield arachidonic acid (AA) and glycerol. The proposed biosynthesis of NADA is the condensation of AA and tyrosine, which results in N-arachidonoyl-tyrosine. Afterwards, N-arachidonoyl-tyrosine is transformed into NADA by the catalysing activity of tyrosine hydroxylase (TH). Synthesis as well as degradation pathway for virodhamine (Viro) and noladin ether (NE) are unknown so far. To date, there are two definitive cannabinoid receptors, cannabinoid receptor 1 (CB_1) and cannabinoid receptor 2 (CB_2). Moreover, endocannabinoids can also bind to transient receptor potential vanilloid type 1 (TRPV1) and to the G protein-coupled receptor 55 (GPR55).

Besides the degradation pathways described above, endocannabinoids can be metabolised by other enzymes, for example by cyclooxygenase-2 (COX-2) into prostaglandin ethanolamides and prostaglandin glycerol esters (Kozak et al., 2002). Endocannabinoid metabolism by COX-2 represents rather a novel pathway for the biosynthesis of further lipid mediators with functions other than endocannabinoids than a mere deactivation mechanism.

1.3.2 Endocannabinoid oxidation by COX-2

In the last decade, paralleling the investigation of the endocannabinoid system, the characterisation of cyclooxygenases (COX) has emerged to a great field of interest. Cyclooygenases convert free fatty acids to prostaglandins. In the early 1990, a second isoform of cyclooxygenase, COX-2 was recovered (Kozak, Prusakiewicz, & Marnett, 2004; O'Neill & Ford-Hutchinson, 1993). While COX-1 is expressed constitutively and acts as a “housekeeping” protein, COX-2 shows a marginally basal expression and can be induced by e.g. growth factors (EGF, PDGF) or inflammatory cytokines (IL-1, TNFα) (Seibert et al., 1997) (Herschman, 1996). However, many cells possess both isoforms, the constitutively active and the inducible one, resulting in no dramatic increase of prostaglandin production even after a strong upregulation of COX-2 (Rouzer & Marnett, 2005; 2008). Moreover, COX-1 and COX-2 share more than 90 % sequence homology. Though what is the functional difference between these two oxygenases? Interestingly, COX-2 possesses an additional binding site. This internal pocket is conserved in all COX-2 genes sequenced up to now suggesting a specific function of COX-2 besides the functions shared with COX-1 (Smith, DeWitt, & Garavito, 2000) (Kozak, Prusakiewicz, Rowlinson, Schneider, & Marnett, 2001b).

Indeed, the first catalytic difference of COX-1 and -2 was uncovered 1997 when COX-2 displayed the ability to create prostaglandin ethanolamides (PG-EA) after incubation with AEA *in vitro*. This finding represents the first marked connection between COX-2 and the endocannabinoid system. Occasionally, COX-1 displayed no metabolism of AEA (Yu, Ives, & Ramesha, 1997). Shortly after, the metabolism of 2-AG by COX-2 was also investigated. Kozak and colleagues showed that 2-AG is metabolised by COX-2 much more efficiently than AEA and even arachidonic acid (Kozak et al., 2004).

Like AEA, 2-AG is a specific substrate for COX-2, but not for COX-1 representing a selective, probably biological meaningful function for COX-2 (Kozak, Rowlinson, & Marnett, 2000). COX-2 action on 2-AG and AEA *in vitro* leads to the production of prostaglandin H_2 glycerol ester (PGH_2-GE) and prostaglandin H_2 ethanol amide (prostamide H_2, PGH_2-EA), respectively. The unstable PGH_2-GE and PGH_2-EA are metabolised by different synthases to a set of PG-GE and PG-EA, respectively (Kozak et al., 2002) (Figure 3).

These prostaglandin analogues are poor substrates for further oxidation steps. Thus, PG-GE and PG-EA are much more stable than their PG counterparts and are able to diffuse from their site of generation (Kozak et al., 2001a).

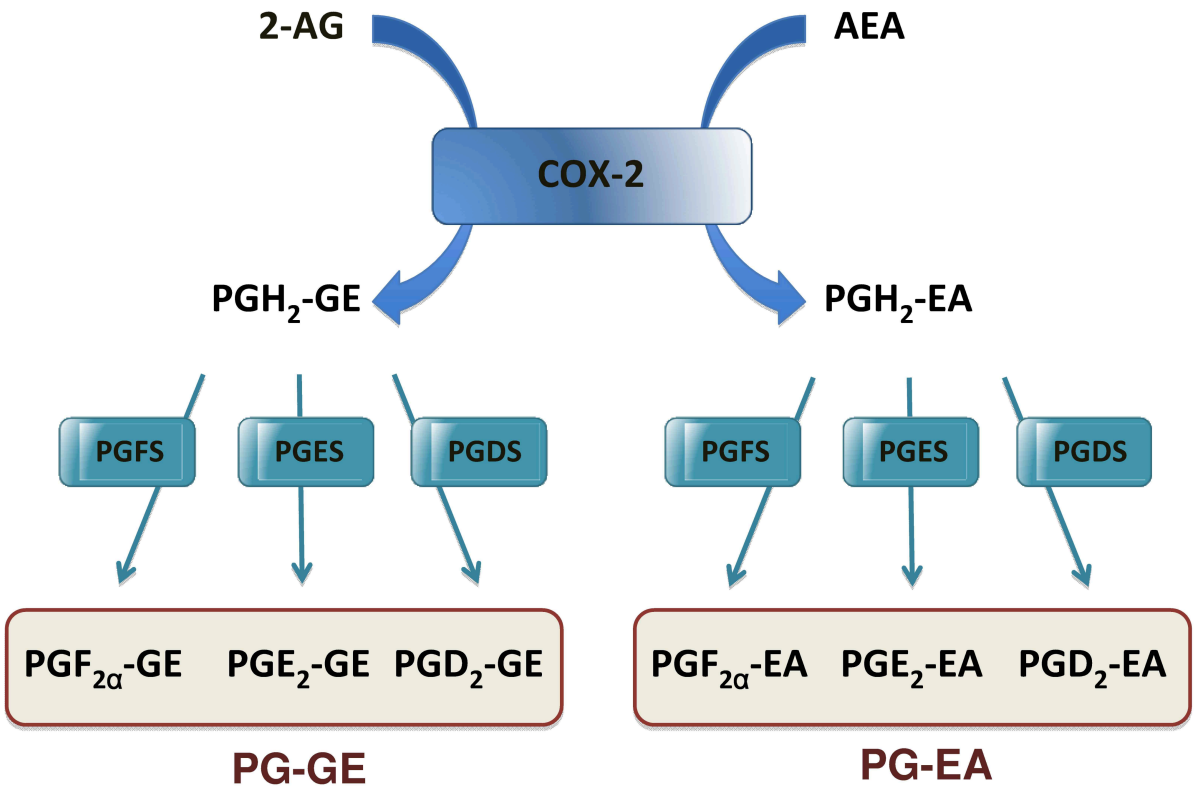

Figure 3. Conversion of 2-arachidonoyl glycerol (2-AG) and Anandamide (AEA) by an oxygenation pathway. 2-AG and AEA are first converted to prostaglandin H_2 glycerol ester (PGH_2-GE) and prostaglandin H_2 ethanolamide (PGH_2-EA, respectively. Afterwards, the prostaglandin-synthases F, E and D (PGFS, PGES, PGDS) metabolise the H_2 derivative to the corresponding prostaglandin-glycerolester (PG-GE) or –ethanolamides (PG-EA).

Less is known about the synthesis of PG-EA and PG-GE *in vivo* and about their biological effects. The COX-2 oxygenation product PGE_2-EA inhibits IL-12 and IL-23 expression in migroglia and macrophages. Their progenitor, AEA, exhibits similar effects. Interestingly, the inhibitory effect of AEA is reversible by treatment with a COX-2 inhibitor. This study suggests that AEA functions not directly in a cannabinoid receptor-dependent way but rather by its metabolism via COX-2 (Correa et al., 2008).

PGE_2-GE induces an increase in the frequency of mIPSCs in mouse hippocampal neurons. This contrasts with the effects of 2-AG and the prostaglandin counterpart PGE_2, which both reduce the frequency. When hippocampal preparations are treated with the COX-2 inhibitor, the frequency decreases suggesting the increase is due to an increase of endocannabinoid-derived PG-GE produced by COX-2 (Sang, Zhang, & Chen, 2006).

In another study, AEA is shown to induce cell death in tumourigenic but not in non-tumourigenic keratinocytes. The authors could show that AEA selectively induces cell death due to the overexpression of COX-2 in the tumour cells and the resulting metabolism of AEA to toxic PG-EA (Van Dross, 2009).

The socalled oxoendocannabinoids produced by COX-2 probably represent a group of unique signalling mediators with activities distinct from their precursors. Previous studies showed, that COX-2 is marginally expressed in the healthy liver. Interestingly, COX-2 expression is strongly upregulated in the injured liver (Jeong et al. 2010) paralleled by the upregulation of the endocannabinoid system. Recent studies showed, that induction of COX-2 leads to growth inhibition in HSCs, therefore having putative anti-fibrotic properties (Davaille et al., 2000; Gallois et al., 1998). However, the role of COX-2 during fibrogenesis is still under discussion.

1.4 Endocannabinoids as key modulators in liver fibrosis

In recent years, several studies showed that the ECS becomes activated and plays important roles in chronic and acute hepatic injury (Siegmund et al., 2008). This activation of the hepatic ECS occurs in early stages of liver disease and remains throughout later stages (Osei-Hyiaman et al., 2005).

It was shown that the cannabinoid receptors CB_1 and CB_2 are expressed marginally or are even absent in the healthy liver. Chronic hepatic injury induces markedly the expression of these receptors (Julien et al., 2005; Teixeira-Clerc et al., 2006). Interestingly, CB_1-deficient mice show a significant decline of fibrosis after bile duct ligation or CCl_4 treatment compared to wild type animals. Furthermore, the CB_1 inhibitor rimonabant reduced profibrogenic markers like α smooth muscle actin. It was suggested that these effects were caused by an increase in cell death and decreased proliferation of myofibroblasts (Teixeira-Clerc et al., 2006). In contrast, $CB_2^{-/-}$ mice display a significant increase of fibrosis after CCl_4 treatment compared to wild type animals and CB_2 receptor inhibition leads to a decrease in cell death and an increase in proliferation of myofibroblasts (Julien et al., 2005). These findings indicate for opposing effects of CB_1 and CB_2 receptors in the liver. Whereas the CB_1 receptor displays pro-fibrogenic, the CB_2 receptor shows anti-fibrogenic properties. This was also confirmed by a study recently published: Trebicka and colleagues could show that steatosis and fibrogenesis are increased in mice lacking the CB_2 receptor and decreased in CB_1 knockout mice (Trebicka et al. 2011). The effects reported here are mediated by cannabinoid receptors expressed on myofibroblasts, but it is important to keep in mind that the CB_1 receptor is also found on endothelial cells and hepatocytes (Julien et al., 2005) (Siegmund et al., 2005b; Teixeira-Clerc et al., 2006). Moreover, CB_2 receptors are primarily found on macrophages such as liver resident Kupffer cells. Thus, CB_2-mediated anti-fibrogenic effects may be a result of its anti-inflammatory actions like suppression of pro-inflammatory factors or the increased production of anti-inflammatory mediators (Figure 4). Interestingly, daily cannabis use was found to accelerate fibrogenesis in patients with hepatitis C. Apparently, pro-

fibrogenic CB_1-mediated signals dominate over the anti-fibrotic actions of CB_2 receptors (Hezode et al., 2005).

Anandamide levels are increased in several disorders such as fatty liver, acute hepatitis or cirrhosis (Biswas et al., 2003; Osei-Hyiaman et al., 2005). Moreover, 2-AG levels are strongly upregulated after hepatic damage in two well-established mouse models of liver fibrogenesis, bile duct ligation and CCL_4 treatment (Siegmund et al., 2007). It is known that lipopolysaccharide (LPS) increases AEA levels in macrophages (Liu et al., 2003). In hepatic fibrosis an elevated level of LPS has been also shown suggesting that LPS can trigger endocannabinoid levels in the liver (Schwabe, Seki, & Brenner, 2006).

The upregulation of AEA was not due an increase in the synthesis pathway but rather by a decline in the expression of the endocannabinoid-degrading enzyme FAAH. FAAH is highly expressed in the parenchymal cells of the liver giving hepatocytes a crucial role in limiting endocannabinoid levels under pathological conditions (Siegmund et al., 2006). Whether the increased 2-AG amounts are caused by an increase in the production or by a decline in the degradation of 2-AG remains to be elucidated.

Recent studies have shown that the regulation of cell death and proliferation of profibrogenic cells are one aspect of the role of endocannabinoids in fibrogenesis. HSCs are highly sensitive to cell death induction by exo- and endocannabinoids. The exogenous cannabinoid THC showed cytotoxic effects towards human hepatic stellate cells in a CB_2 receptor-dependent manner (Julien et al., 2005).

In a primary cell culture model, it was shown that AEA and 2-AG are able to induce necrotic and apoptotic cell death in HSCs, respectively (Figure 4). The endocannabinoid-induced cell death requires membrane cholesterol and is mediated by an increase of reactive oxygen species (ROS). However, 2-AG as well as AEA induces cell death in a receptor-independent way. Hepatocytes are completely resistant to endocannabinoid-mediated cell death (Figure 4). It is believed that less amounts of membrane cholesterol and high expression of the endocannabinoid-degrading enzyme FAAH in hepatocytes are responsible for the different susceptibility of these cell types (Siegmund et al., 2005b) (Siegmund et al., 2007).

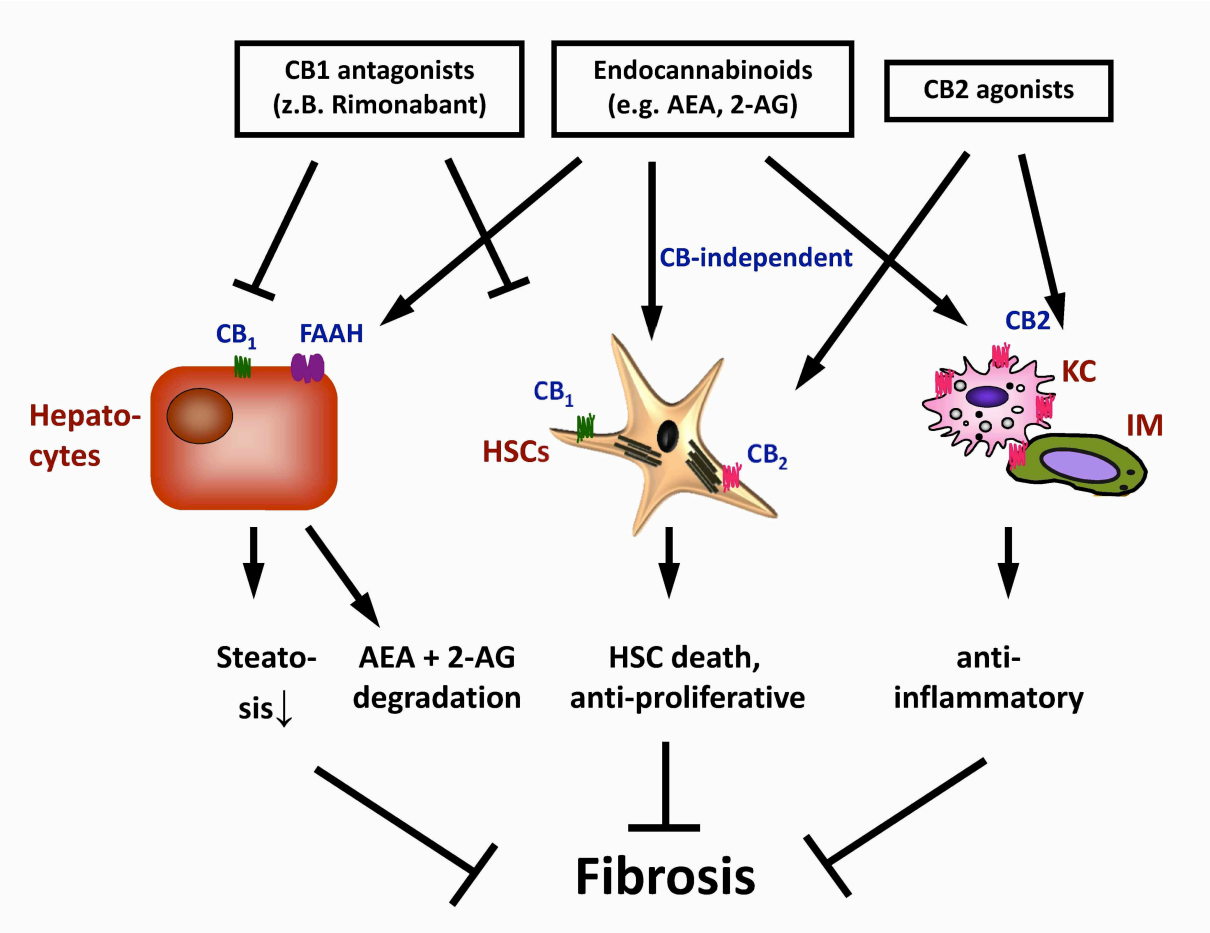

Figure 4. Proposed function of the hepatic endocannabinoid system during fibrogenesis. Antagonists of the endocannabinoid receptor CB_1 such as rimonabant have anti-fibrotic properties by inhibiting CB_1 mediated proliferation of HSCs. Moreover, by blocking CB_1 receptors on hepatocytes, hepatic steatosis by high fat diet is declined. Endocannabinoids like 2-AG and AEA induce cell death in HSCs in a receptor-independent way. Hepatocytes express the endocannabinoid-degrading enzyme FAAH, which leads to resistance to endocannabinoid-induced cell death. CB_2 receptors are expressed on HSCs and inflammatory cells and activation of these receptors suppress the secretion of proinflammatory mediators and thus inhibit fibrogenesis (modified according to Siegmund et al., 2008).

In the last few years it became more and more clear that modulation of the ECS might be utilised for the treatment of fibrosis. CB_1 antagonism showed to have beneficial effects on hepatic steatosis (Despres, Golay, & Sjostrom, 2005; Osei-Hyiaman et al., 2005). Moreover, the anti-inflammatory effects of CB_2 could be exploited by its activation with specific agonist. The possibility of endocannabinoids like 2-AG to induce specifically cell death in HSCs displays potential as antifibrotic mediators (Figure 4).

1.5 Aim of this thesis

The purpose of this study was the investigation of the endocannabinoid system in the injured and fibrotic liver. The effects of the recently identified endocannabinoids noladin ether, virodhamine and NADA are investigated on hepatic cell populations.

To reach this aim, HSCs and hepatocytes were isolated from healthy and injured livers of wild type and different knockout animals. Cell death induced by NADA is analysed in detail by a combination of pharmacological and genetic approaches. These results may be relevant for the design of antifibrotic therapies.

Moreover, cellular origin and mechanisms that lead to increased hepatic 2-AG levels during fibrogenesis are determined. For this purpose, the expression of the synthesis as well as the degradation enzymes of 2-AG is examined in injured and healthy livers. Thus, modulation of the synthesis or the degradation pathways of 2-AG can be used to increase or decrease 2-AG levels in the liver.

A further aim is the investigation of the molecular pathway that underlie the different susceptibility of HSCs and hepatocytes toward 2-AG. A possible role for cyclooxygenase (COX)-2 that converts 2-AG to PG-GE is taken into account in 2-AG-induced cell death. The differential expression of COX-2 and the production of PG-GE is analysed in hepatocytes as well as in HSCs to further characterise 2-AG-induced cell death. This will achieve a better understanding of the role of 2-AG in the injured liver.

In conclusion, the understanding of the role of endocannabinoid-mediated pathways in liver injury allows it to target various components of this system to decrease fibrogenesis in the liver.

2 MATERIAL

2.1 Equipment

Centrifuges	Biofuge fresco, Heraeus Instruments
	Biofuge pico, Heraeus Instruments
	Biofuge stratos, Heraeus Instruments
	Sorvall Evolution RC, Kendro
Magnetic stirrer	MR 3001 K, Heidolph, Fisher
Microplate Analyzer	MRX TC II, Dynex Technologies
pH meter	inoLab, WTW
Spectral photometer	91-ND-1000 UV/Vis, Nanodrop
Sterilising oven	Varioklav 25T, H+P Labortechnik
Vortexer	Vortex-Genie 2, Scientific Industries
Electrophoresis gel chamber	XCellSureLock™, Invitrogen
Blotting chamber	Blot™, Invitrogen
Film processing machine	CP1000, AGFA
Perfusion pump	Pumpdrive5201, Heidolph
Microscope	Nikon Eclipse TS 100
Power supply	PowerEase 500, Invitrogen
Camera	AxioCam MRm, Zeiss
Laminar flow hood	HeraSafe®, Kendro
Cell culture incubator	Binder

2.2 Chemicals and reagents

If not noted otherwise, all reagents used in this work were purchased from Invitrogen, Carl Roth, Merck or Sigma-Aldrich.

2.3 Stimulants for cell culture

2-arachidonoyl glycerol (2-AG)	Cayman Chemicals
Noladin ether	Cayman Chemicals
Actinomycin D (Ac D)	Sigma-Aldrich
Anandamide (AEA)	Sigma-Aldrich
Arachidonic acid (AA)	Sigma-Aldrich
Caspase inhibitor (Z-VAD-FMK)	Promega
CB_1 antagonist AM251	Tocris

CB_2 antagonist SR144528 (SR2)	Sanofi
COMT inhibitor (OR-486)	Tocris
$_{DL}$-buthionine- (*S,R*)-sulfoximine (BSO)	Sigma-Aldrich
Dopamine	Sigma-Aldrich
FAAH inhibitor URB597	Cayman Chemicals
Gluthatione-ethylester (GSH-EE)	Sigma-Aldrich
Methyl-β-cyclodextrin (MCD)	Sigma-Aldrich
N-arachidonoyl dopamine (NADA)	Sigma-Aldrich
Noladin ether (NE)	Sigma-Aldrich
Prostaglandin D_2 glycerol ester (PGD_2-GE)	Sigma-Aldrich
Prostaglandin E_2 glycerol ester (PGE_2-GE)	Sigma-Aldrich
Prostaglandin $F_{2\alpha}$ glycerol ester (PGF_2-GE)	Sigma-Aldrich
Recombinant murine tumour necrosis factor (TNF) α	R&D Systems
TROLOX (6-hydroxy-2,5,7,8-tetramethylchromane-2-carbonacid)	Calbiochem
TRPV1 agonist Capsaicin	Cayman
TRPV1 antagonist capsazepine	Sigma-Aldrich
Virodhamine	Tocris

2.4 Enzymes for cell isolation

2.4.1 HSC isolation

Collagenase D	Roche
DNase I	Roche

2.4.2 Hepatocyte, KC, LSEC isolation

Collagenase CLSII	Biochrom

2.5 Antibodies

2.5.1 Primary antibodies

Antibody against	Source	Obtained from	Dilution
Caspase 3	rabbit	Cell Signaling	1:1000
Catechol-O-methyl transferase (COMT)	rabbit	Santa Cruz biotechnology	1:500

Cleaved Poly (ADP-ribose) polymerase (PARP)	rabbit	Cell Signaling	1:1000
Fatty acid amide hydrolase (FAAH)	rabbit	Cayman Chemical	1:250
Phosphorylated extracellular signal regulated kinase (pERK)	rabbit	Cell Signaling	1:1000
Tyrosine hydroxylase (TH)	rabbit	Cayman Chemical	1:250
α smooth muscle actin (α-SMA)	rabbit	Abcam	1:2000
β-actin	mouse	Sigma-Aldrich	1:10000

Table 1: List of primary antibodies.

2.5.2 Secondary antibodies

Antibody	**Obtained from**	**Dilution**
Anti-rabbit	Abcam	1:5000
Anti-mouse	Sigma Aldrich	1:10000

Table 2: List of secondary antibodies

All secondary antibodies used are linked to “horseradish-peroxidase” (HRP) for detection via ECL-reaction.

2.6 TaqMan assays

All oligonucleotides used in this work were synthesised and delivered by Applied Biosystems. The forward primer of each pair was labelled at the 5’ end with the fluorescent dye FAM or TAMRA.

mRNA to detect	**Assay ID**
18s rRNA	Normalization Standard
COX-2	Mm00478374_m1
DAGLα	Mm00813830_m1
DAGLβ	Mm00523381_m1
FAAH	Mm00515684_m1
MGL	Mm00449274_m1
α-SMA	Mm0072512_s1

Table 3: TaqMan assays

3 METHODS

3.1 Isolation of primary hepatic cells

The establishment of primary hepatic cell isolation and following cultivation was an important step for investigating the pivotal roles of different cell types in the healthy and injured liver.

3.1.1 Animals

C57BL/6 mice (Janvier) and male Sprague-Dawley rats (Charles River) were housed in a temperature-controlled environment with a 12 h light/dark cycle. They were fed with standard mice or rat chow, respectively, and water *ad libitum*. All experimental protocols of this study were performed in accordance with national animal care guidelines (Tierschutzgesetz Germany) and all procedures were approved by the local committees for animal studies (Regierungspräsidium Karlsruhe and Köln).

3.1.2 Solutions

All solutions were filtered trough a 0.22 μm bottle top filter and adjusted to pH 7.4.

10x stock solution	
NaCl	80 g/l
KCl	4 g/l
NaH_2PO_4. H_2O	0.882 g/l
Na_2HPO_4	1.2 g/l
HEPES	2.4 g/l
$NaHCO_3$	3.5 g/l

	EGTA solution	Enzyme solution
10x stock solution	100 ml/l	100 ml/l
EGTA	190 mg/l	-
Glucose	900 mg/l	-
$CaCl_2$. $2H_2O$	-	560 mg/l

	GBSS/A	GBSS/B
NaCl	-	8000 mg/l
KCl		370 mg/l
$MgCl_2$. $6H_2O$		210 mg/l
$MgSO_4$. $7H_2O$		70 mg/l
Na_2HPO_4		59.6 mg/l
KH_2PO_4		30 mg/l
Glucose		991 mg/l
$NaHCO_3$		227 mg/l
$CaCl_2$. $2H_2O$		225 mg/l

3.1.2.1 HSC-specific solutions

Pronase solution

40 mg pronase in 80 ml enzyme solution

Collagenase solution

36 mg collagenase in 120 ml enzyme solution

Pronase/collagenase solution

30 mg pronase, 30 mg collagenase and 10 mg DNase in 100 ml enzyme solution

Nycodenz stock solution

8 g Nycodenz in 27.5 ml of GBSS/A

3.1.2.2 Hepatocyte-specific solutions

Collagenase solution

45 mg collagenase in 120 ml enzyme solution

Percoll solution

50 % (v/v) Percoll in HBSS/B + 10 % FCS

3.1.2.3 Kupffer cell-specific solutions

Solution I

50 mg collagenase in 10 ml HBSS/B

Solution II

40 mg collagenase in 10 ml enzyme solution

Percoll solution 25 %

5 ml Percoll and 15 ml HBSS

Percoll solution 50 %

7.5 ml Percoll and 7.5 ml HBSS

MACS-buffer

PBS; 1 % FCS; 2 mM EDTA

3.1.2.4 LSECs-specific solutions

CA^{2+}deprived medium

L-aspartate	0.1 mM
L-threonine	0.2 mM
L-serine	0.3 mM
Glycine	0.5 mM
L-alanine	0.6 mM
L glutaminic acid	0.9 mM
L-glutamine	0.9 mM
KCl	3 mM
NaH_2PO_4	0.7 mM
$MgCl_2$	0.5 mM
$NaHCO_3$	24 mM
Glucose	20 mM
Fructose	197 mM

MACS-buffer

PBS; 1 % FCS; 2 mM EDTA

Collagenase solution

50 mg collagenase in 100 ml Ca^{2+} deprived medium

3.1.3 Anaesthetic

	rat	mouse
Hostaket (active ingredient: Ketaminhydrochloride)	100 mg/kg bw	100 mg/kg bw
Rompun (active ingredient: Xylazine)	10 mg/kg bw	6 mg/kg bw

The appropriate quantity of Hostaket and Rompun was dissolved in 0.9 % sterile NaCl solution and administered by intraperitoneal (IP) injection.

3.1.4 Isolation of primary murine hepatic stellate cells

The isolation of hepatic stellate cells (HSCs) was conducted by *in situ* digestion followed by density gradient centrifugation which is based on the specific density of vitamin A rich HSCs (Friedman & Roll, 1987; Friedman, Roll, Boyles, & Bissell, 1985; Knook, Seffelaar, & de Leeuw, 1982). This method required high vitamin A content. Since it is known that the size

and also the number of lipid droplets storing vitamin A increase with age, mice older than 240 days were used.

After anaesthetising by IP injection, the mouse was fixed on a Styrofoam platform with the abdomen facing up. The abdominal cavity was opened, the intestines moved to the right and a 27-gauge butterfly needle was inserted into the portal vein. Immediately after, the posterior vena cava above was cut.

Three different perfusion steps, which were performed with a flow-rate of 4.9 ml/min, are necessary to release the HSCs from liver tissue. After rinsing with EGTA solution for 3 min to get rid of blood cells residing in the liver sinusoids and to open the desmosomes of the cell-cell complexes, the liver was perfused first with pronase and afterwards with collagenase solution for approximately 2 and 4 min, respectively. During these steps the liver blanched and the dark red colour changed into a yellow-cream colour. The enzyme-treated liver was excised and kept on ice until livers of three to four animals were obtained. Subsequently, the livers were minced in collagenase/pronase solution in the laminar flow hood and incubated for 5 to 10 min at 37 °C under constant stirring. The resulting suspension was filtered through a nylon mesh (150 μm in diameter) into four 50 ml tubes and centrifuged for 7 min at 500 x g at 4 °C. While stepwise reducing the number of centrifugation tubes by one, the sedimented cells were washed twice with GBSS/B + 1 % FCS. The final pellet was resuspended in 34 ml GBSS/B + 10 % FCS and 13.5 ml of the Nycodenz stock solution were added (final concentration: 8.2 %). After centrifugation for 24 min at 1400 x g at 4 °C without break a whitish stellate cell-enriched fraction was obtained, collected, washed with medium, centrifuged at 500 x g for 7 min at 4 °C and resuspended in plating medium.

Isolated HSCs showed 95 % purity as determined by vitamin A fluorescence two days after isolation. The cells were activated on uncoated plastic tissue culture dishes and were used on day 7 after isolation without any passaging.

3.1.5 Isolation of primary rat hepatic stellate cells

After anaesthetising by IP injection, the rat was fixed on a Styrofoam platform. The abdominal cavity was opened and an 18-gauge butterfly needle was inserted to the portal vein. Further procedures were performed as described in section 3.1.4. The perfusion rate was 15 ml/min and the perfusion times of the three different perfusion steps were three times longer than for primary mouse HSCs.

3.1.6 Isolation of primary murine hepatocytes

The isolation of primary murine hepatocytes was first described by Howard et al. 1967 and improved by Seglen et al. in 1976 (Howard, Christensen, Gibbs, & Pesch, 1967; Seglen, 1976). Anaesthesia, fixation and insertion of the needle were performed as described in section 3.1.4. Isolation of the parenchymal cells of the liver is based on a two-step perfusion

process that includes rinsing with EGTA solution followed by perfusion with collagenase solution both at a flow rate of 8 ml/min for 5 and 10 min, respectively. Subsequently, the liver was excised carefully and placed on a petri dish. After mincing the liver in 40 ml GBSS/B + 10 % FCS, the cell suspension was filtered through a 150 μm gauze into a 50 ml tube. The hepatocyte suspension was centrifuged at 28 x g for 5 min. After repeating this washing step, the pellet was resuspended in Percoll solution and centrifuged at 50 x g for 10 min at 4 °C. Subsequently, the viable cells pelleted and the nonviable cells floated to the top. The cell pellet was washed with medium at 28 x g for 5 min at 4 °C and resuspended in hepatocyte plating medium.

3.1.7 Isolation of primary rat hepatocytes

Isolation of primary rat hepatocytes was conducted as described in section 3.1.6. The rat cell isolation requires a perfusion rate of 15 ml/min and the perfusion times for the EGTA- and collagenase solutions for primary rat hepatocytes were 10 and 30 min, respectively.

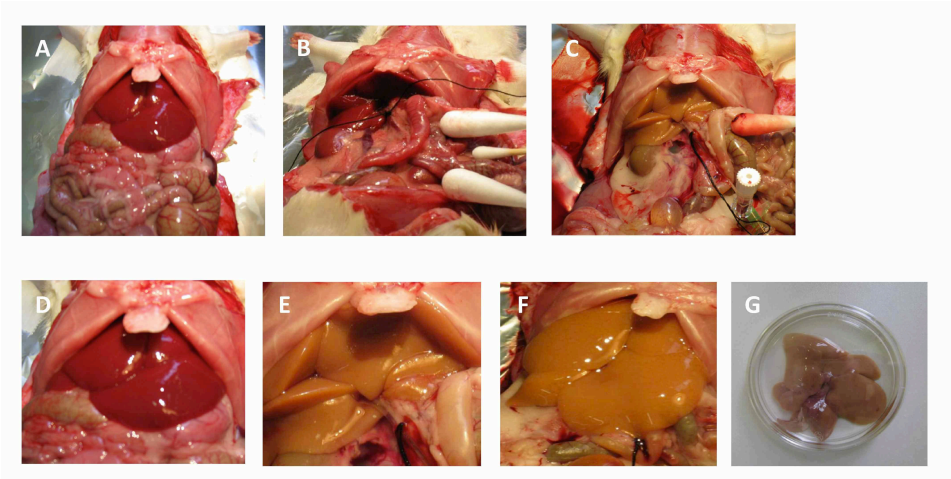

Figure 5. Isolation of primary hepatic cells by *in situ* perfusion. After fixation of the animal, the abdominal wall is cut in a longitudinal line (A) and the intestines are gently moved to the side (B). A cannula is inserted in the portal vein and fixed with a threat silk (C). During the perfusion, the liver blanched from the typical dark red (D) into a yellowish colour (E). The cell-cell contacts are destroyed by perfusion with enzymes. Thus, the liver becomes spongy and achieved a bigger volume (F). After the perfusion, the liver is transferred into a 10 cm dish (G).

3.1.8 Isolation of primary murine Kupffer cells

After sacrificing the mouse by cervical dislocation, the animal was fixated and the perfusion was conducted as described in section 3.1.4. Thereafter, the perfusion of solution I was performed at a perfusion rate of 4 ml/min for 30 sec. Subsequently, the liver was excised and transferred to a 50 ml tube containing solution II until 3 livers were obtained. The liver cells were dissociated mechanically in solution II in a laminar flow hood, transferred in a 50 ml tube and incubated for 17 min under constant shaking with a speed of 250 rpm. Afterwards,

the suspension was passed through a filter (250 μm in diameter), 40 ml HBSS/B were added and centrifuged at 50 x g for 2 min at 4 °C. The supernatant was collected, centrifuged at 800 x g for 10 min at 4 °C and the resulting pellet was washed by repeating the centrifugation step after adding 40 ml HBSS/B. The cells were resuspendend in 10 ml PBS, layered on the top of a two-step Percoll gradient (25 % vs. 50 %, 15 and 20 ml, respectively) and centrifuged at 1350 x g for 30 min at 4 °C. The interface between the upper and the lower cushion was collected, washed with MACS-buffer and centrifuged at 800 x g for 10 min at 4 °C. Subsequently, the cells were counted, labelled with CD11b microbeads (10 µl beads/ 1 x 10^7 total cells) and incubated for 20 min at 4 °C. After centrifugation at 300 g for 10 min, the cells were resuspended in MACS buffer (up to 1 x 10^8 cells/ml) and filtered through a nylon mesh (30 µm in diameter). Afterwards, the cells were sorted magnetically by autoMACS. The MACS sorting was performed by Frank A. Schildberg, Institute of Molecular Medicine and Experimental Immunology, University of Bonn.

3.1.9 Isolation of primary murine liver sinusoidal endothelial cells (LSECs)

Frank A. Schildberg, Institute of Molecular Medicine and Experimental Immunology, carried out the isolation of primary murine LSECs.

After sacrificing the mice by cervical dislocation, fixation and preparation of the animal as described in section 3.1.4, the liver was perfused with the collagenase solution at a perfusion rate of 4 ml/min until up to 10 livers were obtained. The livers were minced well in a laminar flow hood and the resulting suspension was incubated in a rotary water bath at 240 rpm for 20 min at 4 °C. After shaking, the suspension was passed through a filter (mesh size 250 µm in diameter) and washed twice with HBSS/B (300 x g for 10 min at room temperature). Subsequently, the pellet was resuspended in 16.5 % Nycodenz, overlaid carefully with 1 ml HBSS/B and centrifuged at 1400 x g for 20 min at 20 °C without brake. The LSECs were recovered from the top layer and washed once with MACS buffer (300 x g for 10 min). Afterwards, the cells were counted and labelled with anti-LSEC-beads (10 µl beads/ 1 x 10^7 total cells). The next steps were conducted as described previously in section 3.1.8.

3.2 Animal models for liver fibrosis

3.2.1 Carbon tetrachloride- (CCL_4-) induced liver injury

Liver damage was induced in male C57BL/6 mice (n=4) by CCL_4 inhalation three times per week over five weeks. The administration was conducted as follows:

Week	Time span	Cycle number
1	1 min	1
2	1.5 min	1
3	2 min	1
4	2 min	2
5	2 min	2

Moreover, the animals received phenobarbital (Luminol; 0.5 g/l) orally supplemented to the drinking water. This led to an increase of CCl_4-toxicity resulting in accelerated development of liver injury. After the experimental period, the animals were sacrificed and the liver was excised for protein isolation. The experimental procedure for CCl_4-intoxication was conducted by Dr. Jonel Trebicka, Department of Medicine I, University Hospital Bonn.

3.2.2 Bile duct ligation in mice

While anesthetising the animal with isoflurane via inhalation, the abdomen was opened by a midline incision under sterile conditions. The bile duct was carefully isolated, ligated twice and cut between the ligatures. Sham operated animals without ligation of the bile duct served as controls. The abdominal musculature and the skin incision were closed with absorbable suture. Mice were treated with a subcutaneous dose of carprofen® before and after surgery for analgesia. Seven or 14 days after surgery the mice were sacrificed by cervical dislocation and the livers were excised for protein and RNA isolation.

3.3 Cell culture methods

All procedures with cells were performed under sterile conditions in a laminar flow hood.

3.3.1 Cell counting

Cell concentrations were determined with a Neubauer counting chamber. The cell suspension was diluted and –after adding trypan blue to a final concentration of 0.1 % to distinguish viable from non-viable cells- introduced to the chamber. Each large square consists of 9 small squares and has a surface area of 1 mm^2 and a depth of 0.1 mm, which gives a defined volume of 0.1 mm^3. The following calculation gives the cell number per ml:

$$\text{Cells/ml} = \text{average count/square} \times \text{dilution factor} \times 10^4$$

3.3.2 Culturing of primary hepatic cells

Cells were incubated in a humidified incubator at 37 °C in an atmosphere of 5 % CO_2/air.

3.3.2.1 Coating of plastic tissue culture dishes

The rat-tail collagen type I was used at a 1:50 dilution in 1 % acetic acid. The surface of the required cell tissue culture plates were covered with the collagen solution and incubated for 30 min at room temperature under constant shaking. After washing the plates three times with HBSS/B, the dishes were ready to use or were stored up to four weeks at 4 °C.

3.3.2.2 Culturing of primary HSCs

After isolation, cells were cultured on plastic culture dishes in DMEM supplemented with 10 % FCS and 1 % penicillin/streptomycin as previously described (Bataller et al., 1997). The medium was replaced every 48 h.

3.3.2.3 Culturing of primary hepatocytes

Plating medium	Stimulation medium
Waymouth medium	RPMI medium
10 % FCS	-
1 % penicillin/streptomycin	1 % penicillin/streptomycin
1 % glutamine	1 % glutamine
1 mM insulin	1.5 mM insulin
100 μM dexamethason	1 % transferrin/selenium mix

Cells were cultured on plastic tissue culture dishes with rat-tail collagen (see 3.2.2.1) in plating medium for 4 h. Afterwards, the cells were washed three times with HBSS/B and incubated in stimulation medium over night.

3.3.2.4 Culturing of primary KCs

Cells were cultured on plastic culture dishes with rat-tail collagen (see 3.2.21) in DMEM supplemented with 10 % FCS and 1 % penicillin/streptomycin. The cells were used latest 48 h after plating.

3.3.2.5 Culturing of primary LSECs

Cells were cultured on coated plastic culture dishes (see 3.2.2.1) in DMEM with 10 % FCS, 2 % glutamine and 1 % penicillin/streptomycin.

3.3.3 Stimulation experiments

Cells were serum-starved with DMEM containing 0.5 % FCS over night and were treated with the appropriate substance for stimulation or with vehicle.

3.3.4 Adenoviral infection procedures

3.3.4.1 Adenoviral construction

The adenoviruses used were a gift from Schwabe, Columbia University, NY, USA and were constructed as previously described in Siegmund et al. 2006. Mouse fatty acid amide hydrolase (FAAH) was excised from a pcDNA 3.0 and inserted into an AdTrack vector via XbaI and KpnI sites. After linearizing the vector using PmeI, the AdTrack was electroporated into competent BJ 5183-AD1 bacteria, which contain AdEasy1 (Stratagene, La Jolla, CA). The recombinants were linearized using PacI and transfected into HEK293 cells. Subsequent lysing the cells 10 day later, new HEK293 were infected and these lysates were purified on a CsCl density gradient (Siegmund et al., 2006).

3.3.4.2 Adenoviral amplification

For amplification of the viruses, HEK293 cells were infected and incubated until the cytopathic effect was complete (3-5 days). After harvesting, the cells were centrifuged at 500 x g for 7 min at 4 °C. The resulting pellet was frozen and thawed five times and subsequently resuspended in DMEM.

3.3.4.3 Adenoviral infection

Primary HSCs were infected with the FAAH expressing adenovirus AdFAAH or the AdTrack-based green fluorescent protein (GFP)-expressing control adenovirus Ad5GFP at a multiplicity of infection of 50, achieving transduction rates of at least 90 %. After 12 h, the medium was exchanged and stimulated with either NADA or AEA 24 h later.

3.3.5 Detection of reactive oxygen species (ROS) by CM-H_2DCFDA fluorescence

CM-H_2DCFDA is a cell-permeant indicator for reactive oxygen species (ROS), which is nonfluorescent until removal of the acetate groups by oxidation within the cell. After diluting CM-H_2DCFDA with DMSO, the dye was used at a final working concentration of 6 μM. After adding to the medium, the cells were incubated at 37 °C for 30 min and washed with PBS to avoid artificial stainings. Following stimulation with the substance of interest, the fluorescent signal was immediately measured in an ELISA plate reader at a wavelength of 492 nm at different time points.

3.3.6 Wound healing assay

HSCs were cultured to confluence (> 90 %) in 6-well plates. After starvation with DMEM containing 0.5 % FCS for 12 h, a 2-mm-wide linear wound in the cell monolayer was created using a white pipette tip. Cells were treated daily with sublethal concentrations of NADA or vehicle only. Cell migration into the wound was detected using a phase-contrast microscope at day 0, 4 and 6.

3.3.7 Detection of cell death

3.3.7.1 Lactate dehydrogenase (LDH) assay

The lactate dehydrogenase (LDH) assay (Cytotoxicity Detection Kit, Roche Apllied Science) is a colorimetric assay for the quantification of cell death based on the measurements of lactate dehydrogenase (LDH) released from the cytosol of damaged cells in the supernatant.
Cells were serum-starved over night and treated with the substrate of interest or vehicle. After collecting the culture medium at different timepoints, 50 µl of the supernatant were transferred into a 96-well plate in triplicates and incubated with 50 µl of the reaction solution (prepared according to the manufacturer's instructions) for 30 min at room temperature.
To calculate the percentage of cytotoxicity, the following three control reactions had to be performed in each experimental setup: The background control (1), which contains only medium, the low control (2), the supernatant of untreated cells reflecting the spontaneous LDH release, and the high control (3) giving the maximum LDH release. The measurement was conducted at a wavelength of 490 nm in an ELISA plate reader followed by calculation of percentage of cell death:

$$\text{cytotoxicity (\%)} = 100 / (\text{high control} - \text{low control}) \times (\text{sample} - \text{low control})$$

3.3.7.2 Annexin V/propidium iodide staining

The principle of the annexin V/propidium iodide staining assay (Annexin-V-FLUOS staining Kit, Roche Applied Science) is the analysis of phosphatidylserine, which is translocated in apoptotic cells from the inner part of the plasma membrane to the outer layer, by Annexin V staining. Propidium iodide (PI) stains the DNA of leaky necrotic cells that allows the differentiation of apoptotic and necrotic cell death.
For this assay, the cells were washed first with PBS and afterwards incubated with Annexin V-Fluorescein in a HEPES buffer containing PI according to the manufacturer's protocol. The cells were analysed under a fluorescence microscope.

3.3.8 Detection of PGD_2-GE

The assay is based on the conversion of the chemically unstable prostaglandin D_2 (PGD_2) to a stable MOX derivative (Prostaglandin D_2-MOX EIA Kit, Cayman Chemicals). Hepatocytes and HSCs were plated in 24-well plates and treated with 50 µM 2-AG or vehicle for 12 h. The prostaglandin glycerol ester D_2 (PGD_2-GE) concentration was measured by PGD_2-MOX EIA (Cayman Chemical) Kit according to the manufacturer's protocol with reference to a PGD_2-MOX EIA standard provided by the manufacturer. This kit is unable to distinguish between PGs and PG-GEs and therefore PGD_2 and PGD_2-GE were quantified without distinguishing prostaglandins from their glycerol ester derivative.

3.4 Biomolecular methods

3.4.1 RNA isolation

RNA was isolated from cultured cells or frozen liver tissue. The tissue or the cells were homogenised in Trizol (100mg tissue/1 ml Trizol or 10 cm^2 cell-tissue layer/ 1ml Trizol, respectively). After centrifugation for 10 min at 12,000 x g at 4 °C, 50 µl BCP were added to 500 µl supernatant, vortexed for 60 sec and incubated at room temperature for 3 min. The centrifugation step was repeated and after subsequent transfer of the aqueous phase to a fresh tube, 250 µl isopropanol were added. The mix was shortly vortexed, incubated at room temperature for 10 min and centrifuged again under the same conditions. The resulting RNA pellet was washed once with 1 ml 75 % ethanol (12,000 x g; 10 min; 4 °C) and after discarding the supernatant, the dry RNA pellet of cell- or tissue-isolation was dissolved in 30 or 100 µl DEPC water, respectively. After incubation for 15 min at 55-60 °C the RNA concentration was determined.

3.4.2 Determination of RNA concentration

The concentration of RNA was determined by measuring the absorbance at 260 nm (A_{260}) in a spectrophotometer. An absorbance of 1 unit at 260 nm corresponds to 40 µg of RNA per ml (A_{260} = 1 ⇒ 40 µg). The ratio of the readings at 260 nm and 280 nm (A_{260}/A_{280}) provides an estimate of the purity of RNA regarding contaminants that absorb in the UV, such as protein. Pure RNA has an A_{260}/A_{280} ratio of 1.8 to 2.0.

3.4.3 Reverse transcriptase polymerase chain reaction (RT-PCR)

The reverse transcriptase polymerase chain reaction (RT-PCR) is a method used to amplify cDNA copies of RNA.

For each reaction, 2.5 µg RNA were used and the master mix was prepared for each reaction as follows:

0.1 M DTT	2 µl
5x first strand buffer (Invitrogen)	4 µl
H_2O	1 µl
dNTPs (10 mM each)	1 µl
Final volume/sample	8 µl

After adding water to the RNA up to 8 µl, 1 µl oligo(dT) solution was added and cDNA synthesis was conducted as follows:

70 °C	10 min
4 °C	3 min
add 8 µl of master mix	
42 °C	2 min
4 °C	3 min
add 1 µl of reverse transcriptase	
42 °C	60 min
70 °C	15 min
4 °C	10 min

The reaction mix was filled up with water to a final volume of 100 µl.

3.4.4 Real-time reverse transcription-PCR (real-time RT-PCR) using TaqMan Gene expression assays

The real-time RT-PCR is used to quantify the expression of a gene of interest. The TaqMan method uses an oligonucleotide, which is labelled at the 5´ end with a fluorescent group (FAM or VIC) and at the 3´ end by a quenching group (TAMRA or MGB). Primers for the targeted sequence and the oligonucleotides are added to the PCR. When the quenching and the fluorescent group are close together, the TAMRA or MGB absorb the emission of the FAM or VIC dye, respectively, and the fluorescence signal is low. During the PCR, the 5´⇒3´exonuclease activity of the polymerase cleaves the fluorescent part from the oligonucleotide and the signal can be detected. The amount of DNA that is synthesized is proportional to the intensity of the fluorescence detected (Russel, 2001).

5 µl 2x TaqMan gene expression master mix and 0.5 µl 20x TaqMan assay were mixed together with 2.5 µl Rnase/DNase free water and 2 µl cDNA sample were added in a 384well plate.

Quantitative RT-PCR was conducted as follows:

95 °C	10 sec	1x
95 °C	15 sec	40x
60 °C	60 sec	

3.5 Biochemical methods

3.5.1 Protein isolation

3.5.1.1 Lysis buffer

Karnovsky lysis buffer

10 mM Tris
50 mM NaCl
50 mM EDTA
30 mM $Na_4P_2O_7$

Adjusted pH to 7.5

0.5% Triton-X-100

Immediately before use protease inhibitor tablets (1 tablet/10 ml lysis buffer, complete Mini, Roche) were added to the lysis buffer.

3.5.1.2 Protein isolation out of tissue

Freshly removed ore thawed liver tissue were first suspended in three volumes of Karnovsky buffer. The homogenisation was carried out at 0 °C with a plastic homogenizer by up and down movement until removal of all big tissue pieces. A sonification treatment was performed six times of 10 seconds. After a centrifugation step for 10 min at 4 °C at 12,000 g, the protein concentration of the sample was determined.

3.5.1.3 Protein isolation out of cell culture

After removing the medium, Karnovsky buffer was added to the wells (100 µl/ 6-well) and the cells were scraped by pipetting up and down with a 1 ml pipette tip. After transferring into an Eppendorf reaction tube, the cell suspension was sonified 6 times for 5 seconds. After centrifugation for 10 min at 4 °C at 12,000 x g, the protein concentration of the sample was determined.

3.5.2 Determination of protein concentration by BCA Protein Assay Kit (Pierce)

The BCA Protein Assay Kit is a method for colorimetric detection of total protein based on bicinchoninic acid (BCA). Protein concentrations are determined with reference to the standard of bovine serum albumin (BSA) standard. The determination of protein concentration was conducted according to the manufacturers protocol and measured at a wavelength of 592 nm.

3.5.3 Sample preparation for western blotting

The samples were suspended with 6x SDS sample buffer and heated at 95 °C for 10 min to ensure protein denaturation.

6x SDS sample buffer	200 mM 1.5 M Tris-HCl pH 6.8
	8 % SDS
	40 % glycerol
	0.4 % bromphenol blue
	400 mM 1 M DTT

Afterwards, the samples were ready for Sodium dodecyl sulphate-polyacrylamide gel electrophoresis (SDS-PAGE).

3.5.4 Sodium dodecyl sulphate-polyacrylamide gel electrophoresis

Sodium dodecyl sulphate-polyacrylamide gel electrophoresis (SDS-PAGE) is a method that allows the separation of the protein samples of interest. The proteins are electrophoretically separated based on their weight. The electrophoresis was conducted at 200 Volt for 40 min in running buffer (NuPAGE SDS Running Buffer 20x, Invitrogen). NuPAGE 4-12 % Bis-Tris gels (Invitrogen) were used. The molecular weight marker Novex® Sharp Standard (Invitrogen) was used for the confirming of protein transfer and the molecular weight orientation.

3.5.5 Western blot

In a western blot, the separated sample proteins are electrophoretically transferred from a polyacrylamide gel onto a nitrocellulose membrane and the subsequent immuno-detection of the protein of interest.

3.5.5.1 Wet blotting

Proteins separated by SDS-PAGE were transferred from the gel to a nitrocellulose membrane (Whatman) using a “wet” electrophoretic transfer system in transfer buffer (NuPAGE transfer buffer 20x, Invitrogen with 10 % methanol/gel). After SDS-PAGE, the gel

and the membrane were saturated with transfer buffer and sandwiched between saturated filter paper pads and plastic plates as follows:

2 x Blotting Pad
Filter Paper
Transfer Membrane
Gel
Filter Paper
Blotting Pad
Filter Paper
Transfer Membrane
Gel
Filter Paper
2 x Blotting Pad

The transfer was performed in a blotting tank (Invitrogen) for 1 h at 30 Volt constant with an expected current start of 170 mA and an ending current of 110 mA.

3.5.5.2 iBlot® Gel Transfer Stacks

The Western blot using the iBlot® Gel Transfer Stacks (Invitrogen) was conducted according to the manufacturer's instructions.

3.5.5.3 Detection

For the detection of the proteins of interest, following solutions have to be prepared:

10x PBS (phosphate-buffered saline)	10 mM Na_2HPO_4
	2 mM KH_2PO_4
	137 mM NaCl
	2.7 mM KCl
	Adjusted to pH 7.4 (hydrochloride acid)
PBST (phosphate-buffered saline Tween20)	100 ml/l 10xPBS
	0.05 % Tween 20
Blocking solution	PBST
	5 % milk powder

After western blot transfer of the proteins to the nitrocellulose membrane, the membrane was blocked for 1 h in blocking solution at room temperature. The primary antibody was diluted in

blocking solution to the appropriate concentration and the blot was incubated over night at 4 °C. The membrane was then washed three times with PBST for 10 min. Incubation of the blot with the secondary antibody that was conjugated to horseradish peroxidase was carried out for 1-2 h at room temperature. The membrane was washed again for three times 10 min with PBST prior to detection.

For this purpose, the membrane was incubated with ECL western blotting substrate (Pierce) for 1 min and the chemiluminiscent signal was visualized by exposure of Hyperfilm ECL films.

Where indicated, the intensities of the detected bands were evaluated densitometrically using ImageJ (NIH, Bethesda, MD).

3.5.6 Reprobing of western blot membranes

Prior to reprobing the membrane with different antibodies, the previous antibody had to be removed. Therefore, the membrane was incubated twice in stripping buffer on a horizontal shaker for 30 min at room temperature and washed with PBST (three times for 5 min). After blocking the blot for 1 h with blocking solution, a new primary antibody could be applied as described.

Stripping buffer	0.2 M glycine
	0.1 % SDS (w/v)
	1 % Tween 20 (v/v)
	pH to 2.4

3.6 Statistical analysis

All data represent the mean of three independent experiments ± standard error of the mean (SEM), if not otherwise stated. For the determination of statistical significance, unpaired Student's t-test was performed using GraphPad Prism (Version 4.0, GraphPad Software, Inc.). P values of <0.05 (*) were considered to be statistically significant, values of < 0.001 (**) were considered to be statistically highly significant.

4 RESULTS

4.1 Isolation of hepatic stellate cells

Primary hepatic stellate cells (HSCs) undergo activation on uncoated plastic culture dishes, which is similar to the response of these cells to hepatic injury *in vivo.* Thus, isolation of primary HSCs represents an excellent *in vitro* model to study the role of those cells during hepatic fibrosis (Friedman, Roll, Boyles, Arenson, & Bissell, 1989). The isolation was initially conducted in rats due to the bigger size of the animals and thus to a higher number of cells. The need of using knockout mice with a deletion of a specific gene required the isolation murine primary stellate cells.

4.1.1 Primary hepatic stellate cells activate on uncoated plastic culture dishes

Before starting the experiments, the purity and also the activation state of the isolated primary hepatic stellate cells was determined. After plating the cells on uncoated plastic culture dishes, the cells became adherent within the first six hours (Figure 6A). On the first two days, the cells contained a high amount of vitamin A droplets, a characteristic phenotypical feature of unactivated HSCs (Figure 6B). These lipid droplets exhibit a rapidly fading blue-green autofluorescence under UV-light (330 nm), which is also used to examine the purity of the isolated HSCs (Friedman, 2008b). The purity of HSC preparations was over 90 %, which was estimated by autofluorescence on day 2 after isolation (Figure 6 B). Starting from day two, the stellate cells underwent a transformation and developed a star-like shape. The cell density increased compared to day one since the cells started to proliferate (Figure 6A).

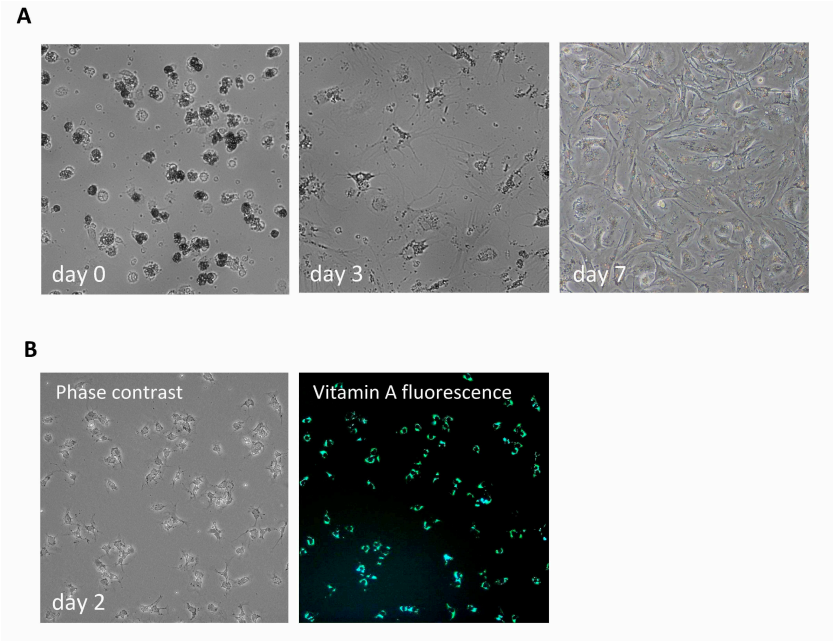

Figure 6. (A) Phase contrast images of HSCs were taken at the indicated time points after isolation. (B) Vitamin A autofluorescence of the lipid droplets of HSCs two days after isolation was visualised under UV light at a wavelength of 330 nm.

In addition, typical for myofibroblasts, the cells expressed α smooth muscle actin (α-SMA) on day 7, which was not observed in freshly isolated cells. Due to its absence in other resident cells in the liver, expression of α-SMA represents a reliable marker of stellate cell activation (Schmitt-Graff, Kruger, Bochard, Gabbiani, & Denk, 1991; Serini & Gabbiani, 1999). The expression of α-SMA was analysed on mRNA level by quantitative RT-PCR (Figure 7A) and on protein level by western blotting (Figure 7B).

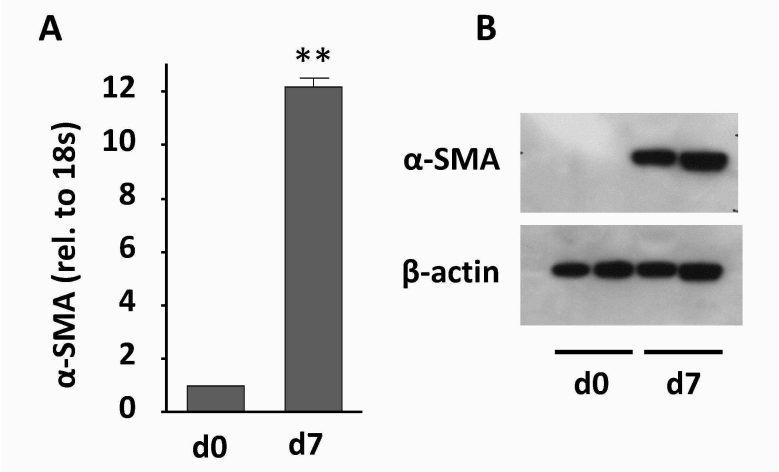

Figure 7. (A) Relative gene expression levels of α-SMA from freshly isolated murine hepatic stellate cells (d0) and from cells seven days after isolation (d7) were examined by quantitative RT PCR. Shown is fold of expression of d0 after normalization to 18s. **p<0.001 vs. d0. (B) α-SMA protein levels were determined by western blotting with antibodies against α-SMA and β-actin.

4.2 Investigation of the effects of noladin ether, virodhamine and NADA on liver cells

It was previously shown that the endogenous cannabinoid AEA blocks proliferation and induces cell death in hepatic stellate cells but not in hepatocytes. However, the effects of other endocannabinoids such as virodhamine (Viro), noladin ether (NE) and N-arachidonoyl dopamine (NADA) on hepatic stellate cells have not been investigated so far.

4.2.1 Virodhamine, noladin ether and N-arachidonoyl dopamine induce cell death specifically in HSCs but not in hepatocytes

Since HSCs are the predominant cellular target of endocannabinoids (ECs) in the injured liver (Julien et al., 2005; Siegmund et al., 2007; Siegmund et al., 2005b; Teixeira-Clerc et al., 2006), the potential antifibrotic effects of noladin ether (NE), virodhamine (Viro), N-arachidonoyl dopamine (NADA) on these cells were investigated.

NADA as well as the two other ECs rapidly and dose-dependently induced cell death in primary rat HSCs (Figure 8). After 2 h of stimulation, NADA significantly induced cell death in 34, 53 and 69 % of the cells at concentrations of 25, 50 and 100 μM, respectively. Moreover, HSCs underwent cell death starting at a concentration of 10 μM NADA after treatment of 4 h. Cell death reached a plateau level after 4 h at NADA concentrations of 50 μM and higher. HSCs treated with NADA concentrations lower than 10 μM did not undergo cell death (Figure 8A).

Similar results were also obtained when the cells were stimulated with virodhamine and noladin ether. Virodhamine showed strong cytotoxic effects starting at a concentration of 25 μM and the percentage of cell death maintained plateau levels at this concentration after 4 h of stimulation. Concentrations of 10 μM or lower showed no effects (Figure 8B). In contrast, noladin ether had a much stronger effect. After a stimulation time of 2 h, a concentration of 10 μM was sufficient to induce cell death in HSCs of 40 % compared to vehicle treated cells and after 4 h even 5 μM were adequate to reach cell toxicity of 53 % (Figure 8C).

To exclude possible effects of the endocannabinoids on parenchymal cells of the liver, primary hepatocytes were exposed to increasing concentrations of NADA, virodhamine and noladin ether for 16 h. In contrast to HSCs, primary hepatocytes showed no signs of cell death up to concentrations of 100 μM although the incubation time was four times longer (Figure 8). Taken together, NADA, virodhamine and noladin ether selectively induced cell death in HSCs but not in hepatocytes.

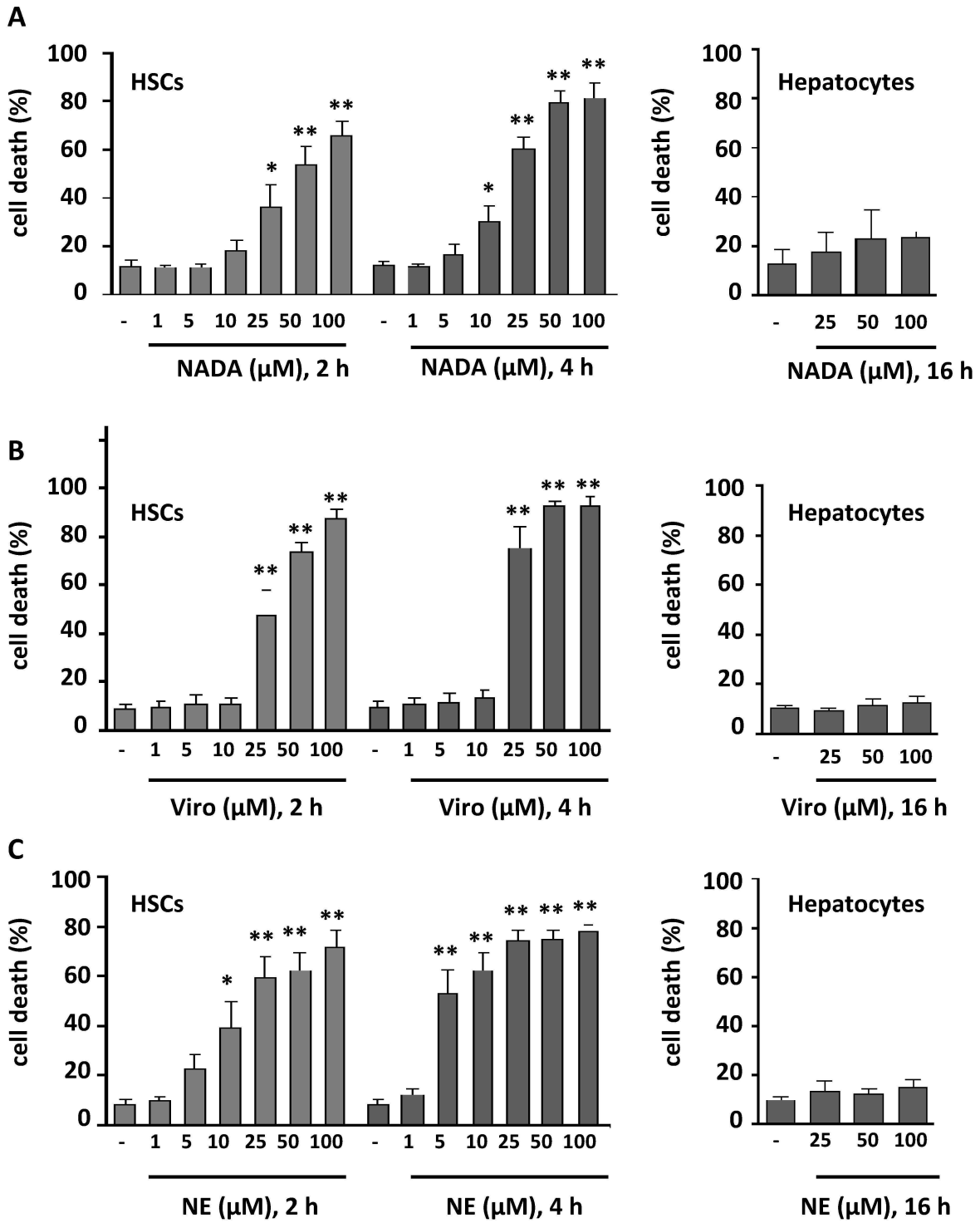

Figure 8. Primary rat HSCs and primary rat hepatocytes were serum-starved for 12 h and treated with the indicated concentrations of NADA (A), virodhamine (B), noladin ether (C) or vehicle (-) for the indicated time intervals. Cell death was determined by measuring the release of LDH into the media. Cell death was measured by LDH assay. *$p<0.05$, **$p<0.001$ vs. vehicle treatment.

4.2.2 Hepatocytes, but not HSCs express the rate-limiting NADA-generating enzyme tyrosine hydroxylase

The mechanism of virodhamine and noladin ether synthesis is unknown so far (Piomelli, 2003). For this reason, only the expression of the putative NADA-generating enzyme, tyrosine hydroxylase (TH) (Hu et al., 2009; Huang et al., 2002), was examined by western blot (Figure 9A). TH was expressed in healthy liver as well as in injured and fibrotic liver of wild type mice that have been intoxicated with CCL_4-inhalation for five weeks. TH was found in hepatocytes but not in HSCs (Figure 9B) leading to the conclusion that hepatocytes but not HSCs are able to produce NADA in normal and diseased states of the liver. As a result of this finding, NADA-induced cell death was further investigated.

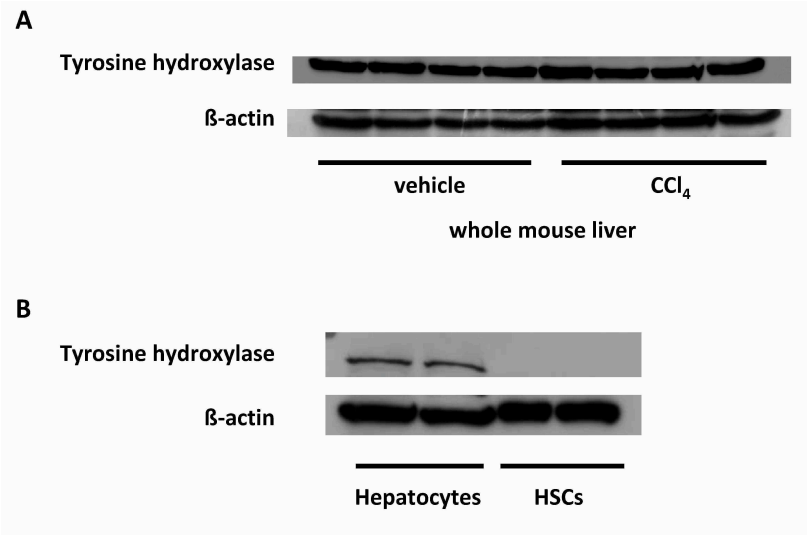

Figure 9. (A) Male C57BL/6 mice (n=4) underwent CCl_4 administration by inhalation three times a week for five weeks to induce fibrosis. TH expression was compared to control mice (n=4) by western blotting. (B) Protein levels in hepatocytes and HSCs of TH were determined by western blotting. A strong expression of TH was observed in hepatocytes.

4.2.3 NADA induces necrosis in activated HSCs

After the discovery that NADA is able to induce pronounced cell death in activated HSCs, the question whether NADA-induced cell death is apoptotic or necrotic was further to confirm. Primary HSCs were treated with NADA, AEA or tumour necrosis factor α (TNFα) and actinomycin D (ActD) as a positive control. The cells were stained with a combination of annexin V (AnnV), which binds to phosphatidylserine in the membrane of apoptotic cells, and propidium iodide (PI), a marker for necrotic cell death. While the treatment with TNFα/Act D showed strong Ann V staining, AEA- as well as NADA-treated stellate cells did not show Ann V binding. In contrast, a strong nuclear PI staining was observed indicating necrotic cell death induced by NADA (Figure 10A). Moreover, HSCs were prestimulated with a specific caspase inhibitor (Z-VAD-FMK) prior to stimulation with NADA or TNFα/ActD. While pretreatment with the caspase inhibitor resulted in 20 % less cell death induced by TNFα/ActD, NADA-induced cell death was not blocked by the costimulation (Figure 10B). These findings underline the necrotic model of NADA-induced cell death in HSCs.

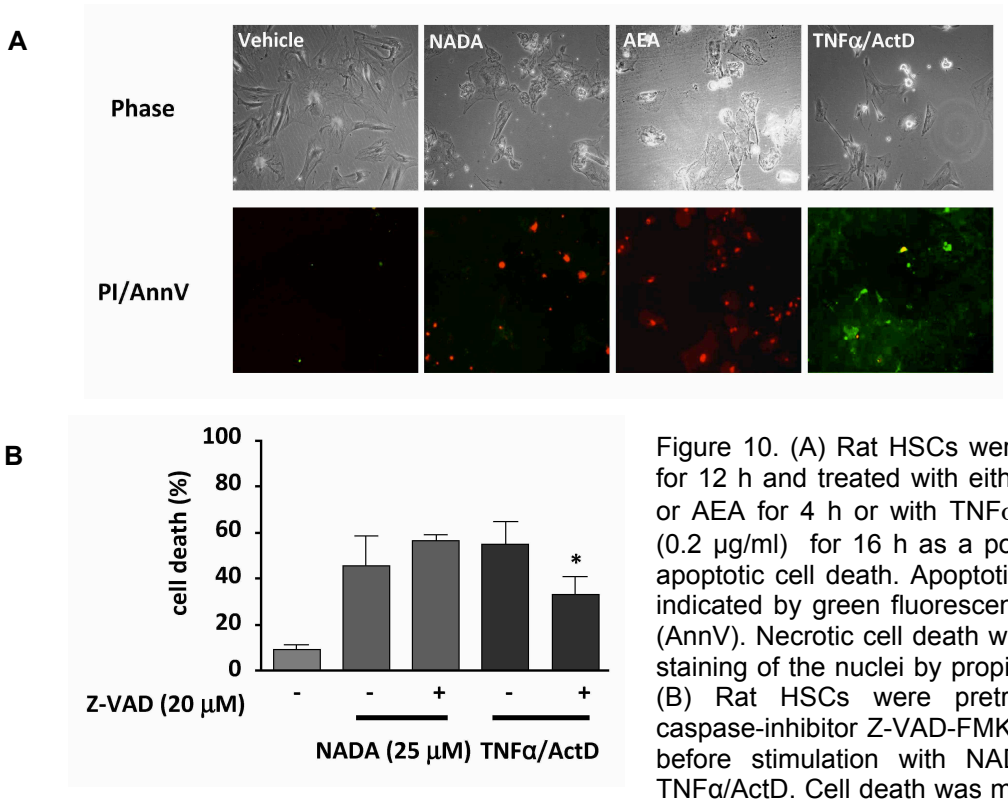

Figure 10. (A) Rat HSCs were serum-starved for 12 h and treated with either 25 μM NADA or AEA for 4 h or with TNFα(30 ng/ml)/ActD (0.2 μg/ml) for 16 h as a positive control for apoptotic cell death. Apoptotic cell death was indicated by green fluorescence of annexin V (AnnV). Necrotic cell death was shown by red staining of the nuclei by propidium iodide (PI). (B) Rat HSCs were pretreated with the caspase-inhibitor Z-VAD-FMK (20 μM) 30 min before stimulation with NADA (25 μM) or TNFα/ActD. Cell death was measured by LDH assay. *p<0.05 vs. TNFα/Act D alone.

4.2.4 Sublethal doses of NADA reduce proliferation and inhibits activation of HSCs

To examine if nanomolar concentrations of NADA can prevent activation of primary HSCs, freshly isolated stellate cells were treated daily with vehicle or NADA at concentrations of 100 nM or 1 μM for seven days. Afterwards, α-SMA expression as a marker of stellate cell activation was determined. Treatment with 1 μM NADA inhibited α-SMA expression on day 3 and 7 after stimulation. Compared to that, no reduction of stellate cell activation was observed at a concentration of 100 nM (Figure 11A).

To confirm the anti-proliferative effect, phosphorylation of ERK (pERK), which is used as a marker for the induction of proliferation, was examined. Therefore, HSCs were incubated with 10 % fetal calf serum (FCS) in the culture media and afterwards treated with 100 nM NADA. A strong induction of ERK phosphorylation was observed directly after FCS stimulation. NADA was shown to strongly diminish the phosphorylation of ERK, thus showing anti-proliferative capacity on activated HSCs (Figure 11B).

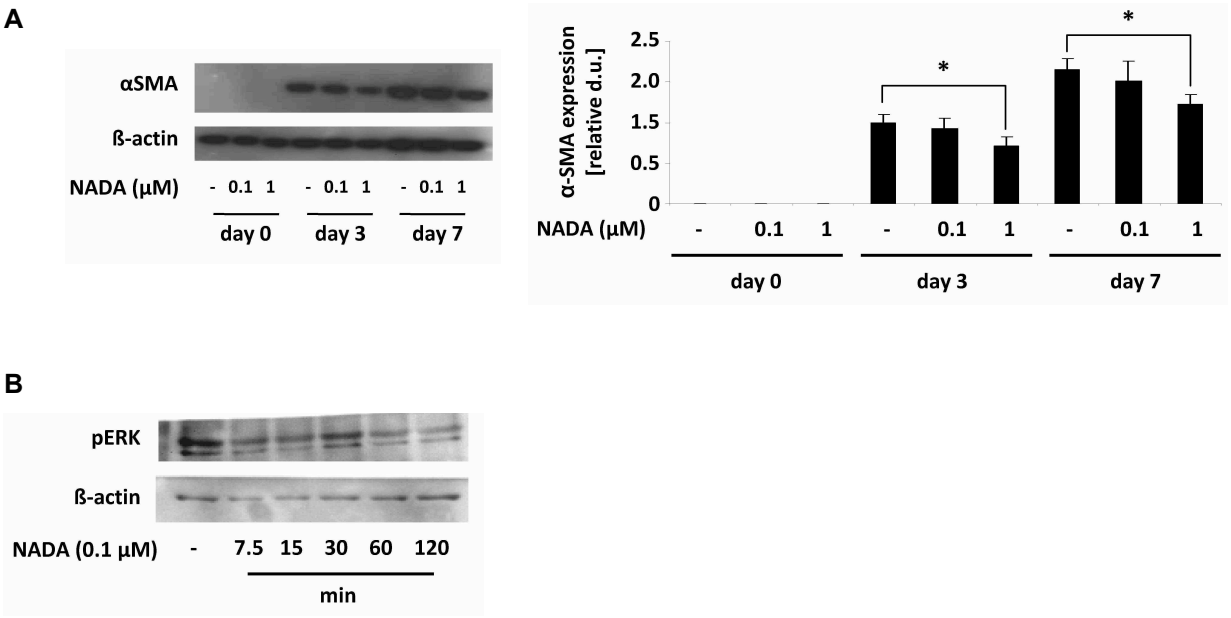

Figure 11. (A) Freshly isolated primary rat HSCs were treated daily with 100 nM or 1 µM NADA directly after stimulation and cells were harvested at the indicated time points. Western blot was performed with antibodies directed against α-SMA and β-actin. Densitometric quantifications are shown in means of relative densitometric units ± SEM compared to α-SMA expression after vehicle treatment at the respective timepoints (day 3 and 7). *$p<0.05$ vs. vehicle (B) HSCs were cultured with DMEM containing 10 % FCS and treated with NADA (100 nM) at the indicated times. Western blot was performed with antibodies directed against pERK and β-actin.

4.2.5 NADA-induced death in HSCs occurs independently of the endocannabinoid receptors CB_1, CB_2 or TRPV1

Endocannabinoids induce various physiologic events via cannabinoid or vanilloid receptors. NADA has been shown to be a full agonist of CB_1- as well as TRPV1 receptors and to a lesser extent of CB_2 receptors (Bisogno et al., 2000; Huang et al., 2002). Using pharmacological and genetic approaches, the involvement of the receptors in NADA-mediated cell death was investigated. Although CB_1, CB_2 and TRPV1 receptors are expressed in HSCs (Siegmund et al., 2005b), neither AM251, a specific antagonist of CB_1, nor SR144528, a specific antagonist of CB_2, nor capsazepine, a specific antagonist of TRPV1, showed cytoprotective effects after NADA-stimulation, indicating independence of these receptors (Figure 12A). Accordingly, activated primary HSCs isolated from wild type and mice lacking the CB_1 receptor and the CB_2 receptor ($CB_1^{-/-}/CB_2^{-/-}$) were equally susceptible toward NADA-mediated cell death (Figure 12B). To provide further evidence of the receptor-independent induction of cell death, HSCs were treated with capsaicin, a TRPV1 agonist, and no cytotoxic effect was observed (Figure 12C).

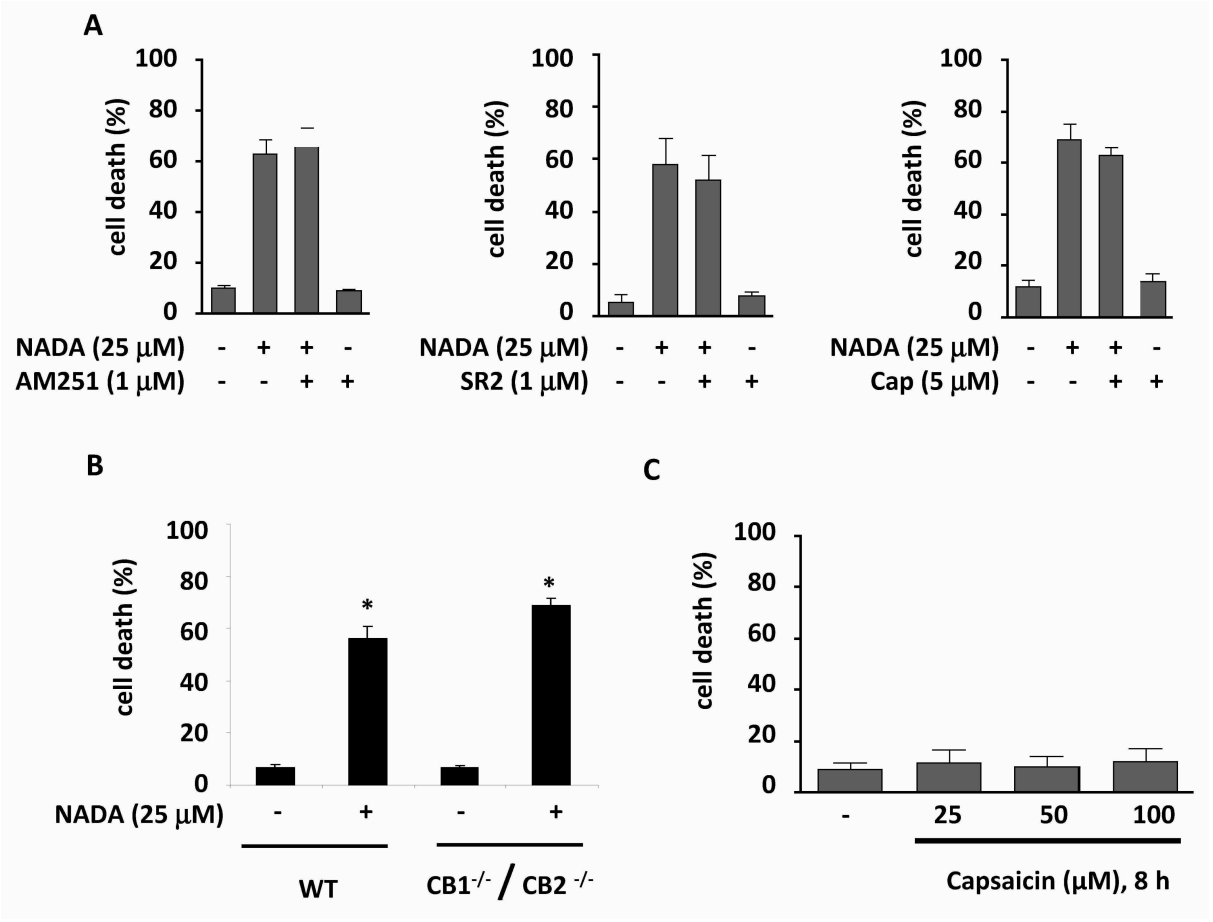

Figure 12. (A) Mouse HSCs were incubated with the specific receptor antagonists AM251 (1 μM), SR144528 (1 μM) or capsazepine (5 μM) for CB_1, CB_2 or TRPV1 receptors, respectively, 30 min prior to addition of NADA (25 μM) for 4 h. (B) HSCs isolated from mice lacking the CB_1 and CB_2 receptor ($CB_1^{-/-}/CB_2^{-/-}$) and from wild type mice were stimulated with 25 μM NADA for 4 h. (C) Mouse HSCs were stimulated with capsaicin or vehicle (-) for 8 h with the indicated concentrations. Cell death was analysed by LDH assay. *$p<0.05$ vs. NADA alone.

4.2.6 NADA-induced cell death does not depend on membrane cholesterol

Previous studies in primary HSCs as well as in other cell types have shown that AEA induces cell death through interaction with phospholipid bilayers via cholesterol-rich lipid rafts (Maccarrone & Finazzi-Agro, 2003; Siegmund et al., 2005b) (Yang, Liu, Zhang, Wu, & Tang). To test whether removing of cholesterol has cytoprotective effects in NADA-stimulated HSCs, the content of cholesterol in the cell membrane was reduced by incubating hepatic stellate cells with MCD (Siegmund et al., 2005b), a membrane cholesterol depletor, prior to stimulation with NADA or AEA. Accordingly, MCD completely inhibited necrosis induced by 25 μM AEA but not by 25 μM NADA (Figure 13). This result indicates that NADA does not require interaction with membrane cholesterol for induction of cell death in HSCs.

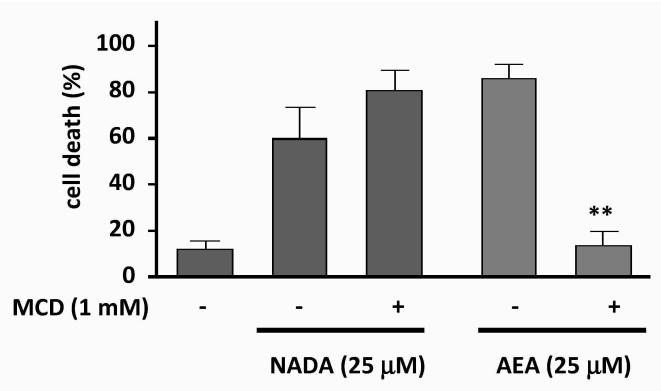

Figure 13. Murine HSCs were incubated with the membrane cholesterol depletor MCD (1 mM) for 1 h and afterwards stimulated with 25 μM NADA or AEA for 4 h. Cell death was analyzed by LDH assay. **p<0.001 vs. NADA or AEA alone.

4.2.7 NADA-induced necrosis is accompanied by an increase in intracellular reactive oxygen species (ROS)

Previous studies showed that ROS formation is involved in AEA-induced cell death (Siegmund et al., 2005b). To anayse whether NADA stimulation promotes ROS formation, the generation of ROS in NADA-treated cells was determined. Comparable to AEA, NADA caused a marked and rapid increase of over 400 % in ROS formation compared to vehicle-treated cells, which started one minute after stimulation at concentrations of 50 and 100 µM. Moreover, 25 µM NADA significantly doubled the ROS amount in the cells after four minutes of stimulation. There are no significant differences in ROS induction between the several NADA concentrations (Figure 14A). The generation of ROS induced by NADA did not differ from the ROS production induced by the corresponding concentrations of AEA (Figure 14B).

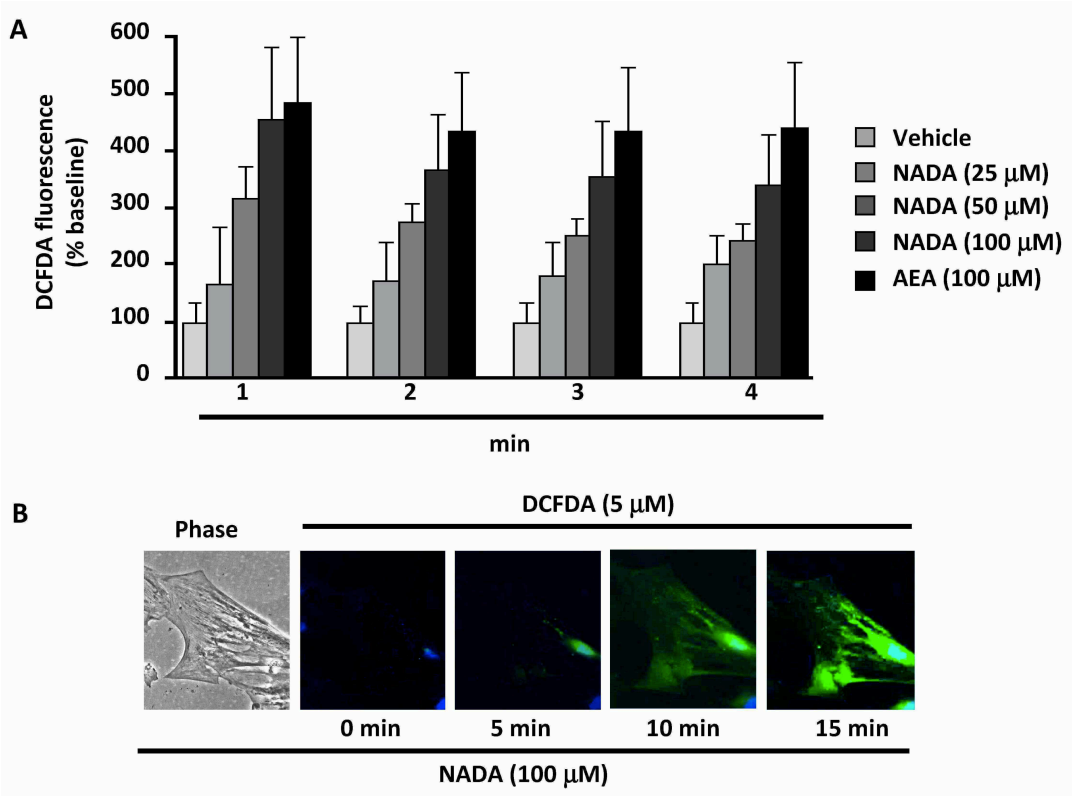

Figure 14. Activated rat HSCs were loaded with CM-H_2DCFDA (5 μM) for 30 min and treated with 100 μM NADA, AEA or vehicle. Reactive oxygen species formation was measured in a platereader in quadruplicates (A) or green fluorescence of CM-H_2DCFDA was visualized on a single cell (B).

Pretreatment with the antioxidants GSH and TROLOX significantly reduced NADA-mediated cell death from 51 % to 16 % and 22 %, respectively (Figure 15A). Moreover, antioxidants ameliorated NADA-induced cell death in HSCs as shown by decreased PI staining of the nuclei (Figure 15B). To provide further evidence for ROS as a key mediator of the cytotoxic effects of NADA, antioxidants in HSCs were depleted by BSO pretreatment resulting in a significant increase in NADA-induced cell death 2 h after stimulation (Figure 15C). These results suggest that antioxidants like GSH or TROLOX protect HSCs from NADA-induced cell death.

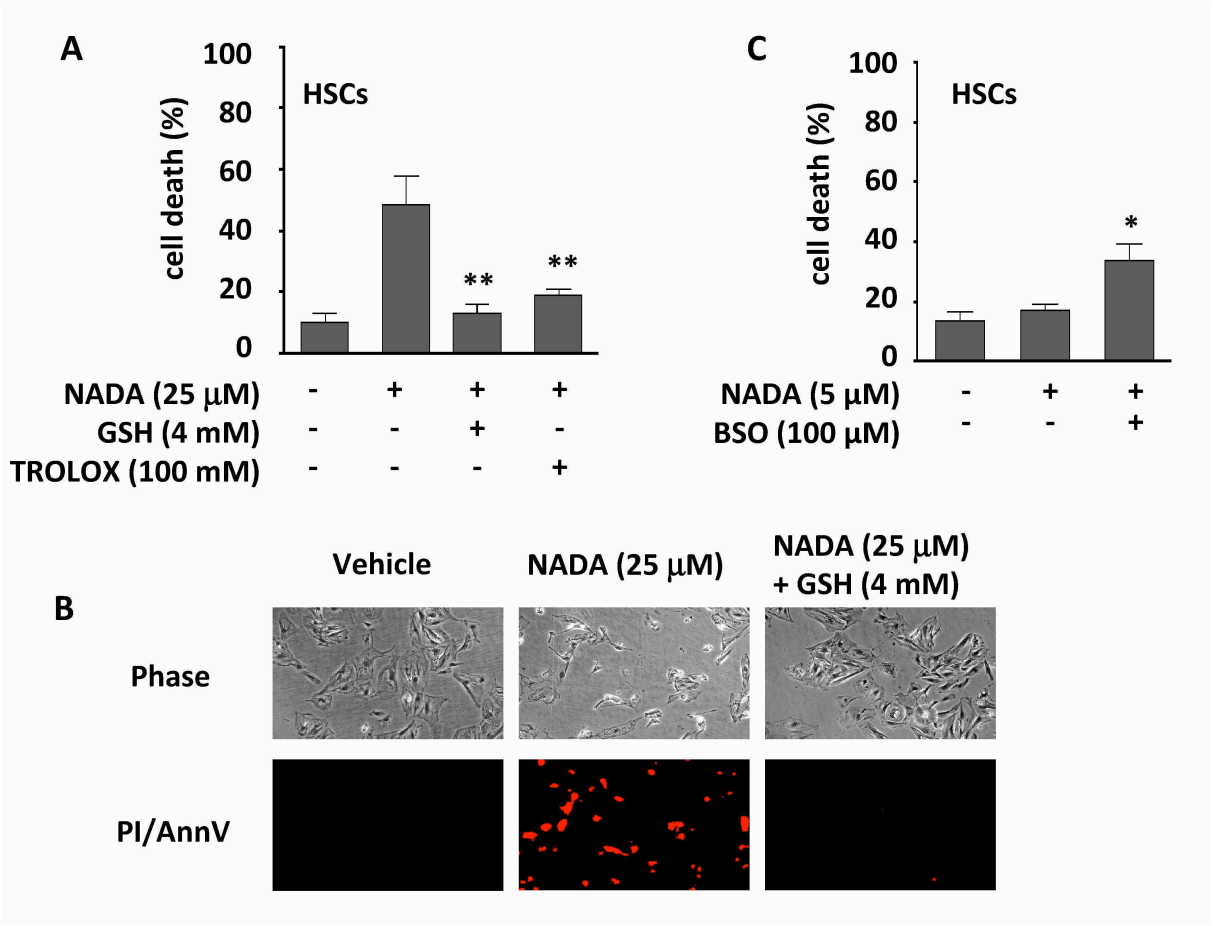

Figure 15. (A) Activated rat HSCs were preincubated with 4 mM GSH or 100 mM TROLOX and treated with NADA (25 µM for 4 h). Cell death was analysed by LDH assay (B). Cells were treated with either NADA (25 µM) plus GSH (4 mM), NADA (25 µM) alone or vehicle (-) for 4 h. Necrotic cell death is shown by red staining of the nuclei by PI (B). (C) After incubation with BSO for 1 h, the cells were stimulated with NADA (5 µM) for 4 h. Cell death was measured by LDH release. *$p<0.05$, **$p<0.001$ vs. NADA alone.

4.2.8 FAAH determines resistance to NADA-mediated cell death in hepatocytes

The expression of catechol-O-methyltransferase (COMT) and fatty acid amid hydrolase (FAAH), which were shown to be able to degrade NADA, was investigated in hepatocytes and in HSCs. COMT-expression was not detected in both cell types. In contrast to HSCs and hepatocytes, HEK293 cells displayed strong expression of the COMT protein (Figure 16A). Furthermore, pharmacological blockade of COMT by OR-486, a specific COMT-inhibitor, showed no difference in response of HSCs to NADA (Figure 16B). Confirming earlier studies (Siegmund et al., 2006), primary hepatocytes express large amounts of FAAH in contrast to primary HSCs (Figure 16A). To investigate whether the different expression of FAAH is responsible for the different susceptibility of hepatocytes and HSCs towards NADA-induced cell death, hepatocytes were first preincubated with URB597, a strong and selective inhibitor of FAAH, and afterwards stimulated with 25 µM NADA. Blocking of FAAH increased NADA-

mediated cell death by 40 % (Figure 16C). Accordingly, hepatocytes isolated from FAAH knockout mice also showed a higher susceptibility towards NADA-induced cell death with 28 %, 46 % and 61 % of cell death after 10 μM, 25 μM and 50 μM, respectively (Figure 16D).

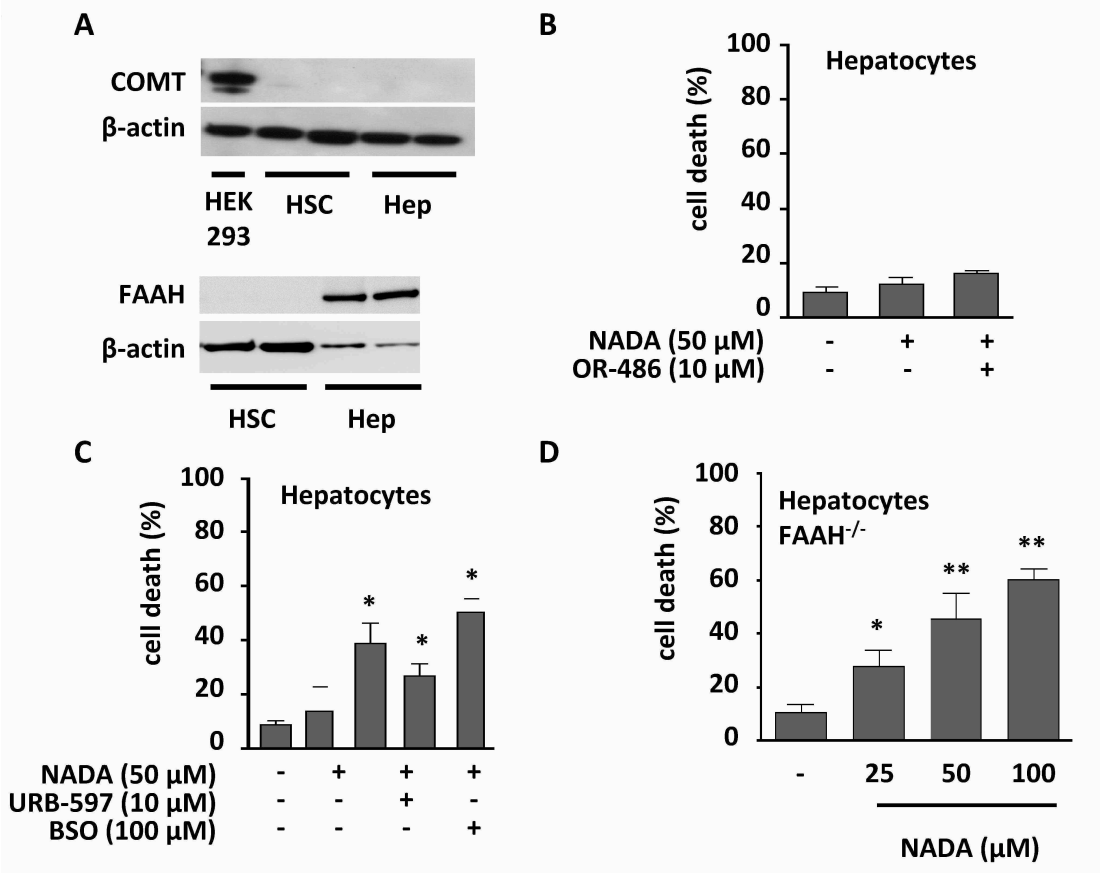

Figure 16. (A) COMT and FAAH protein expression were analysed in rat HSCs and hepatocytes by western blotting. (B) Hepatocytes were either pretreated with vehicle or OR-486 (10 μM) followed by NADA stimulation (25 μM) for 24 h. (C) Hepatocytes were incubated with URB597 (10 μM) or BSO (100 mM) for 1 h followed by NADA stimulation (25 μM) for 24 h. (D) Cell death in FAAH$^{-/-}$ hepatocytes after treatment with indicated NADA concentrations was determined by LDH release. *p<0.05 vs. vehicle.

To further investigate the role of FAAH, rat HSCs were infected with an adenovirus expressing rat FAAH (AdFAAH), which leads to a strong overexpression of the enzyme (Figure 17A). AdFAAH decreased NADA-induced cell death (25 μM) from 55 % to 23 %, similarly to AEA-induced cell death (Figure 17B). In contrast, HSCs infected with the control virus expressing only GFP showed no difference in NADA-induced cell death. NADA is metabolised by FAAH to dopamine and arachidonic acid, a structurally similar polyunsaturated fatty acid. To exclude that these substances have cytotoxic effects, HSCs were incubated with 25 μM of each substance for 4 h. Neither arachidonic acid nor dopamine induced any detectable cell death whereas NADA induced cell death in over 50 % of the cells (Figure 17D).

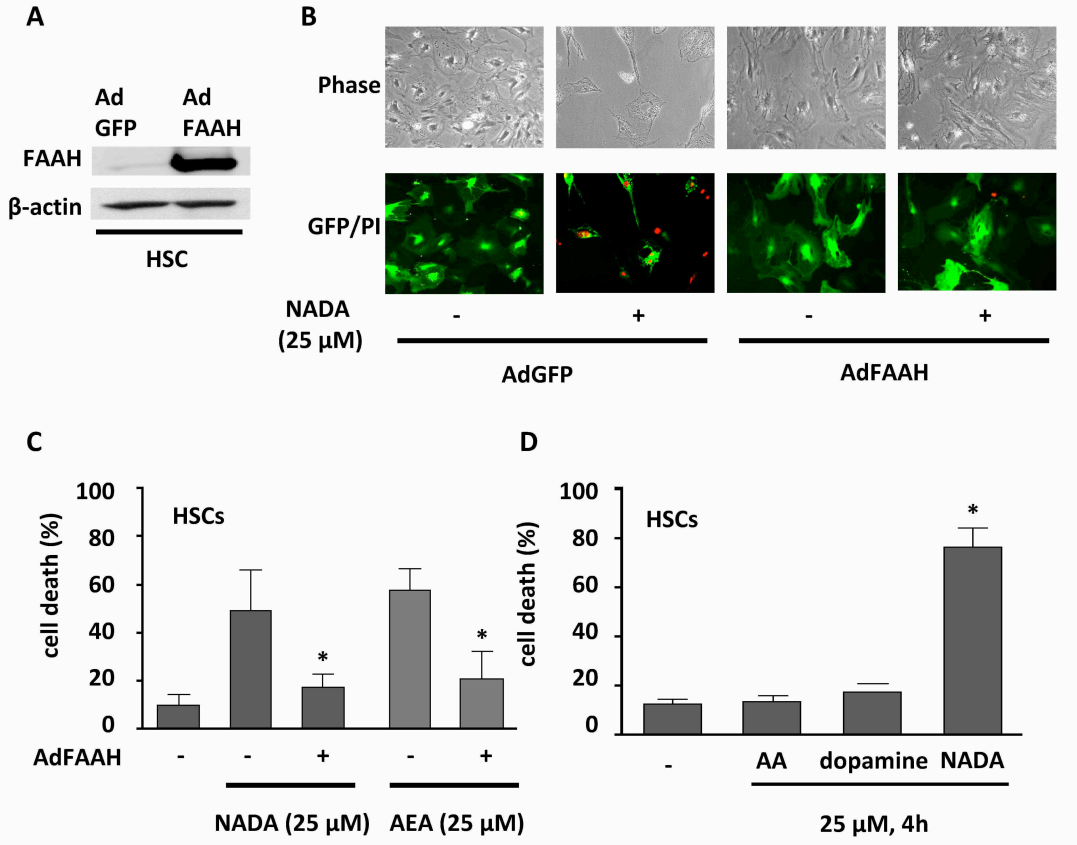

Figure 17. (A) Expression of FAAH protein in HSCs infected with AdGFP or AdFAAH was determined by western blotting. (B, C). HSCs were infected with AdFAAH or AdGFP for 12 h and treated 24 h later with 25 µM NADA for 4 h. PI staining of the nuclei visualised necrosis (B) or LDH release into the media was measured (C). *p<0.05 vs. AdGFP. (D) Cells were treated with arachidonic acid (AA), dopamine or NADA with a concentration of 25 µM for 4 h. Cell death was determined by LDH release. *p<0.05 vs. vehicle.

4.3 Definition of the cellular source of elevated 2-AG levels in the liver

To address upregulated 2-AG levels in the injured liver, first the expression of the synthesising enzymes diacylglycerol lipase (DAGL) α and β as well as the degrading enzymes fatty acid amide hydrolase (FAAH) and monoacyl glycerol lipase (MGL) in whole liver tissue of sham-operated and bile duct ligated mice were examined. The cellular origin of increased 2-AG levels is unknown so far, therefore the expression of proteins involved in production and metabolism of 2-AG were further determined in different cell types of the liver.

4.3.1 Elevated levels of 2-AG in the injured liver by increased synthesis and decreased degradation

To investigate the expression levels of the synthesising and degrading proteins of 2-AG during liver injury, bile duct ligated or sham operated mice were sacrificed on day 7 or day 14

after surgery and mRNA levels of DAGLα and β as well as of FAAH and MGL were examined in whole liver tissue. As shown in Figure 18, the mRNA levels of the 2-AG producing enzyme DAGLα were significantly decreased in the injured liver. Interestingly, DAGLβ expression was four fold higher on day 14 after bile duct ligation compared to DAGLβ levels in sham operated mice. To check which synthesising enzyme is predominantly present in the liver, DAGLβ mRNA levels were compared to DAGLα expression in whole liver tissue. Compared to DAGLα, a 40 fold higher DAGLβ expression was found suggesting that DAGLβ is the main 2-AG-synthesising enzyme in the liver. Moreover, the intrahepatic mRNA expression of FAAH and MGL was significantly decreased seven and 14 days after surgery indicating that elevated expression of DAGLβ and reduced levels of the degrading enzymes of 2-AG are responsible for the upregulated 2-AG levels during fibrogenesis (Figure 18).

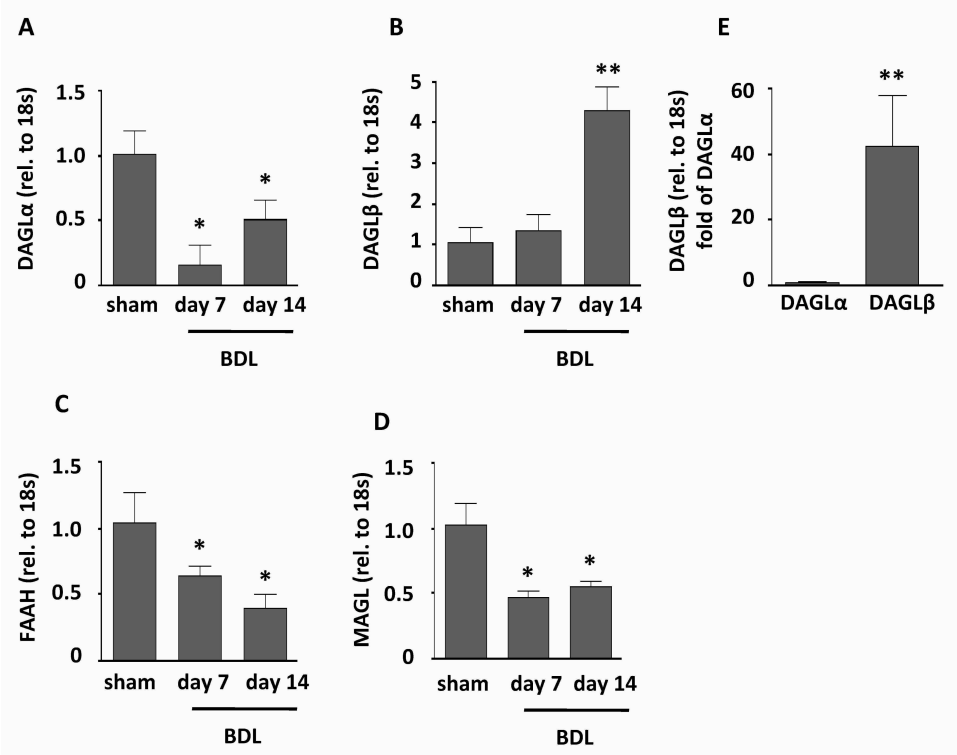

Figure 18: mRNA expression of the 2-AG production enzymes DAGLα (A) and DAGLβ (B) as well as the degradation enzymes FAAH (C) and MGL (D) were examined by quantitative RT-PCR. Shown is fold of expression in sham-operated mice after normalization to 18s. **p<0.001, *p<0.05 vs. sham-operated. (E) DAGLβ mRNA expression is shown as fold of DAGLα expression in whole liver tissue after normalization to 18s RNA. **p<0.001 vs. DAGLα expression.

4.3.2 The non-parenchymal cells of the liver are able to synthesise 2-AG

Since the cellular origin of 2-AG levels in the liver is unknown, DAGLα as well as DAGLβ mRNA expression in isolated primary liver cell populations were determined. A strong expression of DAGLα as well as DAGLβ was found in hepatic stellate cells, Kupffer cells and liver sinusoidal endothelial cells indicating that the non-parenchymal cells are the major source of 2-AG production in the liver (Figure 19). The strongest expression of DAGLα was

found in LSECs with a 20-fold higher expression compared to hepatocytes. The mRNA levels of DAGLα found in HSCs and KCs were still 10-fold higher compared to the level in the parenchymal cells (Figure 19A). Much more pronounced were the differences in DAGLβ expression. The mRNA levels of DAGLβ were 60-times higher in HSCs and LSECs compared to the levels in hepatocytes. While KCs showed lower expression than HSCs or LSECs, the levels of DAGLβ mRNA were still significantly higher than in hepatocytes (Figure 19B).

To check which DAGL type represents the predominant 2-AG producing enzyme in the liver, DAGLα and β expression was compared. Indeed, a significant higher expression of DAGLβ was found in all cell types of the liver compared to DAGLα levels (Figure 19C) confirming the pivotal role of DAGLβ in 2-AG synthesis.

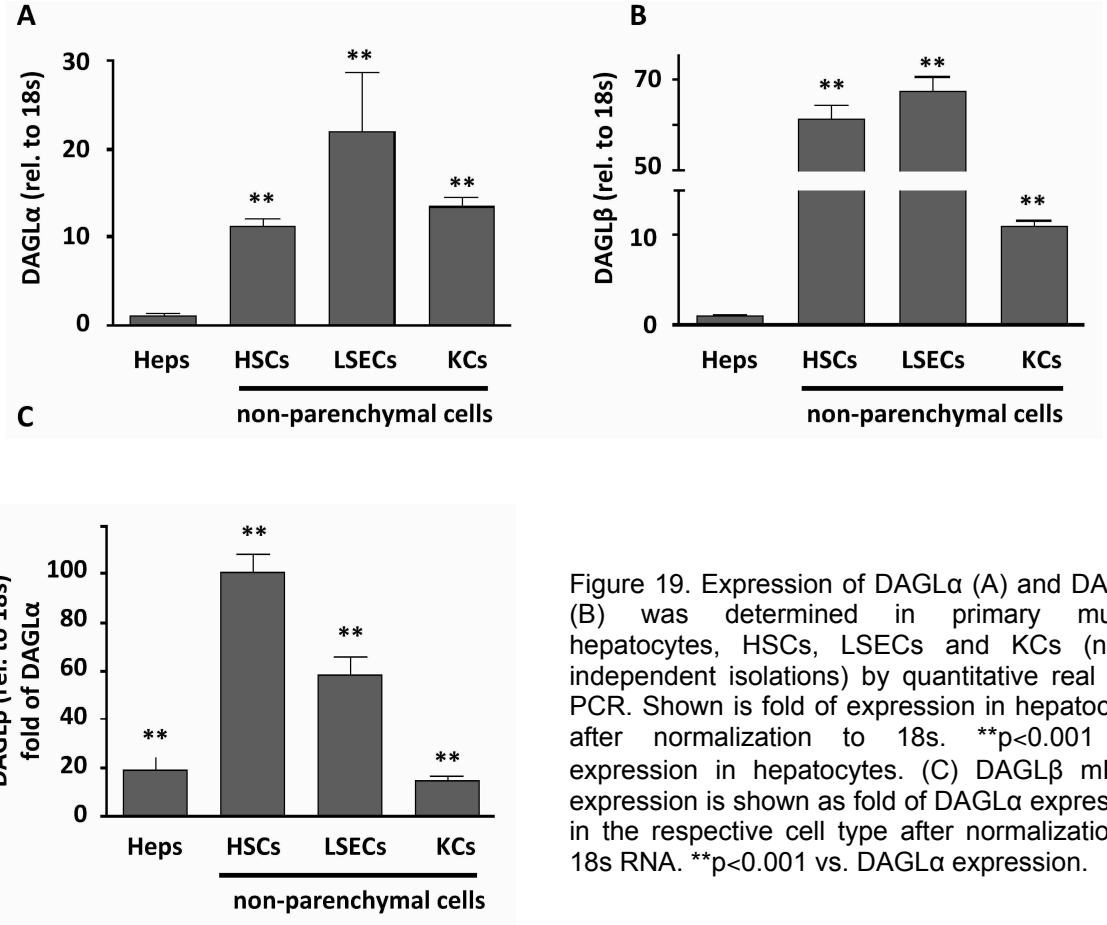

Figure 19. Expression of DAGLα (A) and DAGLβ (B) was determined in primary murine hepatocytes, HSCs, LSECs and KCs (n= 3 independent isolations) by quantitative real time PCR. Shown is fold of expression in hepatocytes after normalization to 18s. **p<0.001 vs. expression in hepatocytes. (C) DAGLβ mRNA expression is shown as fold of DAGLα expression in the respective cell type after normalization to 18s RNA. **p<0.001 vs. DAGLα expression.

4.3.3 FAAH is expressed in hepatocytes whereas MGL was found mainly in HSCs and LSECs

Quantitative real time PCR revealed that FAAH mRNA was mainly expressed in hepatocytes whereas LSECs displayed a marginal expression of FAAH mRNA. HSCs and KCs showed no detectable amounts of FAAH mRNA levels (Figure 20A). The highest MGL mRNA levels

were found in LSECs, where a 130-fold higher expression was observed compared to the expression in hepatocytes. HSCs also express significantly higher levels of MGL than hepatocytes whereas the expression pattern does not differ between KCs and hepatocytes (Figure 20B).

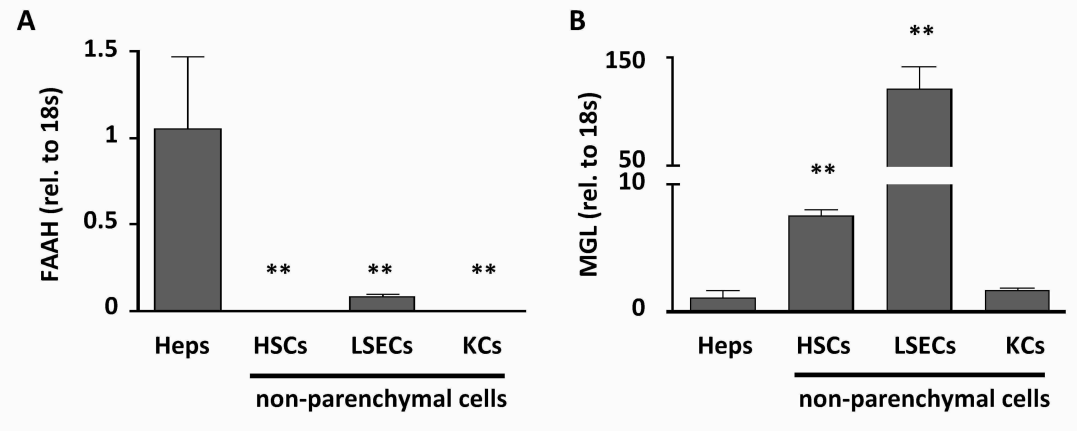

Figure 20. Expression of FAAH (A) and MGL (B) was determined in primary murine hepatocytes, HSCs, LSECs and KCs by quantitative real time PCR. Shown is fold of expression in hepatocytes after normalization to 18s RNA. **p<0.001 vs. expression in hepatocytes.

4.4 Analysis of 2-AG-induced cell death in HSCs

Recently, it was shown that 2-AG is able to induce cell death in HSCs but not in hepatocytes. The exact mechanism of 2-AG-induced HSC death is not clear so far. To answer the question if metabolites of 2-AG are at least in part responsible for the cytotoxic effect of 2-AG, an alternative endocannabinoid metabolic degradation pathway was examined. In this pathway, 2-AG is converted via the enzyme COX-2 in prostaglandin glycerol ester (PG-GE) (Kozak et al., 2002; Kozak et al., 2004). COX-2 could display a possible link between 2-AG stimulation and cell death and may therefore be relevant for the development of hepatoprotective therapies.

4.4.1 COX-2 is expressed in the non-parenchymal cells in the liver and highly upregulated in the injured liver

To determine the expression of COX-2 during fibrogenesis, mRNA levels were determined in sham operated and bile duct ligated mice. COX-2 mRNA levels were more than ten-fold increased seven days after bile duct ligation. Moreover, there was a nearly 60-fold induction of COX-2 expression fourteen days after bile duct ligation demonstrating that liver injury induces COX-2 mRNA expression. Additionally, the cellular source of COX-2 in the liver was determined. There was a 7-fold higher expression level in HSCs compared to the expression levels in hepatocytes (Figure 21).

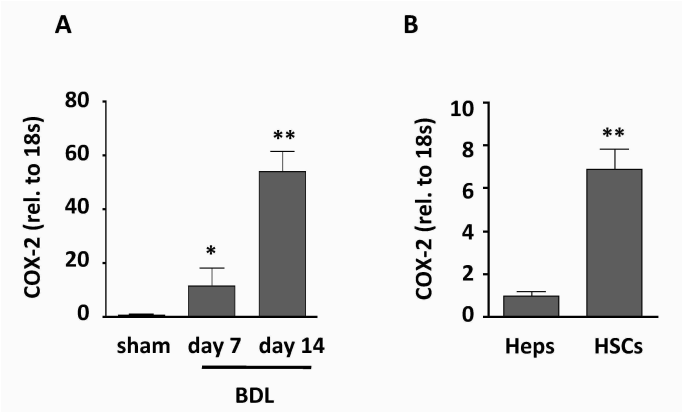

Figure 21. (A) Expression of COX-2 was examined in sham-operated and bile duct ligated mice on day 7 and on day 14 after BDL. Shown is fold of expression in sham-operated mice after normalization to 18s mRNA(B) Expression of COX-2 was examined in primary hepatocytes and HSCs (n=3 independent isolations) by quantitative real time PCR. Shown is fold of expression in hepatocytes after normalization to 18s mRNA. **p<0.001 vs. expression in hepatocytes.

4.4.2 PGD_2-GE but not $–F_{2\alpha}$ and $–E_2$ induces cell death in HSCs

It was recently shown that 2-AG is first metabolised by COX-2 to unstable PGH_2-GE that afterwards acts as a substrate for PGD-, PGE- or PGF-synthases resulting in PGD_2-GE, PGE_2-GE or $PGF_{2\alpha}$-GE, respectively (Kozak et al., 2004). To check whether these possible metabolites of 2-AG were involved in 2-AG-induced cell death, primary HSCs were stimulated with different prostaglandin glycerol esters. Interestingly, only PGD_2-GE showed significant cytotoxic effects on primary stellate cells (Figure 22 A). To exclude that these effects are a result of prostaglandin D_2 (PGD_2), the metabolite of arachidonic acid, the cells were stimulated with PGD_2 with a concentration of 50 µM. In this experiment, no significant induction of cell death by PGD_2 was observed (Figure 22 B). The results suggest that PGD_2-GE and not other PG-GE or PGD_2 are involved in 2-AG-mediated HSC apoptosis.

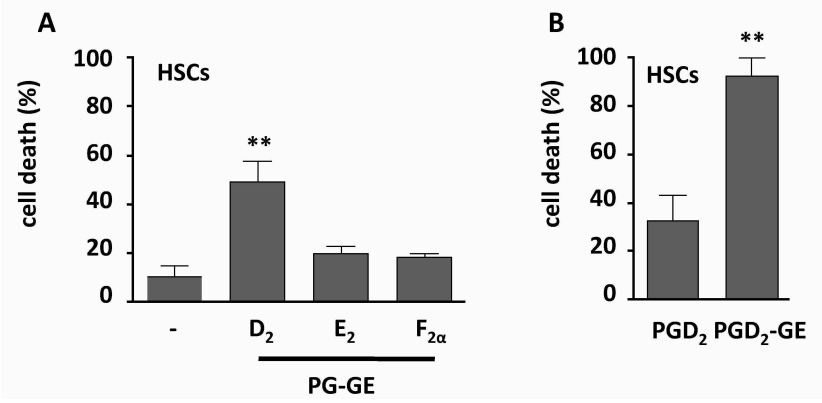

Figure 22. (A) Mouse HSCs were treated with 50 µM PGD_2-GE, PGE_2-GE, $PGF_{2\alpha}$-GE or vehicle (-) (A) and with 50 µM PGD_2, PGD_2-GE or vehicle (-) (B) for 16 h. Cell death was determined by LDH assay. **p<0.001 vs. vehicle.

4.4.3 2-AG is metabolised to PGD_2-GE in HSCs, but not in hepatocytes

To examine whether 2-AG is metabolized by COX-2 to PGH_2-GE and further by PGD-synthase to PGD_2-GE, HSCs as well as hepatocytes were stimulated with 2-AG or vehicle for 16 h. Subsequently, the PGD_2-GE content was measured. No difference was observed in the PGD_2-GE level of treated and untreated hepatocytes. Nevertheless, there was a significant induction of PGD_2-GE production in 2-AG-stimulated HSCs reaching 2000-fold higher PGD_2-GE levels compared to vehicle treated cells indicating that HSCs but not hepatocytes are able to produce PGD_2-GE when stimulated with 2-AG (Figure 23).

Figure 23. Serum-starved primary hepatocytes and HSCs were treated with 50 µM 2-AG or vehicle for 16 h. PGD_2-GE concentration was measured by PGD_2-MOX EIA. **p<0.001 vs. hepatocytes.

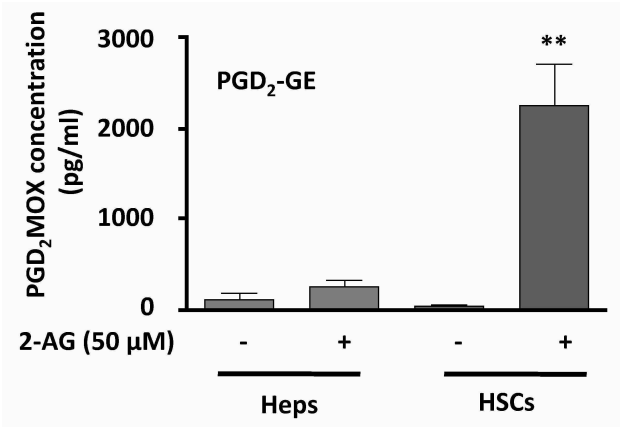

4.4.4 PGD_2-GE induces cell death in HSCs as well as in hepatocytes

To further analyse, whether differential expression of the alternative endocannabinoid degradation pathway by COX-2 contributes to the different susceptibility of HSCs and hepatocytes towards 2-AG, the cells were stimulated with either 50 µM 2-AG or PGD_2-GE. Indeed, stimulation with PGD_2-GE leads to considerable induction of cell death in HSCs as well as in hepatocytes. No cytotoxic effects were observed by stimulating hepatocytes with the adequate concentration of 2-AG suggesting that the metabolism of 2-AG to PGD_2-GE through COX-2 contributes to the apoptotic effect of 2-AG (Figure 24).

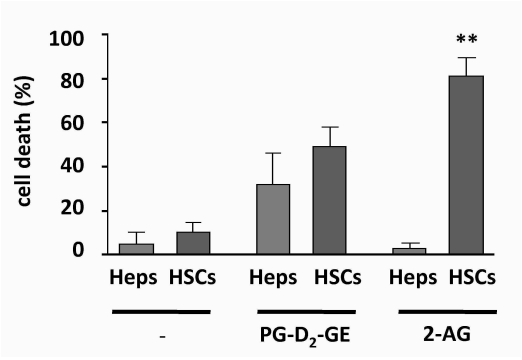

Figure 24. Serum-starved primary mouse hepatocytes and HSCs were treated either with 50 µM PGD_2-GE, 50 µM 2-AG or vehicle (-) for 16 h. Cell death was measured by the release of LDH into the media. **p<0.001 vs. hepatocytes.

4.4.5 PGD_2-GE induces apoptotic cell death in HSCs

To further characterise PGD_2-GE-induced cell death, caspase 3- and PARP-cleavage, two hallmarks of apoptotic cell death, were investigated. PGD_2-GE-treatment showed caspase 3- and PARP cleavage starting 16 h after stimulation (Figure 25) suggesting apoptotic cell death induced by PGD_2-GE.

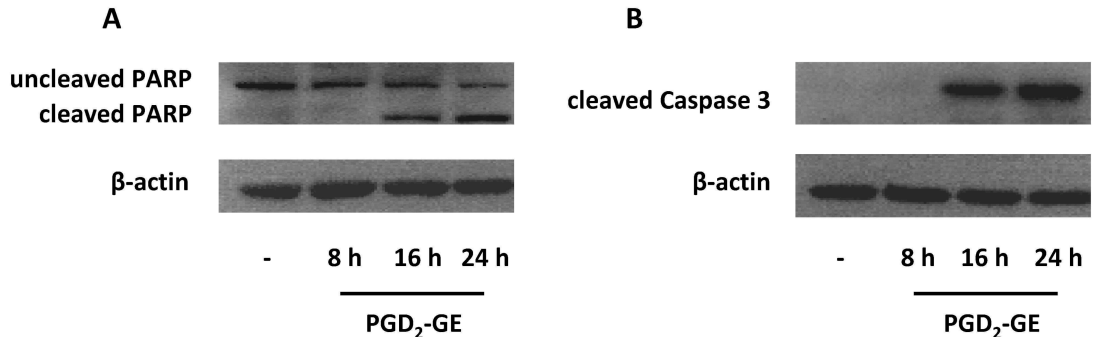

Figure 25 A, B. Primary HSCs were treated with PGD_2-GE (50 µM) or 2-AG (50 µM) as a positive control for the indicated times. Western blotting was performed with antibodies directed against cleaved caspase 3, cleaved PARP and β-actin.

4.4.6 PGD_2-GE-induced cell death is membrane cholesterol independent

It was previously shown that membrane cholesterol depletion prevents HSCs from 2-AG-induced cell death (Siegmund et al., 2007). HSCs were incubated with the membrane cholesterol depletor MCD and afterwards stimulated with either 2-AG or PGD_2-GE. Although preincubation of MCD in 2-AG-treated cells displayed a strong regression in cell death (Figure 26A), no decrease in cytotoxicity was observed in PGD_2-GE treated cells (Figure 26B). Thus, cholesterol seems not to be involved in PGD_2-GE-induced apoptosis.

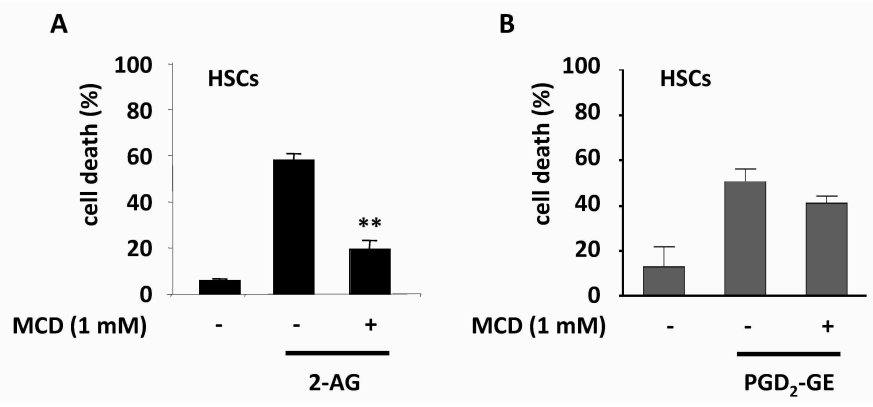

Figure 26 A, B. Primary HSCs were preincubated with the membrane cholesterol depletory MCD (1 mM) 1 h before addition of 2-AG (25 µM) (A) or PGD_2-GE (50 µM) (B) for 16 h. Cell death was assessed by LDH assay.

5 DISCUSSION

Liver fibrosis represents a wound healing response to a variety of chronic injurious stimuli including constant drug or alcohol abuse, viral infections or metabolic disorders (Bataller et al., 2005). This perpetuating wound healing reaction is characterised by excessive accumulation of extracellular matrix (ECM) proteins, which replace the lost parenchyma leading to loss of liver function (Friedman, 2008a). Liver cirrhosis, the end stage of fibrosis, represents a major health problem with high mortality worldwide (Lotersztajn, Julien, Teixeira-Clerc, Grenard, & Mallat, 2005). HSCs are mainly responsible for the increased synthesis and deposition of ECM in the liver. Following liver injury, HSCs activate and transdifferentiate into myofibroblast-like cells expressing large amounts of ECM.

After acute damage of liver cells, ECM proteins are degraded and liver function is recovered. If the hepatic injury becomes chronic, the reconstitution of liver function is not achieved (Friedman, 2008a).

Following removal of the causative agent like eradication of hepatitis C virus infection or cessation of alcohol abuse, liver fibrosis can reverse and result in a complete normal hepatic architecture (Bataller et al., 2005; Siegmund et al., 2005a). Therefore, treatment of the underlying disease is of course the most effective approach. If this is not possible, additional therapeutic options are required. Selective induction of cell death in hepatic stellate cells, the main fibrogenic cell type in the liver, has been linked to the resolution of fibrosis (Iredale et al., 1998). Recently it was shown, that endocannabinoids are able to induce specifically cell death in HSCs but not in hepatocytes making these substrates good candidates for the treatment of liver fibrosis (Siegmund et al., 2007; Siegmund et al., 2005b).

5.1 Cultivation of hepatic stellate cells

Hepatic stellate cells were first described by Kupffer in the 19th century. They represent one third of non-parenchymal cells and 8 % of the total cells in the liver. In their quiescent state, HSCs function as the major vitamin A storing cells in the body containing over 80 % of total vitamin A (Friedman, 2008b). During liver injury, HSCs become activated and transdifferentiate into a myofibroblast-like phenotype, which is known to be the most dominant pathway in fibrogenesis (Enzan et al., 1997; Schmitt-Graff, Desmouliere, & Gabbiani, 1994). Due to its pivotal role in liver injury, the attention regarding the treatment of liver fibrosis turned to the stellate cell. The inhibition of activation or the specific induction of death in HSCs could represent a tool for the treatment of liver fibrosis.

The development of HSC isolation and cultivation represent a major advance to explore the cell function in healthy and injured liver. The isolation is based on *in situ* digestion following density gradient centrifugation, which is again based on the intracellular vitamin A content of

the cells. During the first two days, the cells display a high amount of cytoplasmatic lipid droplets containing retinoids, mostly vitamin A. The autofluorescence of vitamin A under UV-light is used to discriminate HCSs and other resident liver cells that allows the determination of the cell culture purity (Friedman et al., 1985; Volk & Popper, 1950).

After two days of cultivation, the cells act like in the injured liver: they activate and transdifferentiate into myofibroblast-like cells with bundles of numerous microfilaments (Schmitt-Graff et al., 1994). Moreover, they start to proliferate like their counterparts *in vivo*. Therefore, cultivation of primary HSCs represent a good tool for the study of liver fibrosis.

Activation of HSCs in culture can be shown by α smooth muscle actin (α-SMA) expression. α-SMA is localised within the microfilament bundles of myofibroblasts or fibroblasts and is essential for the contractility of the cells (Schmitt-Graff et al., 1991; Serini et al., 1999). Induction of α-SMA is the most reliable marker of stellate cell activation, due to its absence in other resident liver cells (Bataller et al., 2005; Rockey, Boyles, Gabbiani, & Friedman, 1992). Moreover, α-SMA staining is increasingly used as an indicator for hepatic fibrosis in patients even before ECM accumulates (Gawrieh et al., 2005; Russo et al., 2005).

Analysis of inhibition of activation and induction of cell death in HSCs disclose new prospects for patients with end-stage disease in the future.

5.2 Investigation of the effects of noladin ether, virodhamine and NADA on liver cells

Up to now it is known that the hepatic 2-arachidonoyl glycerol (2-AG) and anandamide (AEA) levels as well as the expression levels of their receptors are strongly upregulated in hepatic injury and fibrogenesis (Biswas et al., 2003; Julien et al., 2005; Siegmund et al., 2007; Siegmund et al., 2005b). Furthermore, it was shown that 2-AG induces apoptotic cell death specifically in HSCs but not in hepatocytes (Siegmund et al., 2007). AEA, which belongs to the group of N-acyl-ethanolamines, was shown to induce necrotic cell death in HSCs whereas no cytotoxic effect was shown in the parenchymal cells of the liver (Siegmund et al., 2005b).

In this thesis it is reported the first time that the three recently discovered enocannabinoids, virodhamine, noladin ether and NADA specifically induce necrotic cell death in hepatic stellate cells in a dose-dependent manner. In contrast, hepatocytes are resistant to virodhamine-, noladin ether- as well as to NADA-mediated cell death. As mentioned above, the biosynthetic pathways of virodhamine and noladin ether are not investigated so far. Interestingly, in this study it was shown that the rate-limiting production enzyme of NADA, tyrosine hydroxylase, is expressed in normal as well as in injured liver. Western blotting revealed a strong expression in primary hepatocytes but not in activated primary HSCs, indicating a selective role of hepatocytes in NADA production in the liver. By this finding, the

study of the effects of this endocannabinoid achieves *in vivo* relevance. The focus shifted to further investigations of NADA. Moreover, virodhamine and noladin ether belong to the group of ethanolamides and monoglycerols, respectively, that were both already examined in hepatic cells (Piomelli, 2003). NADA belongs to the N-acyl-dopamines, a novel group of endocannabinoids, which has not been investigated in the liver so far (Bisogno et al., 2000).

The fact that the cytotoxic potency of NADA occurs in the short time period of 2 h after stimulation with 25 µM led to the suggestion that cell death induced by NADA is necrotic. Since endocannabinoids display a volatile appearance due to their production on demand and fast degradation (Di Marzo et al., 2004), the rapid induction of cell death shown here in cell culture experiments assumed a possible cytotoxic effect on HSCs *in vivo*. It has been shown that AEA induces cell death with concentrations of 2-20 µM, depending on the cell type (Contassot, Tenan, Schnuriger, Pelte, & Dietrich, 2004a; Contassot et al., 2004b; Giuliano et al., 2006; Saunders et al., 2009). NADA concentrations may also reach levels comparable to AEA and rapidly induce cell death in HSCs. Therefore, the mainly used concentration of 25 µM NADA in this thesis can be considered to be in the physiological range of NADA levels *in vivo*.

Due to the fact that NADA-induced cell death in other cell types is apoptotic and occurs much later, the necrotic character of NADA-mediated cell death was examined in the present study. To further confirm that the form of cell death induced by NADA was necrotic, cells were treated with propidium iodide, a marker for necrosis, which results in a strong PI staining of the nuclei of NADA-treated cells. As expected, caspase inhibition with a specific caspase-inhibitor (Z-VAD-FMK) decreased TNFα-induced HSC apoptosis, but not NADA-induced death, prefiguring caspase 3-independent necrosis.

Another important question to answer was the impact of nanomolar concentrations of NADA on activated primary HSCs. The results obtained from the wound healing assay demonstrate a remarkable inhibitory effect on proliferation and migration. To analyze the influence of NADA to HSC proliferation in more detail, the phosphorylation of ERK was determined. In a recent study it was shown that the activation of this kinase displays pro-proliferative and anti-fibrotic effects in HSCs (Teixeira-Clerc et al., 2006). In the present thesis, a remarkable inhibition of ERK phosphorylation was observed by exposure of the cells to NADA. Moreover, a lower expression of α-SMA was detected after daily treatment of freshly isolated HSCs with 1000 nM of NADA, indicating that NADA is also able to decelerate HSCs activation, which in contrast was not achieved by comparable concentrations of AEA. These findings represent another aspect of the anti-fibrotic properties of NADA in the liver.

NADA was recently identified as an endogenous ligand for the transient receptor potential vanilloid type 1 (TRPV1) channel due to its vanillyl-amine moiety (Bisogno et al., 2000; De Petrocellis, Bisogno, Davis, Pertwee, & Di Marzo, 2000; Walpole et al., 1993). Moreover,

recent studies have demonstrated that TRPV1 plays a pivotal role in NADA-induced cell death in a neuron-like cell population by generation of reactive oxygen species (ROS) (Davies et al.). In contrast to the findings of Davies and colleagues, the results obtained from the co-stimulatory experiments with NADA and capsazepine, a specific inhibitor of TRPV1, did not show any difference in the susceptibility of NADA-induced cell death. When the cells were exposed to a specific agonist of TRPV1, capsaicin, no cell death could be observed, which argues against an involvement of this receptor in NADA-induced cell death. Moreover, there was no evidence for an involvement of CB_1 receptors in this process, although the binding affinity of NADA to CB_1 receptors is even higher than the affinity of AEA (Bisogno et al., 2000). Additionally, the involvement of the CB_2 receptor, to which NADA shows low affinity, could also be ruled out. Considering that NADA does not display any dopamine receptor activity, although NADA possesses a dopamine moiety (Bisogno et al., 2000), the involvement of these receptors was not investigated. Since all three receptors investigated in this study are expressed on HSCs (Siegmund et al., 2005b), but were shown not to be involved, NADA induced cell death independently of these receptors. Previously it was shown that AEA-mediated cell death requires the presence of membrane cholesterol (Siegmund et al., 2005b). An alternative mechanism might be that NADA, like AEA, acts through membrane cholesterol to induce cell death. This would explain at least in part the different susceptibility of HSCs and hepatocytes, since hepatocytes have significantly less cholesterol in their plasma membrane (Siegmund et al., 2005b). However, the fact that preincubation with the membrane cholesterol depletor MCD did not prevent HSCs from cell death indicated that cholesterol-rich lipid rafts are not involved. However, the exact signal transduction from cellular uptake to initiation of death induced by NADA remains to be elucidated.

NADA stimulation induced a rapid induction of ROS in similar ranges as AEA. High amounts of rapidly generated ROS are known to lead to damage of intracellular macromolecules thus initiating necrosis (Raffray & Cohen, 1997). In the present study, treatment of HSCs with antioxidants (GSH, TROLOX) blocked the induction of cell death. In line with that, after the depletion of antioxidants, 10 µM NADA was sufficient to significantly induce cell death suggesting a pivotal role of ROS generation in the process.

As mentioned above, a stable expression of tyrosine hydroxylase (TH), the rate limiting NADA-generating enzyme, was found in hepatocytes, but not in HSCs, indicating that hepatocytes possess the capability for NADA production. Since NADA-mediated death of HSCs was triggered by rapid induction of noxious ROS production and could be ameliorated by incubation of the cells with antioxidants, it was first checked whether depletion of GSH in hepatocytes could render susceptibility toward NADA-mediated death. Indeed, hepatocytes resistance toward NADA-induced cell death was due to the effective antioxidant defence

mechanism of high GSH expression. Moreover, additional factors that may confer resistance against NADA-mediated cell death were investigated. Hu and colleagues revealed in 2009 that NADA represents a good substrate for catechol-O-methyl transferase (COMT) (Hu et al., 2009). NADA is converted by COMT to its less potent 3-O-methyl derivative. However, COMT expression in hepatocytes as well as in HSCs were under the detection level in the experiment discussed here, although there was a strong expression in HEK293 cells. Consequently, this degradation pathway did not contribute to NADA resistance observed in hepatocytes, since selective inhibition of COMT by the specific inhibitor OR-486 did not rescue hepatocytes from the cytotoxic effects of NADA.

Another degradation pathway of NADA is its hydrolysation by fatty acid amide hydrolase (FAAH) into arachidonic acid and dopamine (Hu et al., 2009; Huang et al., 2002). FAAH has initially been identified as the primary degradation enzyme for AEA (Cravatt et al., 1996). It has been shown that NADA is also metabolised by FAAH but five-fold slower than AEA due to the higher metabolic stability of NADA regarding to the dopamine derivative (Hu et al., 2009). Consistent with previous studies, FAAH is highly expressed in hepatocytes but not in HSCs (Siegmund et al., 2006). Treatment with URB597, a specific inhibitor of FAAH, rendered hepatocytes susceptibility to NADA-induced cell death. Additionally, hepatocytes isolated from FAAH $^{-/-}$ mice are sensitised to NADA-mediated death. To further elucidate these findings, FAAH was overexpressed in HSCs using a FAAH-expressing adenovirus resulting in resistance against NADA. The results of these studies underline the pivotal role for FAAH in mediating resistance of the liver parenchyma to the cytotoxic effects of NADA. Similar results were obtained in recent studies, where FAAH was shown to play a crucial role in the resistance of hepatocytes against AEA-induced cell death (Siegmund et al., 2006).

In conclusion, NADA mediates cell death specifically in HSCs due to increased generation ROS (Figure 27). NADA does not induce cell death in hepatocytes due to their high levels of antioxidants and FAAH. FAAH was also shown to be a putative synthesising enzyme for NADA (Hu et al., 2009), but since FAAH primarily conferred resistance against NADA-induced cell death, FAAH displays rather a pivotal role in NADA degradation in these cells than in synthesis.

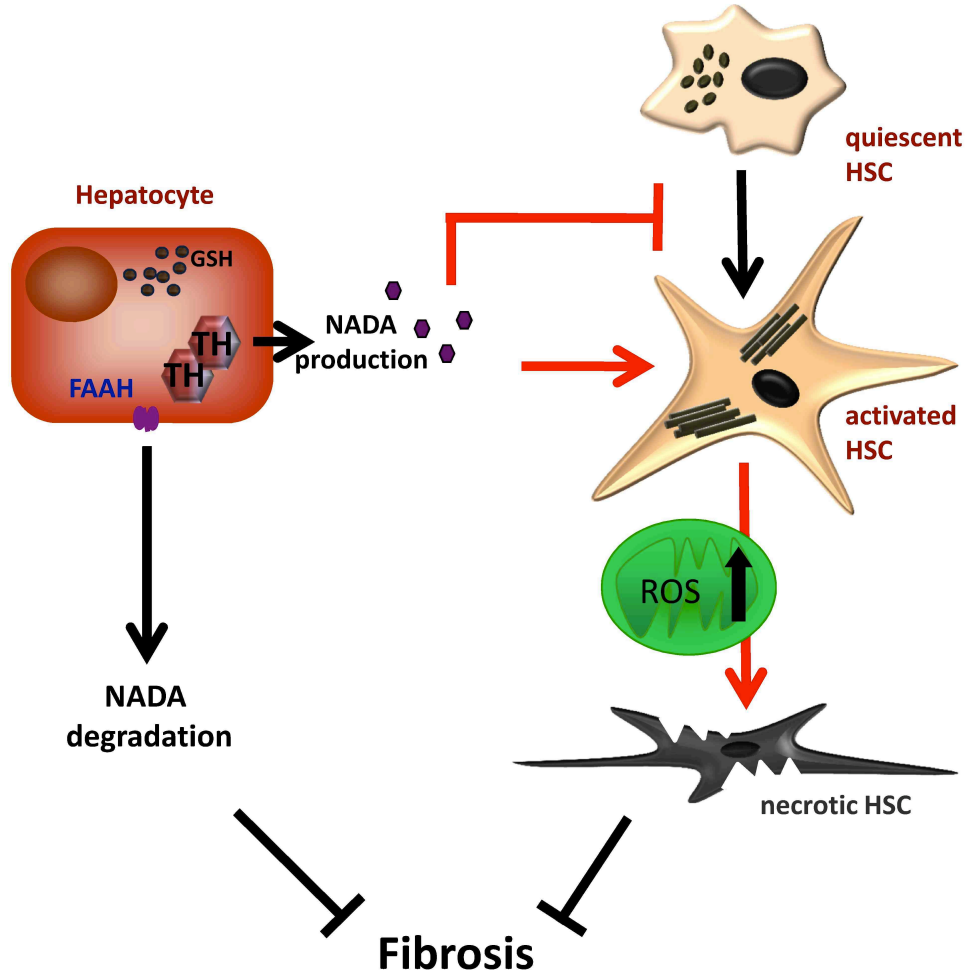

Figure 27. Scheme of the proposed NADA-induced cell death. Hepatocytes produce N-arachidonoyl dopamine (NADA) catalysed by tyrosine hydroxylase (TH). After release, NADA inhibit activation of hepatic stellate cells (HSCs) by a yet unknown mechanism. Furthermore, NADA induces necrotic cell death in HSCs by a strong induction of reactive oxygen species (ROS) generation. Hepatocytes are protected against NADA-mediated cell death due to high levels of antioxidants (GSH) and strong expression of fatty acid amide hydrolase (FAAH), which is able to degrade NADA.

The selective expression of effective defence systems (antioxidants, FAAH) and the selective expression of the rate-limiting NADA producing enzyme TH in hepatocytes as well as the selective induction of cell death in HSCs shown by the present analyses proposes NADA as a novel anti-fibrotic endogenous agent.

5.3 Definition of the cellular source of elevated 2-AG levels in the liver

2-arachidonoyl glycerol (2-AG) is an endogenous arachidonic acid derivative released on demand from membrane precursors (Piomelli, 2003). In 1995, 2-AG was distributed to the group of endocannabinoids. Many of the effects of 2-AG are mediated by the cannabinoid receptors CB_1 and CB_2 (Mechoulam et al., 1995). The normal, healthy liver contains only

small amounts of 2-AG. However, liver injury caused by ischemia/reperfusion triggers significantly augmented 2-AG levels. Furthermore, ethanol feeding in mice led to an upregulation in hepatic 2-AG levels (Batkai et al., 2007; Jeong et al., 2008). A significant increase in 2-AG levels was also found in two well-established mouse models of liver injury and fibrosis. For the induction of hepatic injury and fibrogenesis, mice underwent either ligation of the common bile duct leading to cholestatic liver disease or were treated with CCl_4 causing toxic liver damage. In both models an approximately three-fold elevation of 2-AG was observed (Siegmund et al., 2007). Taken together, 2-AG is strongly upregulated in hepatic injury and fibrogenesis. Up to now, it is not known whether an increase in the synthesis or a decline in the expression of degradation enzymes is responsible for this effect. 2-AG is produced via the hydrolysis of diacylglycerol (DAG) with arachidonate, which is catalysed by one of two highly related DAG lipases (DAGLα and β), depending on the cell type (Gao et al.). To examine the role of 2-AG synthesis in liver fibrogenesis, the expression of DAGLα and β were examined in bile duct ligated mice. The expression of DAGLα was clearly decreased, excluding that this lipase is responsible for elevated 2-AG levels found in the injured liver. Although there was no significant induction of DAGLβ expression seven days after surgery, the results showed clearly a five-fold significant increase in DAGLβ mRNA levels on day 14. In whole liver tissue, 40-fold higher levels of DAGLβ compared to DAGLα were observed. A previous study showed that DAGLα is expressed in the liver and there is a 60 % reduction in 2-AG levels in DAGLα$^{-/-}$ mice. Nevertheless, loss of DAGLβ results in an almost 90 % decrease of 2-AG (Gao et al.) suggesting that DAGLβ is the main 2-AG producing enzyme in the liver. On the cellular level, these findings were confirmed since the amount of DAGLβ mRNA is up to 100-fold higher than the amount of DAGLα in all examined liver cells. These data and the data published by Gao et al. prefigure DAGLβ rather than DAGLα as the main 2-AG-producing enzyme in the liver.

The late onset of DAGLβ expression as the dominant synthesising machinery in the liver may be at least in part responsible for the elevated 2-AG levels in the injured liver. The fact that an increased 2-AG content could already be detected three days after bile duct ligation (Siegmund et al., 2007) implies the involvement of other mechanisms in the upregulation of 2-AG levels during liver injury and fibrogenesis. Therefore, the focus of the present study switched to the investigation of changes in 2-AG degradation pathways.

After its cellular uptake, 2-AG is rapidly degraded by intracellular hydrolysis catalysed by the serine hydrolase monoacylglycerol lipase (MGL) (Bisogno, Ligresti, & Di Marzo, 2005; Dinh et al., 2004). Moreover, it was shown, that FAAH is able to degrade 2-AG *in vitro* (Muccioli). In the bile duct ligated mice analysed here, a significant decline in FAAH as well as in MGL levels were observed seven days after surgery. This reduction in the metabolism of 2-AG possibly explains its upregulation in the early state of liver damage. Since it was shown that

FAAH$^{-/-}$ mice showed unchanged tissue levels of 2-AG (Muccioli) (Patel et al., 2005), MGL rather than FAAH seems to be the responsible enzyme for increased 2-AG levels.

Up to now, no data exists on the contribution of different cell types in the liver to the production and metabolism of 2-AG. To investigate which cells are mainly involved in the production of 2-AG, the expression levels of DAGLα as well as DAGLβ were examined in hepatocytes and non-parenchymal cells. In contrast to the low DAG lipase levels in hepatocytes, a strong expression of DAGLα as well as β in the non-parenchymal cells of the liver was observed suggesting that these cells are the major source of 2-AG production. In recent studies, it was increasingly recognized that substances produced from non-parenchymal cells regulate many functions of the liver conducted by hepatocytes. It is possible that endocannabinoids are also produced by this cell fraction and interact with the parenchyma. Lately it has been shown that 2-AG produced in HSCs mediated an induction of CB_1 receptors on hepatocytes, which indicates a paracrine signalling mechanism between these liver cell populations (Jeong et al., 2008).

The results presented here demonstrate that LSECs and to a lesser extend HSCs are the main DAGLβ expressing cells in the liver. This is partly consistent with a previous study, which has shown that HSCs are the main source for increased hepatic 2-AG levels after ethanol feeding in mice. Indeed, no expression of DAGLβ and no upregulated 2-AG levels were found in hepatocytes (Jeong et al., 2008). Nevertheless, other cell types in the liver, like LSECs were not investigated so far. LSECs are responsible for the secretion of various cytokines and due to the fact that they possess the synthesising machinery of 2-AG, they appear to be able to produce and secrete 2-AG for autocrine or paracrine signalling in the liver. This corresponds to the finding that LSECs possess CB_1 as well as CB_2 receptors, which are both receptors for 2-AG (Batkai et al., 2001; Batkai et al., 2007). In this study, it is shown the first time, that LSECs crucially contribute to 2-AG production and may be mainly responsible for the upregulation of 2-AG levels in the injured and fibrotic liver. Interestingly, LSECs and HSCs express the highest levels of MGL in the liver, leading to the conclusion that these cell types possess the production and the degradation machinery for 2-AG.

FAAH is mainly expressed in hepatocytes, but only marginally in the non-parenchymal cells. This finding is in good agreement with similar results from previous studies, where FAAH expression levels were examined in HSCs and hepatocytes. However, in the study at hand it was shown that other non-parenchymal cell types do not express FAAH. Thus, hepatocytes are able to degrade endocannabinoids such as 2-AG although they lack the capability of their synthesis.

In conclusion, 2-AG in the liver is mainly produced and degraded by LSECs and HSCs. Elevated 2-AG levels occurring during fibrogenesis are rather driven by decreased degradation than by upregulation of production. The data further point towards LSECs and

HSCs rather than to other cell types as being the most important hepatic cell populations for 2-AG metabolism during liver injury and fibrogenesis.

5.4 Analysis of 2-AG-induced cell death in HSCs

After identification of the cellular source and the enzymes responsible for 2-AG upregulation, the focus shifted to the analysis of the potential, anti-fibrogenic properties of 2-AG. 2-AG induces cell death in HSCs, the main fibrogenic cell type in the liver, which is accompanied by a dramatic increase in the generation of mitochondrial reactive oxygen species (ROS). In contrast to HSCs, hepatocytes were completely resistant to 2-AG-induced cell death. However, the reason for the different susceptibility and the exact mechanism underlying this effect is unclear so far (Siegmund et al., 2007).

The cytotoxic effects of 2-AG could not be explained by activation of the known receptors or by metabolism via its degradation enzymes MGL and FAAH. Inhibition of the receptors or MGL did neither alter the sensitivity of 2-AG induced cell death in HSCs nor in hepatocytes (Siegmund et al., 2007). Furthermore, due to the lack of FAAH expression in HSCs, the involvement of metabolites of FAAH was also excluded (Siegmund et al., 2006).

The presence of a arachidonoyl moiety in the structure of 2-AG suggests that it is able to serve as a substrate for metabolism by other enzymes beside FAAH and MGL (Kozak et al., 2004). Indeed, a few years ago COX-2 was shown to metabolise AEA and 2-AG to prostamides and prostaglandin glycerol esters (PG-GE), respectively (Kozak et al., 2002).

However, in liver fibrogenesis the effects of COX-2 are discussed controversially and a definitive role for COX-2 has not been elucidated so far (Yu et al., 2008). It is known that COX-2 is marginally expressed in healthy liver. In response to inflammation, COX-2 is highly inducible by inflammatory cytokines and has been reported to be increased in several types of liver injury such as chronic hepatitis or cirrhosis (Jeong et al.). COX-2 inhibitors were shown to decrease α-SMA expression in HSCs (Cheng et al., 2002) and were able to reduce CCl_4-induced liver fibrosis in mice (Horrillo et al., 2007). In contrast, COX-2 displayed hepato-protective activities in models of toxic liver injury in mice and in CCL_4-induced liver fibrosis in rats (Hui et al., 2006; Reilly et al., 2001).

To analyse the expression pattern of COX-2 under fibrogenic conditions in an animal model, livers of sham operated and bile duct ligated mice were investigated for COX-2 expression. A significant increase of 13-fold or more than 60-fold was found seven days and fourteen days after surgery, respectively. It seems that the expression of COX-2 is strongly upregulated in the early states of hepatic inflammation and injury. The cells in the liver that are typically involved in the inflammatory response are KCs, the resident macrophages in the liver. Previously it was shown that KCs represent the primary source for COX-2 in alcoholic liver disease (Nanji et al., 1997). In contrast, hepatocytes in primary culture as well as *in vivo* are

not able to express high amounts of COX-2 even after onset of inflammation (Martin-Sanz, Mayoral, Casado, & Bosca). This is consistent with the results of this study, since hepatocytes only marginally expressed COX-2. Interestingly, HSCs showed seven-fold higher levels of COX-2 compared to hepatocytes. Julien and colleagues showed that increasing levels of COX-2 have growth-inhibitory effects on HSCs, which were reduced by specific COX-2 inhibitors. In their study, the exogenous cannabinoid THC was responsible for the upregulation of COX-2 (Julien et al., 2005). Moreover, cannabinoids are also able to induce COX-2 expression in neuroglioma and lung cancer cells (Bifulco, Laezza, Pisanti, & Gazzerro, 2006). If cannabinoid-induced upregulation of COX-2 leads to growth arrest in HSCs, endocannabinoids such as 2-AG represent a possible antifibrotic tool. Indeed, it is known that 2-AG also evokes growth arrest by a yet unidentified mechanism (Jacobsson, Wallin, & Fowler, 2001).

In the injured liver, paralleling the overexpression of COX-2, 2-AG is also strongly upregulated (Siegmund et al., 2007). The question rose whether COX-2 plays a noteworthy role in 2-AG-induced cell death. 2009, it was shown that the endocannabinoid anandamide selectively induces cell death in keratinocytes due to elevated COX-2 expression and the resulting metabolism of AEA to cytotoxic prostaglandin ethanol amides. This work reflects the significance of endocannabinoid metabolic products in the initiation of cell death (Van Dross, 2009). COX-2 was shown to metabolise 2-AG more efficiently than AEA (Kozak et al., 2004). The cytotoxic effects of 2-AG could correlate with the catalytic activity of COX-2, which metabolises this endocannabinoid to prostaglandin glycerol esters.

To examine, whether PG-GEs have any effects on HSCs and hepatocytes, primary cells were treated with various PG-GE to determine the contribution of each to induce cell death.

Interestingly, only prostaglandin D_2 glycerol ester (PGD_2-GE) was found to have cytotoxic effects. It is known that 2-AG induces apoptotic cell death in HSCs but not in hepatocytes (Siegmund et al., 2007). After oxygenation of 2-AG to PGD_2-GE, cell type specific toxicity is not present anymore and the COX-2 metabolite induced apoptosis in HSCs as well as in hepatocytes via a caspase-3- and PARP-dependent pathway.

Less is known about the biosynthesis of PG-GE *in vivo*. In a previous study it was shown that COX-2 converted exogenous 2-AG to PGH_2-GE. PGD synthase converted the H_2 derivative to PGD_2-GE as the final glycerol ester product in a macrophage cell line (Kozak et al., 2000). Indeed, HSCs were able to metabolise the endocannabinoid 2-AG to PGD_2-GE, in contrast to hepatocytes, which failed to produce prostaglandins. These findings represent a possible explanation for the resistance of hepatocytes to 2-AG-mediated cell death due to the lack of COX-2 expression. However, less is known about PGD_2-GE and the role of this metabolite in 2-AG-induced apoptosis has to be further characterised.

It was previously shown that PGD_2-GE could spontaneously be converted to its prostaglandin counterpart (PGD_2). PGD_2 inhibits cell proliferation and induces apoptosis in various cell types including non-small cell lung carcinoma (Wang & Mak), leukaemia cells (Azuma, Watanabe, Date, Daito, & Ohura, 2004) and colon cancer cells (Yoshida et al., 1998). Interestingly, in this thesis, rather PGD_2-GE than PGD_2 is responsible for the cytotoxic effect of 2-AG in HSCs.

Up to now, limited data is available regarding the metabolism of endocannabinoids as a source of novel lipid mediators. COX-2 activity was mainly found in the central nervous system, inflammatory cells and also in liver cells paralleling the distribution of cannabinoid receptors (Kozak et al., 2000). Nevertheless, the connection between the endocannabinoid system and COX-2 has slowly been uncovered. The experimental results in this study suggest that part of the cytotoxic effects of 2-AG in HSCs is attributed to high COX-2 expression and conversion of 2-AG by COX-2 to cytotoxic PG-D_2-GE (Figure 28).

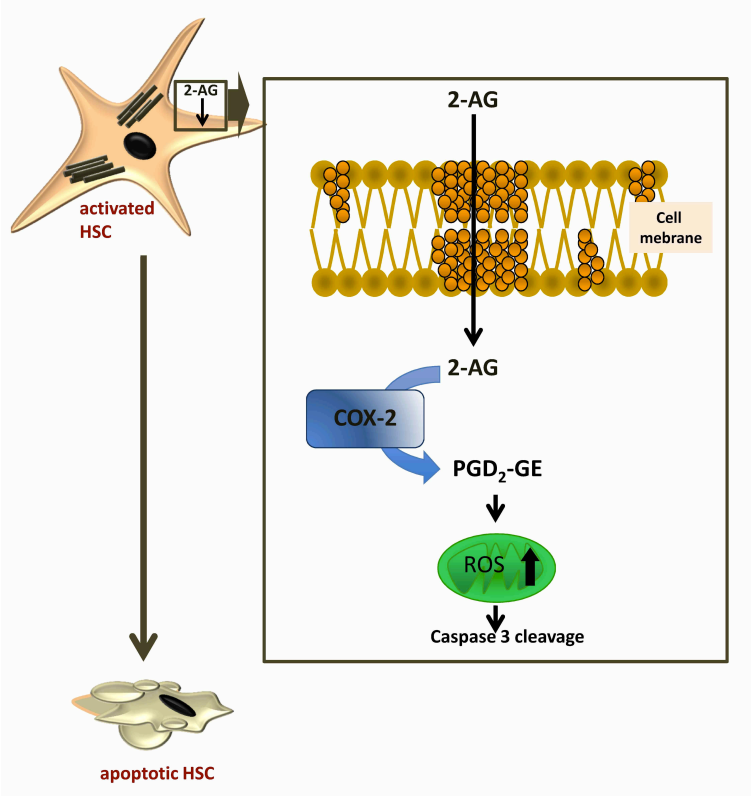

Figure 28. Scheme of proposed 2-arachidonoyl glycerol (2-AG) death signalling. 2-AG bind to unknown structures in cholesterol rich lipid rafts. Inside the cell, 2-AG is metabolised to prostaglandin D2 glycerol ester (PGD2-GE) catalysed by cyclooxygenase-2 (COX-2). PGD_2-GE possibly upregulates the generation of reactive oxygen species (ROS) and induces caspase-3-dependent apoptotic cell death in hepatic stellate cells (HSCs).

In this study, the advantage of COX-2 catalytic activity was explored. The results showed that the metabolites of 2-AG were toxic specifically in HSCs, which express high amounts of COX-2. Since COX-2 is expressed specifically in HSCs and it is possible to induce an

upregulation of COX-2 by endocannabinoids, 2-AG may be useful for the treatment of liver fibrosis. The data reported in this study suggest that COX-2 expression provides a supply of bioactive lipids-protect against liver injury.

5.5 Conclusion and future directions

The results presented in this work provide new insights in the role of the endocannabinoid system in the liver. Modulating this system seems to be a promising target for the treatment of hepatic injury.

HSCs are highly sensitive to endocannabinoid-induced cell death. In recent studies it was shown that 2-AG and AEA are able to induce specifically cell death in HSCs (Siegmund et al., 2007; Siegmund et al., 2005b). However, their susceptibility to enzymatic hydrolysis reduces the efficiency and more stable endocannabinoids may serve better for a model of drug development. In addition, due to their fast degradation, a rapid induction of cell death is necessary for using these lipid mediators as an approach for antifibrotic therapy. This thesis showed that NADA-induced cell death occurred very fast. In contrast to 2-AG and AEA, NADA is much more stable and is degraded 5-times slower by FAAH than AEA (Hu et al., 2009). Thus, NADA has the conditions to function as an antifibrotic tool.

Moreover, hepatocytes are shown to be able to produce NADA in the injured liver. The hypothesis is that after its release, NADA can act on HSCs and inhibit activation or –in higher doses- induce cell death. Unquestionably, more work is necessary to examine the exact mechanism how NADA participate in the pathophysiology of liver fibrosis. However, the findings of this work provide new insights of the possible role of NADA as an antifibrotic tool. In future studies, the effects of NADA on other hepatic cell types should be investigated. Are Kupffer and LSEC cells protected against NADA-induced cell death?

Another question rose: Does NADA also have physiological functions in the healthy liver? Indeed, the NADA synthesising enzyme TH is expressed in normal liver. However, further information is required to fully understand the role of NADA in the healthy as well as the injured liver.

It is known that 2-AG levels are strongly upregulated during hepatic fibrogenesis (Siegmund et al., 2007). This thesis showed that the expression of the 2-AG-synthesising enzyme DAGLβ is elevated in liver injury whereas the levels of MGL, which is responsible for 2-AG degradation, are significantly decreased. These findings can certainly offer new therapeutic perspectives: modulation of DAGLβ as well as MGL levels can be used to keep 2-AG levels upregulated and decelerate fibrogenesis by its antifibrotic effects.

One believed antifibrotic effect of 2-AG is cell death induction specifically in HSCs (Siegmund et al., 2007). The results of this thesis suggested that the cytotoxic effect of 2-AG is due to its conversion to PGD_2-GE by COX-2. This finding provides new insights in the understanding of

the molecular mechanisms of 2-AG-induced cell death. Moreover, the results of this work shifted the focus from 2-AG to PGD_2-GE as an antifibrotic substance. Needless to say, further studies are required to investigate the role of COX-2 in 2-AG-induced cell death.

In this work, NADA, 2-AG and also PGD_2-GE as antifibrotic agents are effective in cultures of activated HSCs. In future studies, the next step has to be the investigation in experimental models of liver fibrosis *in vivo*. The findings of endocannabinoid treatment in liver-injured animals may have clinical relevance in the development of antifibrotic therapies.

Another important problem to solve will be the specific targeting of activated HSCs. The agent should not bind to myofibroblasts in other tissues or to quiescent HSCs. Moreover, it has to reach the regions with active fibrogenesis. Future work should be focus on novel carriers which bind specifically to activated HSCs. like to the collagen type VI receptor (Beljaars et al., 2000).

In conclusion, due to the lack of antifibrotic drugs at present, the investigation of endocannabinoids and their promising functions in fibrogenesis will be an important issue in future work.

6 SUMMARY

Liver fibrosis is the response to chronic hepatic injury and results from an excessive deposition of connective scar tissue. Liver cirrhosis, the end stage of fibrosis, leads to further severe complications like ascites and peritonitis resulting in a high mortality rate worldwide. Hepatic stellate cells (HSCs) are the main responsible cells for the increased synthesis of extracellular tissue. While cell death in hepatocytes, the parenchymal cells in the liver, plays a pivotal role in the activation of HSCs and deterioration of this disease, removal of activated HSCs preceded amelioration of fibrosis.

In this thesis it was shown the first time, that the endocannabinoids virodhamine, noladin ether and N-arachidonoyl dopamine (NADA) specifically induce cell death in HSCs. Due to the selective expression of effective defense systems like antioxidants and the NADA degradation enzyme fatty acid amide hydrolase (FAAH), hepatocytes showed resistance to NADA-induced cell death. The rate limiting enzyme of NADA, tyrosine hydroxylase, was shown to be strongly expressed in hepatocytes in the healthy as well as the injured liver. Thus, NADA has potential as an antifibrotic endogenous agent.

It was recently demonstrated that the endogenous cannabinoid 2-arachidonoyl glycerol (2-AG) is strongly upregulated in the injured liver. The present study showed that the main 2-AG producing cells are liver sinusoidal endothelial cells (LSECs). They showed a strong expression of the 2-AG synthesising enzyme DAGLβ as well as of the degradation enzyme monoacylglycerol lipase (MGL). Elevated 2-AG levels during fibrogenesis are rather driven by decreased degradation than by upregulation of 2-AG production.

It is known that 2-AG specifically induces cell death in HSCs but not in hepatocytes. To examine the different susceptibility of HSCs and hepatocytes to 2-AG-induced cell death, the role of an alternative metabolic pathway of 2-AG was investigated. In this pathway, 2-AG is converted to prostaglandin glycerol esters (PG-GEs) by the catalytic activity of cyclooxygenase-2 (COX-2). It could be shown, that COX-2 is highly expressed in HSCs but not in hepatocytes. Furthermore, HSCs are able to produce PGD_2-GE after 2-AG exposure. PGD_2-GE had cytotoxic effects on HSCs as well as on hepatocytes. Hepatocytes are resistant to 2-AG-induced cell death possibly due to the lack of COX-2 and the missing production of cytotoxic PGD_2-GE. The results in this study represent an important step in the understanding of 2-AG-mediated pathways in liver injury and make it possible to specifically target components of this system to decrease hepatic fibrogenesis.

In conclusion, the present study has provided new findings about the mechanism of 2-AG-signalling in liver injury. Moreover, a possible functional role of NADA during liver injury was investigated. These results faciliate the use of components of the endocannabinoid system for antifibrotic, therapeutical purposes.

7 REFERENCES

Arthur, M. J. (2000). Fibrogenesis II. Metalloproteinases and their inhibitors in liver fibrosis, *Am J Physiol Gastrointest Liver Physiol* (pp. G245-9).

Azuma, Y., Watanabe, K., Date, M., Daito, M., & Ohura, K. (2004). Possible involvement of p38 in mechanisms underlying acceleration of proliferation by 15-deoxy-Delta(12,14)-prostaglandin J2 and the precursors in leukemia cell line THP-1. *J Pharmacol Sci* 94, 261-70.

Bataller, R., & Brenner, D. A. (2005). Liver fibrosis, *J Clin Invest* (pp. 209-18).

Bataller, R., Nicolas, J. M., Gines, P., Esteve, A., Nieves Gorbig, M., Garcia-Ramallo, E., Pinzani, M., Ros, J., Jimenez, W., Thomas, A. P., Arroyo, V., & Rodes, J. (1997). Arginine vasopressin induces contraction and stimulates growth of cultured human hepatic stellate cells. *Gastroenterology* 113, 615-24.

Batkai, S., Jarai, Z., Wagner, J. A., Goparaju, S. K., Varga, K., Liu, J., Wang, L., Mirshahi, F., Khanolkar, A. D., Makriyannis, A., Urbaschek, R., Garcia, N., Jr., Sanyal, A. J., & Kunos, G. (2001). Endocannabinoids acting at vascular CB1 receptors mediate the vasodilated state in advanced liver cirrhosis. *Nat Med* 7, 827-32.

Batkai, S., Osei-Hyiaman, D., Pan, H., El-Assal, O., Rajesh, M., Mukhopadhyay, P., Hong, F., Harvey-White, J., Jafri, A., Hasko, G., Huffman, J. W., Gao, B., Kunos, G., & Pacher, P. (2007). Cannabinoid-2 receptor mediates protection against hepatic ischemia/reperfusion injury. *FASEB J* 21, 1788-800.

Beljaars, L., Molema, G., Schuppan, D., Geerts, A., De Bleser, P. J., Weert, B., Meijer, D. K., & Poelstra, K. (2000). Successful targeting to rat hepatic stellate cells using albumin modified with cyclic peptides that recognize the collagen type VI receptor. *J Biol Chem* 275, 12743-51.

Beltramo, M., & Piomelli, D. (2000). Carrier-mediated transport and enzymatic hydrolysis of the endogenous cannabinoid 2-arachidonylglycerol. *Neuroreport* 11, 1231-5.

Bifulco, M., Laezza, C., Pisanti, S., & Gazzerro, P. (2006). Cannabinoids and cancer: pros and cons of an antitumour strategy. *Br J Pharmacol* 148, 123-35.

Bisogno, T., Ligresti, A., & Di Marzo, V. (2005). The endocannabinoid signalling system: biochemical aspects. *Pharmacol Biochem Behav* 81, 224-38.

Bisogno, T., Melck, D., Bobrov, M., Gretskaya, N. M., Bezuglov, V. V., De Petrocellis, L., & Di Marzo, V. (2000). N-acyl-dopamines: novel synthetic CB(1) cannabinoid-receptor ligands and inhibitors of anandamide inactivation with cannabimimetic activity in vitro and in vivo. *Biochem J* 351 Pt 3, 817-24.

Biswas, K. K., Sarker, K. P., Abeyama, K., Kawahara, K., Iino, S., Otsubo, Y., Saigo, K., Izumi, H., Hashiguchi, T., Yamakuchi, M., Yamaji, K., Endo, R., Suzuki, K., Imaizumi, H., & Maruyama, I. (2003). Membrane cholesterol but not putative receptors mediates anandamide-induced hepatocyte apoptosis. *Hepatology* 38, 1167-77.

Brown, S. M., Wager-Miller, J., & Mackie, K. (2002). Cloning and molecular characterization of the rat CB2 cannabinoid receptor. *Biochim Biophys Acta* 1576, 255-64.

Capasso, R., Matias, I., Lutz, B., Borrelli, F., Capasso, F., Marsicano, G., Mascolo, N., Petrosino, S., Monory, K., Valenti, M., Di Marzo, V., & Izzo, A. A. (2005). Fatty acid amide hydrolase controls mouse intestinal motility in vivo. *Gastroenterology* 129, 941-51.

Chang, M. H., Chen, C. J., Lai, M. S., Hsu, H. M., Wu, T. C., Kong, M. S., Liang, D. C., Shau, W. Y., & Chen, D. S. (1997). Universal hepatitis B vaccination in Taiwan and the incidence of hepatocellular carcinoma in children. Taiwan Childhood Hepatoma Study Group. *N Engl J Med* 336, 1855-9.

Cheng, J., Imanishi, H., Liu, W., Iwasaki, A., Ueki, N., Nakamura, H., & Hada, T. (2002). Inhibition of the expression of alpha-smooth muscle actin in human hepatic stellate cell line, LI90, by a selective cyclooxygenase 2 inhibitor, NS-398. *Biochem Biophys Res Commun* 297, 1128-34.

Contassot, E., Tenan, M., Schnuriger, V., Pelte, M. F., & Dietrich, P. Y. (2004a). Arachidonyl ethanolamide induces apoptosis of uterine cervix cancer cells via aberrantly expressed vanilloid receptor-1. *Gynecol Oncol* 93, 182-8.

Contassot, E., Wilmotte, R., Tenan, M., Belkouch, M. C., Schnuriger, V., de Tribolet, N., Burkhardt, K., & Dietrich, P. Y. (2004b). Arachidonylethanolamide induces apoptosis of human glioma cells through vanilloid receptor-1. *J Neuropathol Exp Neurol* 63, 956-63.

Correa, F., Docagne, F., Clemente, D., Mestre, L., Becker, C., & Guaza, C. (2008). Anandamide inhibits IL-12p40 production by acting on the promoter repressor element GA-12: possible involvement of the COX-2 metabolite prostamide E(2). *Biochem J* 409, 761-70.

Cravatt, B. F., Giang, D. K., Mayfield, S. P., Boger, D. L., Lerner, R. A., & Gilula, N. B. (1996). Molecular characterization of an enzyme that degrades neuromodulatory fatty-acid amides. *Nature* 384, 83-7.

Davaille, J., Gallois, C., Habib, A., Li, L., Mallat, A., Tao, J., Levade, T., & Lotersztajn, S. (2000). Antiproliferative properties of sphingosine 1-phosphate in human hepatic myofibroblasts. A cyclooxygenase-2 mediated pathway. *J Biol Chem* 275, 34628-33.

Davies, J. W., Hainsworth, A. H., Guerin, C. J., & Lambert, D. G. Pharmacology of capsaicin-, anandamide-, and N-arachidonoyl-dopamine-evoked cell death in a homogeneous transient receptor potential vanilloid subtype 1 receptor population. *Br J Anaesth* 104, 596-602.

Day, C. P. (2005). Natural history of NAFLD: remarkably benign in the absence of cirrhosis, *Gastroenterology* (pp. 375-8).

De Petrocellis, L., Bisogno, T., Davis, J. B., Pertwee, R. G., & Di Marzo, V. (2000). Overlap between the ligand recognition properties of the anandamide transporter and the VR1 vanilloid receptor: inhibitors of anandamide uptake with negligible capsaicin-like activity. *FEBS Lett* 483, 52-6.

Despres, J. P., Golay, A., & Sjostrom, L. (2005). Effects of rimonabant on metabolic risk factors in overweight patients with dyslipidemia. *N Engl J Med* 353, 2121-34.

Devane, W. A., Hanus, L., Breuer, A., Pertwee, R. G., Stevenson, L. A., Griffin, G., Gibson, D., Mandelbaum, A., Etinger, A., & Mechoulam, R. (1992). Isolation and structure of a brain constituent that binds to the cannabinoid receptor. *Science* 258, 1946-9.

Di Marzo, V., Bifulco, M., & De Petrocellis, L. (2004). The endocannabinoid system and its therapeutic exploitation. *Nat Rev Drug Discov* 3, 771-84.

Di Marzo, V., Bisogno, T., De Petrocellis, L., Melck, D., Orlando, P., Wagner, J. A., & Kunos, G. (1999). Biosynthesis and inactivation of the endocannabinoid 2-arachidonoylglycerol in circulating and tumoral macrophages. *Eur J Biochem* 264, 258-67.

Di Marzo, V., & Matias, I. (2005). Endocannabinoid control of food intake and energy balance. *Nat Neurosci* 8, 585-9.

Dinh, T. P., Kathuria, S., & Piomelli, D. (2004). RNA interference suggests a primary role for monoacylglycerol lipase in the degradation of the endocannabinoid 2-arachidonoylglycerol. *Mol Pharmacol* 66, 1260-4.

Dixon, J. B., Bhathal, P. S., Hughes, N. R., & O'Brien, P. E. (2004). Nonalcoholic fatty liver disease: Improvement in liver histological analysis with weight loss. *Hepatology* 39, 1647-54.

Dong, M. H., & Saab, S. (2008). Complications of cirrhosis. *Dis Mon* 54, 445-56.

Duffield, J. S., Forbes, S. J., Constandinou, C. M., Clay, S., Partolina, M., Vuthoori, S., Wu, S., Lang, R., & Iredale, J. P. (2005). Selective depletion of macrophages reveals distinct, opposing roles during liver injury and repair, *J Clin Invest* (pp. 56-65).

Dufour, J. F., & Oneta, C. M. (2004). [Alcoholic and non-alcoholic steatohepatitis]. *Ther Umsch* 61, 505-12.

Enzan, H., Himeno, H., Hiroi, M., Kiyoku, H., Saibara, T., & Onishi, S. (1997). Development of hepatic sinusoidal structure with special reference to the Ito cells. *Microsc Res Tech* 39, 336-49.

Farrell, G. C., & Larter, C. Z. (2006). Nonalcoholic fatty liver disease: from steatosis to cirrhosis, *Hepatology* (pp. S99-S112).

Fezza, F., Bisogno, T., Minassi, A., Appendino, G., Mechoulam, R., & Di Marzo, V. (2002). Noladin ether, a putative novel endocannabinoid: inactivation mechanisms and a sensitive method for its quantification in rat tissues. *FEBS Lett* 513, 294-8.

Fisar, Z. (2009). Cannabinoids and atherosclerosis. *Prague Med Rep* 110, 5-12.

Friedman, S. L. (2000). Molecular regulation of hepatic fibrosis, an integrated cellular response to tissue injury, *J Biol Chem* (pp. 2247-50).

Friedman, S. L. (2004). Stellate cells: a moving target in hepatic fibrogenesis, *Hepatology* (pp. 1041-3).

Friedman, S. L. (2008a). Hepatic fibrosis -- overview. *Toxicology* 254, 120-9.

Friedman, S. L. (2008b). Hepatic stellate cells: protean, multifunctional, and enigmatic cells of the liver, *Physiol Rev* (pp. 125-72).

Friedman, S. L., & Roll, F. J. (1987). Isolation and culture of hepatic lipocytes, Kupffer cells, and sinusoidal endothelial cells by density gradient centrifugation with Stractan. *Anal Biochem* 161, 207-18.

Friedman, S. L., Roll, F. J., Boyles, J., Arenson, D. M., & Bissell, D. M. (1989). Maintenance of differentiated phenotype of cultured rat hepatic lipocytes by basement membrane matrix. *J Biol Chem* 264, 10756-62.

Friedman, S. L., Roll, F. J., Boyles, J., & Bissell, D. M. (1985). Hepatic lipocytes: the principal collagen-producing cells of normal rat liver. *Proc Natl Acad Sci U S A* 82, 8681-5.

Gallois, C., Habib, A., Tao, J., Moulin, S., Maclouf, J., Mallat, A., & Lotersztajn, S. (1998). Role of NF-kappaB in the antiproliferative effect of endothelin-1 and tumor necrosis factor-alpha in human hepatic stellate cells. Involvement of cyclooxygenase-2. *J Biol Chem* 273, 23183-90.

Gao, Y., Vasilyev, D. V., Goncalves, M. B., Howell, F. V., Hobbs, C., Reisenberg, M., Shen, R., Zhang, M. Y., Strassle, B. W., Lu, P., Mark, L., Piesla, M. J., Deng, K., Kouranova, E. V., Ring, R. H., Whiteside, G. T., Bates, B., Walsh, F. S., Williams, G., Pangalos, M. N., Samad, T. A., & Doherty, P. Loss of retrograde endocannabinoid signaling and reduced adult neurogenesis in diacylglycerol lipase knock-out mice. *J Neurosci* 30, 2017-24.

Gaoni, Y., & Mechoulam, R. (1971). The isolation and structure of delta-1-tetrahydrocannabinol and other neutral cannabinoids from hashish. *J Am Chem Soc* 93, 217-24.

Gawrieh, S., Papouchado, B. G., Burgart, L. J., Kobayashi, S., Charlton, M. R., & Gores, G. J. (2005). Early hepatic stellate cell activation predicts severe hepatitis C recurrence after liver transplantation. *Liver Transpl* 11, 1207-13.

Giampieri, M. P., Jezequel, A. M., & Orlandi, F. (1981). The lipocytes in normal human liver. A quantitative study. *Digestion* 22, 165-9.

Giuliano, M., Calvaruso, G., Pellerito, O., Portanova, P., Carlisi, D., Vento, R., & Tesoriere, G. (2006). Anandamide-induced apoptosis in Chang liver cells involves ceramide and JNK/AP-1 pathway. *Int J Mol Med* 17, 811-9.

Glaser, S. T., Abumrad, N. A., Fatade, F., Kaczocha, M., Studholme, K. M., & Deutsch, D. G. (2003). Evidence against the presence of an anandamide transporter. *Proc Natl Acad Sci U S A* 100, 4269-74.

Hanus, L., Abu-Lafi, S., Fride, E., Breuer, A., Vogel, Z., Shalev, D. E., Kustanovich, I., & Mechoulam, R. (2001). 2-arachidonyl glyceryl ether, an endogenous agonist of the cannabinoid CB1 receptor. *Proc Natl Acad Sci U S A* 98, 3662-5.

Harrison, S., De Petrocellis, L., Trevisani, M., Benvenuti, F., Bifulco, M., Geppetti, P., & Di Marzo, V. (2003). Capsaicin-like effects of N-arachidonoyl-dopamine in the isolated guinea pig bronchi and urinary bladder. *Eur J Pharmacol* 475, 107-14.

Herschman, H. R. (1996). Prostaglandin synthase 2. *Biochim Biophys Acta* 1299, 125-40.

Hezode, C., Roudot-Thoraval, F., Nguyen, S., Grenard, P., Julien, B., Zafrani, E. S., Pawlotsky, J. M., Dhumeaux, D., Lotersztajn, S., & Mallat, A. (2005). Daily cannabis smoking as a risk factor for progression of fibrosis in chronic hepatitis C. *Hepatology* 42, 63-71.

Ho, W. S., & Hiley, C. R. (2004). Vasorelaxant activities of the putative endocannabinoid virodhamine in rat isolated small mesenteric artery. *J Pharm Pharmacol* 56, 869-75.

Horrillo, R., Planaguma, A., Gonzalez-Periz, A., Ferre, N., Titos, E., Miquel, R., Lopez-Parra, M., Masferrer, J. L., Arroyo, V., & Claria, J. (2007). Comparative protection against liver inflammation and fibrosis by a selective cyclooxygenase-2 inhibitor and a nonredox-type 5-lipoxygenase inhibitor. *J Pharmacol Exp Ther* 323, 778-86.

Howard, R. B., Christensen, A. K., Gibbs, F. A., & Pesch, L. A. (1967). The enzymatic preparation of isolated intact parenchymal cells from rat liver. *J Cell Biol* 35, 675-84.

Hu, S. S., Bradshaw, H. B., Benton, V. M., Chen, J. S., Huang, S. M., Minassi, A., Bisogno, T., Masuda, K., Tan, B., Roskoski, R., Jr., Cravatt, B. F., Di Marzo, V., & Walker, J. M. (2009). The biosynthesis of N-arachidonoyl dopamine (NADA), a putative endocannabinoid and endovanilloid, via conjugation of arachidonic acid with dopamine. *Prostaglandins Leukot Essent Fatty Acids* 81, 291-301.

Huang, S. M., Bisogno, T., Trevisani, M., Al-Hayani, A., De Petrocellis, L., Fezza, F., Tognetto, M., Petros, T. J., Krey, J. F., Chu, C. J., Miller, J. D., Davies, S. N., Geppetti, P., Walker, J. M., & Di Marzo, V. (2002). An endogenous capsaicin-like substance with high potency at recombinant and native vanilloid VR1 receptors. *Proc Natl Acad Sci U S A* 99, 8400-5.

Hui, A. Y., Leung, W. K., Chan, H. L., Chan, F. K., Go, M. Y., Chan, K. K., Tang, B. D., Chu, E. S., & Sung, J. J. (2006). Effect of celecoxib on experimental liver fibrosis in rat. *Liver Int* 26, 125-36.

Iredale, J. P. (2007). Models of liver fibrosis: exploring the dynamic nature of inflammation and repair in a solid organ, *J Clin Invest* (pp. 539-48).

Iredale, J. P., Benyon, R. C., Pickering, J., McCullen, M., Northrop, M., Pawley, S., Hovell, C., & Arthur, M. J. (1998). Mechanisms of spontaneous resolution of rat liver fibrosis. Hepatic stellate cell apoptosis and reduced hepatic expression of metalloproteinase inhibitors. *J Clin Invest* 102, 538-49.

Jacobsson, S. O., Wallin, T., & Fowler, C. J. (2001). Inhibition of rat C6 glioma cell proliferation by endogenous and synthetic cannabinoids. Relative involvement of cannabinoid and vanilloid receptors. *J Pharmacol Exp Ther* 299, 951-9.

Jeong, S. W., Jang, J. Y., Lee, S. H., Kim, S. G., Cheon, Y. K., Kim, Y. S., Cho, Y. D., Kim, H. S., Lee, J. S., Jin, S. Y., Shim, C. S., & Kim, B. S. Increased expression of cyclooxygenase-2 is associated with the progression to cirrhosis. *Korean J Intern Med* 25, 364-71.

Jeong, W. I., Osei-Hyiaman, D., Park, O., Liu, J., Batkai, S., Mukhopadhyay, P., Horiguchi, N., Harvey-White, J., Marsicano, G., Lutz, B., Gao, B., & Kunos, G. (2008). Paracrine activation of hepatic CB1 receptors by stellate cell-derived endocannabinoids mediates alcoholic fatty liver. *Cell Metab* 7, 227-35.

Julien, B., Grenard, P., Teixeira-Clerc, F., Van Nhieu, J. T., Li, L., Karsak, M., Zimmer, A., Mallat, A., & Lotersztajn, S. (2005). Antifibrogenic role of the cannabinoid receptor CB2 in the liver. *Gastroenterology* 128, 742-55.

Klein, T. W., Newton, C., Larsen, K., Lu, L., Perkins, I., Nong, L., & Friedman, H. (2003). The cannabinoid system and immune modulation. *J Leukoc Biol* 74, 486-96.

Knook, D. L., Seffelaar, A. M., & de Leeuw, A. M. (1982). Fat-storing cells of the rat liver. Their isolation and purification. *Exp Cell Res* 139, 468-71.

Kozak, K. R., Crews, B. C., Morrow, J. D., Wang, L. H., Ma, Y. H., Weinander, R., Jakobsson, P. J., & Marnett, L. J. (2002). Metabolism of the endocannabinoids, 2-arachidonylglycerol and anandamide, into prostaglandin, thromboxane, and prostacyclin glycerol esters and ethanolamides. *J Biol Chem* 277, 44877-85.

Kozak, K. R., Crews, B. C., Ray, J. L., Tai, H. H., Morrow, J. D., & Marnett, L. J. (2001a). Metabolism of prostaglandin glycerol esters and prostaglandin ethanolamides in vitro and in vivo. *J Biol Chem* 276, 36993-8.

Kozak, K. R., Prusakiewicz, J. J., & Marnett, L. J. (2004). Oxidative metabolism of endocannabinoids by COX-2. *Curr Pharm Des* 10, 659-67.

Kozak, K. R., Prusakiewicz, J. J., Rowlinson, S. W., Schneider, C., & Marnett, L. J. (2001b). Amino acid determinants in cyclooxygenase-2 oxygenation of the endocannabinoid 2-arachidonylglycerol. *J Biol Chem* 276, 30072-7.

Kozak, K. R., Rowlinson, S. W., & Marnett, L. J. (2000). Oxygenation of the endocannabinoid, 2-arachidonylglycerol, to glyceryl prostaglandins by cyclooxygenase-2. *J Biol Chem* 275, 33744-9.

Kozlowska, H., Baranowska, M., Schlicker, E., Kozlowski, M., Laudanski, J., & Malinowska, B. (2008). Virodhamine relaxes the human pulmonary artery through the endothelial cannabinoid receptor and indirectly through a COX product. *Br J Pharmacol* 155, 1034-42.

Lang, A., Schoonhoven, R., Tuvia, S., Brenner, D. A., & Rippe, R. A. (2000). Nuclear factor kappaB in proliferation, activation, and apoptosis in rat hepatic stellate cells. *J Hepatol* 33, 49-58.

Leon, D. A., Shkolnikov, V. M., McKee, M., Kiryanov, N., & Andreev, E. (2010). Alcohol increases circulatory disease mortality in Russia: acute and chronic effects or misattribution of cause?, *Int J Epidemiol* (pp. 1279-90).

Liu, J., Batkai, S., Pacher, P., Harvey-White, J., Wagner, J. A., Cravatt, B. F., Gao, B., & Kunos, G. (2003). Lipopolysaccharide induces anandamide synthesis in macrophages via CD14/MAPK/phosphoinositide 3-kinase/NF-kappaB independently of platelet-activating factor. *J Biol Chem* 278, 45034-9.

Lotersztajn, S., Julien, B., Teixeira-Clerc, F., Grenard, P., & Mallat, A. (2005). Hepatic fibrosis: molecular mechanisms and drug targets. *Annu Rev Pharmacol Toxicol* 45, 605-28.

Ludwig, J., Viggiano, T. R., McGill, D. B., & Oh, B. J. (1980). Nonalcoholic steatohepatitis: Mayo Clinic experiences with a hitherto unnamed disease. *Mayo Clin Proc* 55, 434-8.

Maccarrone, M., & Finazzi-Agro, A. (2003). The endocannabinoid system, anandamide and the regulation of mammalian cell apoptosis. *Cell Death Differ* 10, 946-55.

Maher, J. J. (2001). Interactions between hepatic stellate cells and the immune system, *Semin Liver Dis* (pp. 417-26).

Martin-Sanz, P., Mayoral, R., Casado, M., & Bosca, L. COX-2 in liver, from regeneration to hepatocarcinogenesis: what we have learned from animal models? *World J Gastroenterol* 16, 1430-5.

Matsuda, L. A., Lolait, S. J., Brownstein, M. J., Young, A. C., & Bonner, T. I. (1990). Structure of a cannabinoid receptor and functional expression of the cloned cDNA. *Nature* 346, 561-4.

Matsuoka, M., & Tsukamoto, H. (1990). Stimulation of hepatic lipocyte collagen production by Kupffer cell-derived transforming growth factor beta: implication for a pathogenetic role in alcoholic liver fibrogenesis. *Hepatology* 11, 599-605.

Mechoulam, R., Ben-Shabat, S., Hanus, L., Ligumsky, M., Kaminski, N. E., Schatz, A. R., Gopher, A., Almog, S., Martin, B. R., Compton, D. R., & et al. (1995). Identification of an endogenous 2-monoglyceride, present in canine gut, that binds to cannabinoid receptors. *Biochem Pharmacol* 50, 83-90.

Miranda-Mendez, A., Lugo-Baruqui, A., & Armendariz-Borunda, J. Molecular basis and current treatment for alcoholic liver disease. *Int J Environ Res Public Health* 7, 1872-88.

Muccioli, G. G. Endocannabinoid biosynthesis and inactivation, from simple to complex. *Drug Discov Today* 15, 474-83.

Munro, S., Thomas, K. L., & Abu-Shaar, M. (1993). Molecular characterization of a peripheral receptor for cannabinoids. *Nature* 365, 61-5.

Nanji, A. A., Miao, L., Thomas, P., Rahemtulla, A., Khwaja, S., Zhao, S., Peters, D., Tahan, S. R., & Dannenberg, A. J. (1997). Enhanced cyclooxygenase-2 gene expression in alcoholic liver disease in the rat. *Gastroenterology* 112, 943-51.

Nithipatikom, K., Isbell, M. A., Endsley, M. P., Woodliff, J. E., & Campbell, W. B. Anti-proliferative effect of a putative endocannabinoid, 2-arachidonylglyceryl ether in prostate carcinoma cells. *Prostaglandins Other Lipid Mediat* 94, 34-43.

O'Neill, G. P., & Ford-Hutchinson, A. W. (1993). Expression of mRNA for cyclooxygenase-1 and cyclooxygenase-2 in human tissues. *FEBS Lett* 330, 156-60.

O'Sullivan, S. E., Kendall, D. A., & Randall, M. D. (2004). Characterisation of the vasorelaxant properties of the novel endocannabinoid N-arachidonoyl-dopamine (NADA). *Br J Pharmacol* 141, 803-12.

O'Sullivan, S. E., Kendall, D. A., & Randall, M. D. (2005). Vascular effects of delta 9-tetrahydrocannabinol (THC), anandamide and N-arachidonoyldopamine (NADA) in the rat isolated aorta. *Eur J Pharmacol* 507, 211-21.

Oka, S., Tsuchie, A., Tokumura, A., Muramatsu, M., Suhara, Y., Takayama, H., Waku, K., & Sugiura, T. (2003). Ether-linked analogue of 2-arachidonoylglycerol (noladin ether) was not detected in the brains of various mammalian species. *J Neurochem* 85, 1374-81.

Okamoto, Y., Morishita, J., Tsuboi, K., Tonai, T., & Ueda, N. (2004). Molecular characterization of a phospholipase D generating anandamide and its congeners. *J Biol Chem* 279, 5298-305.

Okazaki, I., Watanabe, T., Hozawa, S., Arai, M., & Maruyama, K. (2000). Molecular mechanism of the reversibility of hepatic fibrosis: with special reference to the role of matrix metalloproteinases. *J Gastroenterol Hepatol* 15 Suppl, D26-32.

Onaivi, E. S., Ishiguro, H., Gong, J. P., Patel, S., Perchuk, A., Meozzi, P. A., Myers, L., Mora, Z., Tagliaferro, P., Gardner, E., Brusco, A., Akinshola, B. E., Liu, Q. R., Hope, B., Iwasaki, S., Arinami, T., Teasenfitz, L., & Uhl, G. R. (2006). Discovery of the presence and functional expression of cannabinoid CB2 receptors in brain. *Ann N Y Acad Sci* 1074, 514-36.

Osei-Hyiaman, D., DePetrillo, M., Pacher, P., Liu, J., Radaeva, S., Batkai, S., Harvey-White, J., Mackie, K., Offertaler, L., Wang, L., & Kunos, G. (2005). Endocannabinoid activation at hepatic CB1 receptors stimulates fatty acid synthesis and contributes to diet-induced obesity. *J Clin Invest* 115, 1298-305.

Patel, S., Carrier, E. J., Ho, W. S., Rademacher, D. J., Cunningham, S., Reddy, D. S., Falck, J. R., Cravatt, B. F., & Hillard, C. J. (2005). The postmortal accumulation of brain N-arachidonylethanolamine (anandamide) is dependent upon fatty acid amide hydrolase activity. *J Lipid Res* 46, 342-9.

Pinzani, M., & Marra, F. (2001). Cytokine receptors and signaling in hepatic stellate cells, *Semin Liver Dis* (pp. 397-416).

Piomelli, D. (2003). The molecular logic of endocannabinoid signalling. *Nat Rev Neurosci* 4, 873-84.

Porter, A. C., Sauer, J. M., Knierman, M. D., Becker, G. W., Berna, M. J., Bao, J., Nomikos, G. G., Carter, P., Bymaster, F. P., Leese, A. B., & Felder, C. C. (2002). Characterization of a novel endocannabinoid, virodhamine, with antagonist activity at the CB1 receptor. *J Pharmacol Exp Ther* 301, 1020-4.

Raffray, M., & Cohen, G. M. (1997). Apoptosis and necrosis in toxicology: a continuum or distinct modes of cell death? *Pharmacol Ther* 75, 153-77.

Reilly, T. P., Brady, J. N., Marchick, M. R., Bourdi, M., George, J. W., Radonovich, M. F., Pise-Masison, C. A., & Pohl, L. R. (2001). A protective role for cyclooxygenase-2 in drug-induced liver injury in mice. *Chem Res Toxicol* 14, 1620-8.

Rivera, C. A., Bradford, B. U., Hunt, K. J., Adachi, Y., Schrum, L. W., Koop, D. R., Burchardt, E. R., Rippe, R. A., & Thurman, R. G. (2001). Attenuation of CCl(4)-induced hepatic fibrosis by GdCl(3) treatment or dietary glycine, *Am J Physiol Gastrointest Liver Physiol* (pp. G200-7).

Rockey, D. C., Boyles, J. K., Gabbiani, G., & Friedman, S. L. (1992). Rat hepatic lipocytes express smooth muscle actin upon activation in vivo and in culture. *J Submicrosc Cytol Pathol* 24, 193-203.

Rouzer, C. A., & Marnett, L. J. (2005). Structural and functional differences between cyclooxygenases: fatty acid oxygenases with a critical role in cell signaling. *Biochem Biophys Res Commun* 338, 34-44.

Rouzer, C. A., & Marnett, L. J. (2008). Non-redundant functions of cyclooxygenases: oxygenation of endocannabinoids. *J Biol Chem* 283, 8065-9.

Russel, S. a. (2001). *Molecular Cloning A Laboratory Manual*. New York: Cold Spring Harbor Laboratory Press.

Russo, M. W., Firpi, R. J., Nelson, D. R., Schoonhoven, R., Shrestha, R., & Fried, M. W. (2005). Early hepatic stellate cell activation is associated with advanced fibrosis after liver transplantation in recipients with hepatitis C. *Liver Transpl* 11, 1235-41.

Ryberg, E., Larsson, N., Sjogren, S., Hjorth, S., Hermansson, N. O., Leonova, J., Elebring, T., Nilsson, K., Drmota, T., & Greasley, P. J. (2007). The orphan receptor GPR55 is a novel cannabinoid receptor. *Br J Pharmacol* 152, 1092-101.

Saario, S. M., Savinainen, J. R., Laitinen, J. T., Jarvinen, T., & Niemi, R. (2004). Monoglyceride lipase-like enzymatic activity is responsible for hydrolysis of 2-arachidonoylglycerol in rat cerebellar membranes. *Biochem Pharmacol* 67, 1381-7.

Saile, B., Knittel, T., Matthes, N., Schott, P., & Ramadori, G. (1997). CD95/CD95L-mediated apoptosis of the hepatic stellate cell. A mechanism terminating uncontrolled hepatic stellate cell proliferation during hepatic tissue repair. *Am J Pathol* 151, 1265-72.

Sang, N., Zhang, J., & Chen, C. (2006). PGE2 glycerol ester, a COX-2 oxidative metabolite of 2-arachidonoyl glycerol, modulates inhibitory synaptic transmission in mouse hippocampal neurons. *J Physiol* 572, 735-45.

Saunders, C. I., Fassett, R. G., & Geraghty, D. P. (2009). Up-regulation of TRPV1 in mononuclear cells of end-stage kidney disease patients increases susceptibility to N-arachidonoyl-dopamine (NADA)-induced cell death. *Biochim Biophys Acta* 1792, 1019-26.

Schmitt-Graff, A., Desmouliere, A., & Gabbiani, G. (1994). Heterogeneity of myofibroblast phenotypic features: an example of fibroblastic cell plasticity. *Virchows Arch* 425, 3-24.

Schmitt-Graff, A., Kruger, S., Bochard, F., Gabbiani, G., & Denk, H. (1991). Modulation of alpha smooth muscle actin and desmin expression in perisinusoidal cells of normal and diseased human livers. *Am J Pathol* 138, 1233-42.

Schwabe, R. F., Seki, E., & Brenner, D. A. (2006). Toll-like receptor signaling in the liver. *Gastroenterology* 130, 1886-900.

Seglen, P. O. (1976). Preparation of isolated rat liver cells. *Methods Cell Biol* 13, 29-83.

Seibert, K., Zhang, Y., Leahy, K., Hauser, S., Masferrer, J., & Isakson, P. (1997). Distribution of COX-1 and COX-2 in normal and inflamed tissues. *Adv Exp Med Biol* 400A, 167-70.

Serini, G., & Gabbiani, G. (1999). Mechanisms of myofibroblast activity and phenotypic modulation. *Exp Cell Res* 250, 273-83.

Siegmund, S. V., Dooley, S., & Brenner, D. A. (2005a). Molecular mechanisms of alcohol-induced hepatic fibrosis. *Dig Dis* 23, 264-74.

Siegmund, S. V., Qian, T., de Minicis, S., Harvey-White, J., Kunos, G., Vinod, K. Y., Hungund, B., & Schwabe, R. F. (2007). The endocannabinoid 2-arachidonoyl glycerol induces death of hepatic stellate cells via mitochondrial reactive oxygen species. *FASEB J* 21, 2798-806.

Siegmund, S. V., & Schwabe, R. F. (2008). Endocannabinoids and liver disease. II. Endocannabinoids in the pathogenesis and treatment of liver fibrosis. *Am J Physiol Gastrointest Liver Physiol* 294, G357-62.

Siegmund, S. V., Seki, E., Osawa, Y., Uchinami, H., Cravatt, B. F., & Schwabe, R. F. (2006). Fatty acid amide hydrolase determines anandamide-induced cell death in the liver. *J Biol Chem* 281, 10431-8.

Siegmund, S. V., Uchinami, H., Osawa, Y., Brenner, D. A., & Schwabe, R. F. (2005b). Anandamide induces necrosis in primary hepatic stellate cells. *Hepatology* 41, 1085-95.

Smith, W. L., DeWitt, D. L., & Garavito, R. M. (2000). Cyclooxygenases: structural, cellular, and molecular biology. *Annu Rev Biochem* 69, 145-82.

Sobesky, R., Mathurin, P., Charlotte, F., Moussalli, J., Olivi, M., Vidaud, M., Ratziu, V., Opolon, P., & Poynard, T. (1999). Modeling the impact of interferon alfa treatment on liver fibrosis progression in chronic hepatitis C: a dynamic view. The Multivirc Group. *Gastroenterology* 116, 378-86.

Steffens, M., Zentner, J., Honegger, J., & Feuerstein, T. J. (2005). Binding affinity and agonist activity of putative endogenous cannabinoids at the human neocortical CB1 receptor. *Biochem Pharmacol* 69, 169-78.

Storr, M., Yuce, B., & Goke, B. (2006). [Perspectives of cannabinoids in gastroenterology]. *Z Gastroenterol* 44, 185-91.

Straiker, A., & Mackie, K. (2006). Cannabinoids, electrophysiology, and retrograde messengers: challenges for the next 5 years. *AAPS J* 8, E272-6.

Teixeira-Clerc, F., Julien, B., Grenard, P., Tran Van Nhieu, J., Deveaux, V., Li, L., Serriere-Lanneau, V., Ledent, C., Mallat, A., & Lotersztajn, S. (2006). CB1 cannabinoid receptor antagonism: a new strategy for the treatment of liver fibrosis. *Nat Med* 12, 671-6.

Trebicka, J., Racz, I., Siegmund, S. V., Cara, E., Granzow, M., Schierwagen, R., Klein, S., Wojtalla, A., Hennenberg, M., Huss, S., Fischer, H. P., Heller, J., Zimmer, A., & Sauerbruch, T. Role of cannabinoid receptors in alcoholic hepatic injury: steatosis and fibrogenesis are increased in CB(2) receptor-deficient mice and decreased in CB(1) receptor knockouts. *Liver Int* 31, 862-72.

Trim, N., Morgan, S., Evans, M., Issa, R., Fine, D., Afford, S., Wilkins, B., & Iredale, J. (2000). Hepatic stellate cells express the low affinity nerve growth factor receptor p75 and undergo apoptosis in response to nerve growth factor stimulation. *Am J Pathol* 156, 1235-43.

van der Stelt, M., Trevisani, M., Vellani, V., De Petrocellis, L., Schiano Moriello, A., Campi, B., McNaughton, P., Geppetti, P., & Di Marzo, V. (2005). Anandamide acts as an intracellular messenger amplifying Ca2+ influx via TRPV1 channels. *EMBO J* 24, 3026-37.

Van Dross, R. T. (2009). Metabolism of anandamide by COX-2 is necessary for endocannabinoid-induced cell death in tumorigenic keratinocytes. *Mol Carcinog* 48, 724-32.

Volk, B. W., & Popper, H. (1950). The influence of dispersion upon the absorption of Vitamin A and fat as studied by fluorescence microscopy. *Gastroenterology* 14, 549-57.

Wake, K. (1971). "Sternzellen" in the liver: perisinusoidal cells with special reference to storage of vitamin A. *Am J Anat* 132, 429-62.

Walpole, C. S., Wrigglesworth, R., Bevan, S., Campbell, E. A., Dray, A., James, I. F., Masdin, K. J., Perkins, M. N., & Winter, J. (1993). Analogues of capsaicin with agonist activity as novel analgesic agents; structure-activity studies. 3. The hydrophobic side-chain "C-region". *J Med Chem* 36, 2381-9.

Wang, J. J., & Mak, O. T. Induction of apoptosis in non-small cell lung carcinoma A549 cells by PGD2 metabolite, 15d-PGJ2. *Cell Biol Int*.

WHO. (2002). Hepatitis C. In **http://www.who.int/csr/disease/hepatitis/whocdscsrlyo2003/en/index.html** (Ed.): World health organisation.

Yang, Q., Liu, H. Y., Zhang, Y. W., Wu, W. J., & Tang, W. X. Anandamide induces cell death through lipid rafts in hepatic stellate cells. *J Gastroenterol Hepatol* 25, 991-1001.

Yoshida, T., Ohki, S., Kanazawa, M., Mizunuma, H., Kikuchi, Y., Satoh, H., Andoh, Y., Tsuchiya, A., & Abe, R. (1998). Inhibitory effects of prostaglandin D2 against the proliferation of human colon cancer cell lines and hepatic metastasis from colorectal cancer. *Surg Today* 28, 740-5.

Yu, J., Wu, C. W., Chu, E. S., Hui, A. Y., Cheng, A. S., Go, M. Y., Ching, A. K., Chui, Y. L., Chan, H. L., & Sung, J. J. (2008). Elucidation of the role of COX-2 in liver fibrogenesis using transgenic mice. *Biochem Biophys Res Commun* 372, 571-7.

Yu, M., Ives, D., & Ramesha, C. S. (1997). Synthesis of prostaglandin E2 ethanolamide from anandamide by cyclooxygenase-2. *J Biol Chem* 272, 21181-6.

8 SUPPLEMENTAL

8.1 Publications

Schildberg, F. A., Wojtalla, A., Siegmund, S. V., Endl, E., Diehl, L., Abdullah, Z., Kurts, C., & Knolle, P. A. (2011) Hepatic stellate cells veto CD8 T cell activation by a CD54-dependent mechanism. *Hepatology*.

Trebicka, J., Racz, I., Siegmund, S. V., Cara, E., Granzow, M., Schierwagen, R., Klein, S., Wojtalla, A., Hennenberg, M., Huss, S., Fischer, H. P., Heller, J., Zimmer, A., & Sauerbruch, T. (2011) Role of cannabinoid receptors in alcoholic hepatic injury: steatosis and fibrogenesis are increased in CB(2) receptor-deficient mice and decreased in CB(1) receptor knockouts. *Liver Int* **31,** 862-72.

Wojtalla A., Herweck F., Granzow M., Trebicka J., Sauerbruch T., Singer M. V., Zimmer A., Siegmund S. V. The endocannabinoid N-arachidonoyl dopamine (NADA) induces cell death in primary hepatic stellate cells, **in Revision**

8.2 Declaration

I hereby solely declare that I prepared this thesis entitled: “Liver fibrosis and endocannabinoids” entirely by myself except otherwise stated. All text passages that are literally or correspondingly taken from published or unpublished papers/writings are indicated as such. All materials or services provided by other persons are equally indicated.

Danksagung

Mein besonderer Dank gilt Prof. Dr. Stefan Wölfl für die Begutachtung meiner Arbeit.
Mein Dank gilt ebenfalls Prof. Dr. Singer, denn er ermöglichte es mir, meine Doktorarbeit in seiner Arbeitsgruppe zu beginnen.
Prof. Dr. Andreas Zimmer danke ich zum einen für die Übernahme der Funktion des Zweitgutachters. Zum anderen möchte ich mich aber vor allem für die freundliche Aufnahme in seine Arbeitsgruppe bedanken, in der ich mich sofort wohl gefühlt habe. Hier hatte ich unter ausgezeichneter Betreuung und Unterstützung die Möglichkeit, meine Arbeit abzuschließen.
Dr. Sören Siegmund danke ich für die Überlassung des Themas, für seinen fachlichen Rat und die fortdauernde Unterstützung während der gesamten Zeit meiner Doktorarbeit und Betreuung meiner Arbeit sowohl in Mannheim als auch in Bonn. Vielen Dank für die Hilfestellungen in den Endzügen meiner Arbeit und auch die Verbesserungsvorschläge während des Schreibprozesses.
Frank Herweck danke ich für eine super Zusammenarbeit in Mannheim. Ohne ihn wäre vieles nicht machbar gewesen.
Svenja, Eva, Anna-Lena, Pamela, Britta, Caro, Irene und David – Schätzeleins, ihr habt mir die Zeit sowohl im Labor als auch Freizeittechnisch in Bonn erheblich verschönt!
Eva und Micha: Vielen, vielen, vielen Dank für die Endloskorrekturen meiner Endlosmanuskripte.
...und Micha, ich würde sagen: ICH RASTE AUS!!! ☺

Benni, danke für alles

Mama, ohne Dich wäre das nicht möglich gewesen: Danke